The Role of Perineurial Glia in Peripheral Nerve Regeneration

Gwendolyn Maura Lewis
Charlottesville, Virginia

B.S., James Madison University, 2004

A Dissertation presented to the Graduate Faculty
of the University of Virginia in Candidacy for the Degree of
Doctor of Philosophy

Department of Biology

University of Virginia
August, 2015

_____

_____

_____

_____

_____

Abstract

The vertebrate peripheral nervous system (PNS) encompasses a complex network of nerves responsible for transmitting information between the central nervous system (CNS) and the body. When peripheral nerves are damaged, this flow of vital sensory and motor information is disrupted, and the result can be debilitating. The PNS has the remarkable capability to regenerate, however patients with severe injuries often do not regain full functional recovery, leaving substantial room for improvement in therapies. Although peripheral nerve regeneration has been studied extensively with respect to axons, Schwann cells, and even macrophages, the role of the perineurium in this process is poorly understood.

Here, I present the first detailed characterization of perineurial behavior after nerve injury in a live animal. First, I present my development of a novel assay to study glial responses to nerve transection in live zebrafish larvae. This assay uses laser-mediated nerve transection followed by *in vivo* time-lapse microscopy. Using this assay, I show that perineurial glia respond to nerve injury with rapid and dynamic changes in behavior. Perineurial glia send highly motile membrane processes toward injury sizes, phagocytize debris, and eventually bridge the gap between proximal and distal nerve stumps. In the absence of these bridges, axon regrowth is impaired, suggesting that perineurial glia are essential for successful regeneration. Finally, I present evidence that perineurial glia communicate and coordinate with Schwann cells and macrophages after injury. This work introduces perineurial glia as active and influential players in the early response to nerve injury.

Dedication

This work is dedicated with love and gratitude to the family, friends, and fellow scientists who made it possible. Thank you for everything. To my Mom and Dad, for their unconditional love and support, and to the rest of my wonderful family- Tim, Sarah, Jack, Mommom, Poppop, Grandpa, Bill, Kim, Chad, Janice, Jessi, Ian, Micki, and Oma, for their love and encouragement. To my mentor Sarah Kucenas, for her support and guidance through my atypical path through graduate school. To the past and present members of the Kucenas lab, particularly Jessica, Angie, Rebecca and Cody, who listened to my madness, kept me laughing, contributed valuable scientific insight, and helped me achieve my dream of creating a Peepnado. To my husband Travis, for being so supportive, for being the greatest husband and father, and for loving me through everything. Someone should give him a Ph.D. in being awesome. Finally, to my two beautiful and hilarious children, Bryant and Allie. Thank you for the love and laughter you've brought me, and for putting it all in perspective…

Table of Contents

Figures, Tables and Movies

Chapter 1

Introduction: Development and regeneration of the perineurium

The vertebrate nervous system is composed of the central nervous system (CNS), which consists of the brain and spinal cord, and the peripheral nervous system (PNS), which encompasses the nerves responsible for transmitting information between the CNS and almost all tissues and organs. In this way, the PNS controls every movement and sensation. Peripheral nerves are composed of axons, surrounded by layers of glia and connective tissue. During development, the cells that form these layers must precisely coordinate their migration and differentiation to ensure the nerve is assembled properly. After an injury, peripheral nerves have the remarkable ability to regenerate, and this process again requires the coordination of multiple cells. Unfortunately, clinical evidence suggests that less than 10% of peripheral nerve injury patients achieve full functional recovery (Witzel et al., 2005; Zochodne, 2012). In order to design better therapies, we first need a comprehensive understanding of the regenerative process.

Peripheral nerves are populated by at least five distinct cell types, but previous research on regeneration has focused primarily on investigating the actions of only two, neurons and Schwann cells. In this dissertation, I use the zebrafish motor nerve as a model to investigate how perineurial glia, another prominent and essential PNS cell type, respond to nerve injury and coordinate with other cells during regeneration. In this introduction I will review what is known about perineurial glia, their role in development, and their interactions with other cells. I will also review what previous literature has

revealed about the perineurium during regeneration, and highlight significant knowledge gaps in our understanding of perineurial behavior after nerve injury.

Organization of the adult peripheral nerve

The construction of the peripheral nerve is designed to ensure that information is transmitted quickly and nerve components are protected. Within the nerve, neurons relay information by propagating action potentials down their axons. These axons are wrapped by glia, called Schwann cells, which can be either myelinating or non-myelinating. Myelinating Schwann cells associate with segments of large caliber axons in a 1:1 ratio and wrap them in a spiral fashion. This produces many layers of membrane that compact to form the myelin sheath. This sheath is lipid rich and acts as insulation, allowing for the fast, saltatory conduction of action potentials (Quarles et al., 2006). Non-myelinating Schwann cells ensheath groups of small-caliber axons, creating Remak bundles. These axon-Schwann cell complexes are then surrounded by the endoneurium, perineurium, and epineurium (Kaplan et al., 2009; Geuna et al., 2009). The endoneurium encompasses the space around and between the Schwann cells and is formed of loose connective tissue embedded with a capillary network. The perineurium bundles axons, Schwann cells, and endoneurium into fascicles, and the epineurium forms the outermost protective sheath of dense connective tissue (Figure 1-1A). While all of these sheaths function to protect the nerve, their composition is quite different. The endoneurium and epineurium are composed primarily of connective tissue and scattered fibroblasts, whereas the perineurium is a cellular sheath formed by flattened, interdigitated perineurial glia (Thomas and Olsson, 1984; Kucenas et al., 2008; Clark et al., 2014).

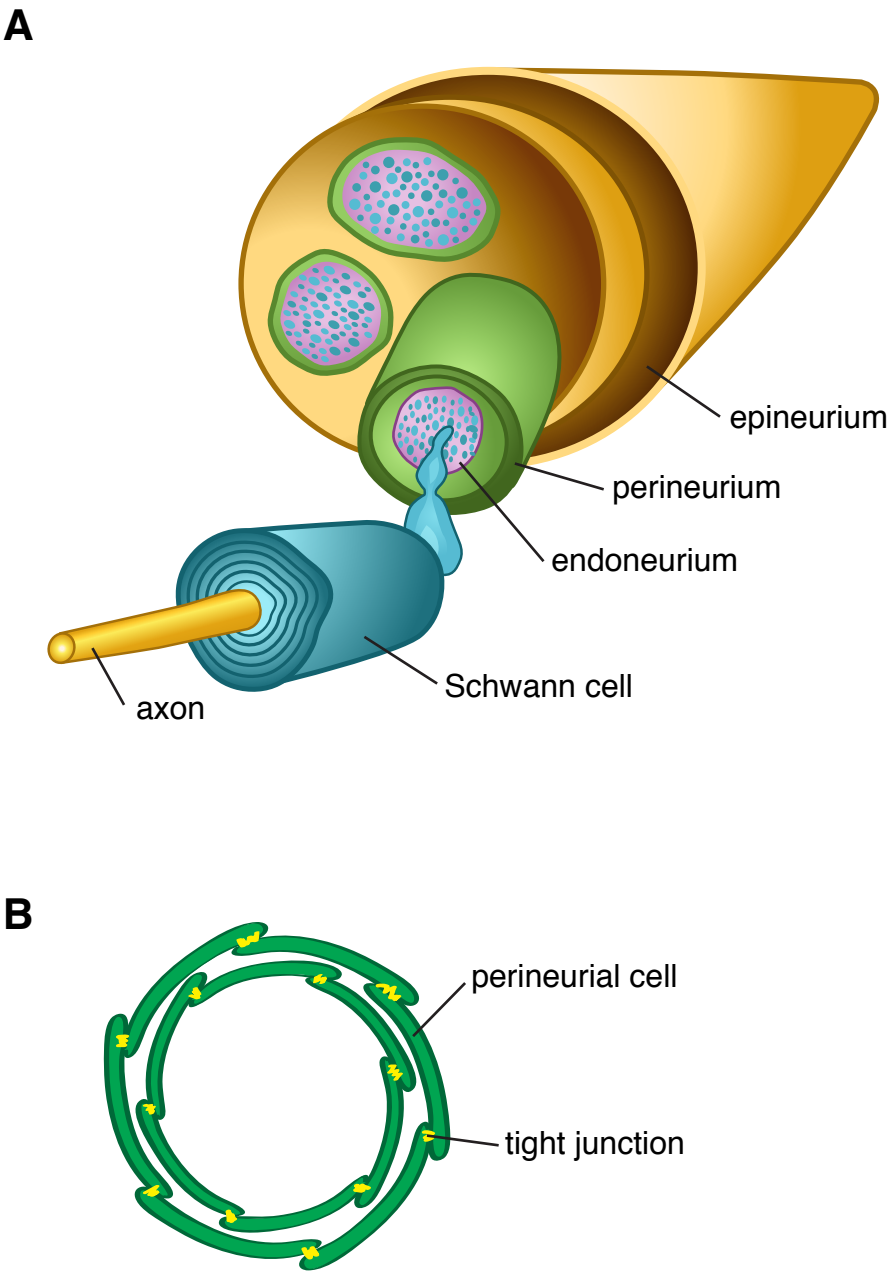

Figure 1-1: Structure of the adult peripheral nerve and perineurium. (A) Diagram of a cross section through an adult peripheral nerve illustrating major nerve components. Axons (tan) are wrapped by Schwann cells (blue), which are surrounded by the endoneurium (pink) and bundled into a fascicle by the perineurium (green). The epineurium is the outermost layer surrounding several fascicles (tan). (B) Simplified diagram of the perineurial sheath, illustrating the overlaping of processes and tight junctions (yellow) between adjacent cells.

Function of the perineurial sheath

The perineurium is a mechanically strong and metabolically active barrier that surrounds the fascicle and separates the endoneurial space from the rest of the body. The functional significance of the perineurium was first described by Key and Retzius in 1876. They observed that fluid injected beneath the perineurial sheath flowed easily through the nerve for considerable distances, whereas fluid injected outside the perineurium diffused and spread only a short distance (Key and Retzius, 1876; Sullivan and Mortensen, 1934). This suggested the perineurium served as a diffusion barrier, which was later confirmed by others using protein tracers (Thomas and Olsson, 1984; Kristensson and Olsson, 1971). Structurally, the perineurium consists of flattened cells, which contain characteristic pinocytic vesicles and have a double basal lamina. These cells coalesce into compact, concentrically arranged layers with overlapping membranes that often interlock (Figure 1-1B) (Thomas and Jones, 1967; Akert et al., 1976; Burkel, 1967; Bourne, 1968). Collagen and elastin fibrils fill the spaces between perineurial lamella, and are usually oriented longitudinally to the nerve. Fibroblast-like cells have also been observed within the perineurial layers, but differ morphologically from the ensheathing cells in that they do not have a basal lamina or extensive processes (Thomas, 1963; Thomas and Jones, 1967). Tight junctions are present at the contacts between adjacent ensheathing cells (Figure 1-1B), which prevent unwanted diffusion of materials through the extracellular space and allow perineurial cells to regulate the transport of material between the interior and exterior of the fascicle (Akert et al., 1976; Burkel, 1967; Bourne, 1968; Thomas and Olsson, 1984; Kristensson and Olsson, 1971). Together with the cells that line the capillaries, this creates the blood-nerve-barrier (BNB). As part of the BNB, perineurial

cells serve to isolate the endoneurial space and protect it from toxins and infection, while also regulating fluid pressure and ionic flux (Geuna et al., 2009). In this way, the perineurium regulates both the support and protection of vital nerve components and is essential for proper nerve function.

Motor nerve development

Before discussing regeneration, it is pertinent to address the origin and relationship of nerve cells during development. Vertebrate peripheral nerves are composed of sensory and motor fibers, which transmit information to and from the CNS respectively. Although these branches are structurally and functionally similar, they have different developmental origins. Motor and sensory roots are separate from each other proximal to the spinal cord, but often join together distally to create mixed nerves. In my work, I have utilized the zebrafish spinal motor nerve root (a region not mixed with sensory fibers) to study the role of perineurial glia and their interactions with Schwann cells in regeneration. Thus, development of motor nerve associated glia and studies in zebrafish will be particularly emphasized here.

i. Motor axons

Motor neurons are specified in the pMN domain of the spinal cord through a combinatorial code of morphogens and transcription factors. These neurons keep their cell bodies in the CNS and project axons into the periphery through ventrally located motor exit points (MEPs). Once in the periphery, these axons pathfind along stereotypical paths, guided by cues from the local environment, until target cells are reached and

innervated. In zebrafish, two classes of motor neurons innervate muscle fibers, primary and secondary. Primary motor neurons arise first and establish the first functional circuitry in the embryo. This governs essential survival behaviors, such as swimming. Three primary motor neurons are generated in each segment, which project axons through a single MEP and pioneer the three major spinal motor nerve tracts. Two of these neurons project axons ventrally to form the rostral and caudal nerve tracts, while the third neuron projects its axon dorsally and forms the middle tract. Secondary motor neurons arise a few hours later and project axons through the same MEP and along similar paths as the primary axons. As axons reach their targets, their growth cones meet with pre-patterned acetylcholine receptors on the muscle fibers, and functional neuromuscular junctions are formed. When axogenesis is complete, approximately 70 motor axons will have exited through each MEP (Figure 1-2) (Myers et al., 1986; Eisen, 1991; Lin et al., 2001).

ii. Schwann cell differentiation

Development of Schwann cells begins with the delamination of neural crest cells, which originate from the dorsal neural tube during neurulation. A subset of these cells migrates along a ventral path and associates with outgrowing motor axons. This marks the beginning of a series of changes in cell state that eventually lead to the formation of mature Schwann cells. Neural crest cells that have associated with axons are Schwann cell precursors (SCPs), which differentiate into immature Schwann cells (ISCs), then finally mature Schwann cells (Jessen and Mirsky, 2005). Each of these steps in the Schwann cell lineage accompanies changes in expression and behavior. SCPs are

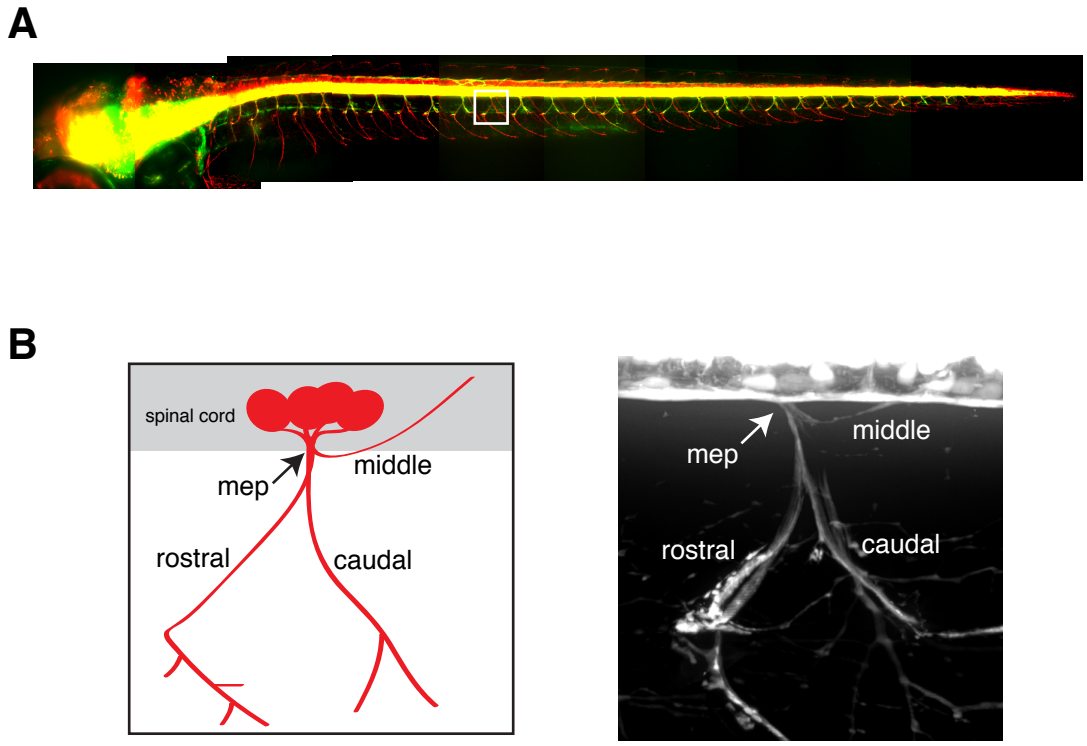

Figure 1-2: Zebrafish motor nerves. (A) Full length confocal image of a 6 dpf *Tg(nkx2.2a:megfp; olig2:dsred)* zebrafish larva with dorsal to top and anterior to left. Motor axons (red) are present in each segment and are wrapped by perineurial glia (green). White box denotes region represented in (B). (B) Diagrammatic and actual representation of the zebrafish spinal motor nerve root at 6 dpf. The rostral, caudal, and middle nerve tracts are labeled in the diagram and are evident in the image. mep, motor exit point.

multipotent precursor cells that are that are migratory, proliferative, and dependent on survival signals from axons (Joseph et al., 2004). ISCs are also migratory and proliferative, but the change from SCP to ISC accompanies a switch from paracrine to autocrine survival (Meier et al., 1999), the creation of a basal lamina, and commitment to the Schwann cell fate (Jessen and Mirsky, 2005). As ISCs begin to differentiate into mature Schwann cells, they invade the axon bundle and begin radial sorting, whereby Schwann cells associate with a single axon and begin myelination.

Although the expression pattern of Schwann cells change as they differentiate, the expression of several essential factors is maintained throughout the lineage. One of these is the transcription factor Sox10 (SRY (sex determining region Y)-box 10). Sox10 is initially expressed in all migratory neural crest, but is turned down in several other neural crest-derived lineages. It remains expressed in Schwann cells throughout development and is essential for their generation. In accordance with this, Sox10 null mice and zebrafish *colourless* (*cls*) mutants, which are deficient for *sox10*, do not have Schwann cells along peripheral nerves (Britsch et al., 2001; Dutton et al., 2001; Kucenas et al., 2008).

Progression down the Schwann cell lineage is driven, at least in part, by signals from axons. Arguably the best studied of these signals is Neuregulin 1 (Nrg1), which is alternatively spliced into several isoforms. The type III isoform is a transmembrane ligand that is abundant on peripheral axons and signals to Schwann cells through the tyrosine kinase receptor complex Erbb2/Erbb3 (Garratt et al., 2000a). This complex only functions as a heterodimer, as Erbb3 contains the Nrg1 binding domain, but has no intrinsic kinase activity, while Erbb2 has kinase activity but no binding domain

(Birchmeier, 2009). Erbb2/Erbb3 receptor activation potently activates the extracellular-signal-regulated-kinase (ERK) 1/2 cascade, and signaling through this receptor is required continuously throughout development to promote Schwann cell proliferation, migration, differentiation, and myelination (Birchmeier and Nave, 2008; Riethmacher et al., 1997; Morris et al., 1999; Taveggia et al., 2005; Lyons et al., 2005; Garratt et al., 2000b). Similar to Sox10 mutants, Erbb2 and Erbb3 mutant mice lack Schwann cells along peripheral nerves (Morris et al., 1999; Britsch et al., 2001). Interestingly, Sox10 directly modulates Erbb3 transcription (Prasad et al., 2011), suggesting decreased Erbb3 expression in Sox10 mutants is at least one reason why Schwann cells do not develop. Zebrafish *erbb2* and *erbb3* mutants also exhibit Schwann cell defects. Imaging studies in *erbb3* larvae revealed that Schwann cells did not develop along the posterior lateral line nerve (PLLn), a prominent sensory nerve in fish, and the expression of several Schwann cell markers was absent in both *erbb2* and *erbb3* mutants (Lyons et al., 2005). These studies demonstrate Nrg1-Erbb signaling is a critical and conserved driver of Schwann cell development in vertebrates.

Recently, the G protein-coupled receptor Gpr126 has gained attention for its role in mediating later stages of Schwann cell development. Gpr126 is localized on the surface of Schwann cells and interacts with laminin in the extra cellular matrix (ECM) (Petersen et al., 2015). Signaling through this receptor is required autonomously in Schwann cells and has duel roles in regulating radial sorting and myelination (Petersen et al., 2015). In both mouse and zebrafish Gpr126 mutants, Schwann cells are present along peripheral nerves in normal numbers, indicating early migration and proliferation is normal, but they later stall at the pro-myelinating stage. These Schwann cells do not

myelinate axons and fail to terminally differentiate (Monk et al., 2009; Monk et al., 2011). These studies suggest that signaling through Gpr126 is essential for Schwann cell differentiation and myelination.

iii. Perineurium and other sheaths

Following the association of Schwann cells with outgrowing motor axons, these components become encased by the endoneurium, perineurium and epineurium, although the development of these sheaths is less well understood. Fate mapping studies in mice have suggested that endoneurial fibroblasts share a neural crest origin with Schwann cells (Joseph et al., 2004). These cells likely arise from the multi-potent SCPs that associate with nascent axons. The origin of epineurial fibroblasts is not known, although it has been suggested that they develop from mesenchyme similar to other fibroblasts. Until recently, the origin of the perineurium was debated, with researchers suggesting origins such as neural crest or mesenchyme (Burkel, 1967; Du Plessis et al., 1997; Bourne, 1968; Bunge et al., 1989). However, studies in both zebrafish and mice have now demonstrated that perineurial cells along the motor nerve are derived from precursors that originate in the p3 domain of the spinal cord. (Kucenas et al., 2008; Clark et al., 2014).

One reason it has been difficult to study the development of peripheral nerve sheaths is due to the lack of available markers for cells in these layers. The relatively recent discovery that motor nerve perineurial cells in zebrafish express the transcription factor *nkx2.2a* has led to significant advances in our understanding of perineurial development. In zebrafish, developing motor nerve perineurial cells can be visualized using the transgenic reporter line *Tg(nkx2.2a:megfp)*, which uses regulatory sequences

from the *nkx2.2a* gene to drive membrane tethered EGFP in all *nkx2.2a* expressing cells. Using *in vivo* time-lapse imaging of this line, Kucenas et al. demonstrated that early in zebrafish development, *nkx2.2a*$^{+}$ cells were restricted to the p3 domain of the spinal cord. After the association of SCPs with motor axons, *nkx2.2a*$^{+}$ cells migrated out of the spinal cord and into the periphery through MEPs. Once in the periphery, these cells migrated along motor axons, ensheathed on top of Schwann cells and axons, and eventually differentiated into the mature perineurium. Reflecting the neural origin of these *nkx2.2a*$^{+}$ cells, I will hereafter refer to them as perineurial glia. In this same study, the authors showed that disrupting the specification of perineurial glia through the use of an *nkx2.2a* morpholino oligonucleotide (MO) prevented their migration into the periphery. Subsequently, motor axons exited ectopically, were defasciculated, and Schwann cells failed to wrap nerves (Kucenas et al., 2008). Consistent with the findings in zebrafish, a recent study in mice concluded that a subset of cells in the mammalian perineurium is centrally derived. These cells also expressed Nkx2.2, and conditional knockouts for Nkx2.2 exhibited motor neuron and Schwann cell defects similar to those described in zebrafish (Clark et al., 2014). Taken together, these studies suggest that perineurial glia are essential for motor nerve development, and that the origin of perineurial glia is conserved among vertebrates.

Unlike Schwann cells, few studies have investigated the molecular cues that drive perineurial glial development. As stated above, *nkx2.2a* is required for perineurial glial specification. After specification, only two signaling cascades are known to regulate perineurial development, Notch and Desert Hedgehog (Dhh)-Patched (Ptc). In zebrafish, Notch signaling is active in perineurial glia around the time they migrate from the spinal

cord, and remains active until migration ceases. Disrupting Notch signaling before perineurial exiting leads to a failure of cells to migrate into the periphery, and disrupting Notch signaling after exiting results in defective perineurial maturation and sheath formation (Binari et al., 2013). This suggests perineurial glia utilize Notch signaling for their migration and maturation, although the source of Notch ligand is still unknown. Dhh-Ptc signaling has been shown to regulate later stages of perineurial development. Dhh is a morphogen expressed by Schwann cells (Parmantier et al., 1999; Bitgood and McMahon, 1995). Perineurial cells express the Dhh receptor Ptc. In *Dhh* mouse mutants, the perineurium is thin, disorganized, and forms small minifascicles. Perineurial tight junctions are abnormal, and the BNB is compromised. Notably, these defects are only seen in older animals, and initial sheath formation is normal (Parmantier et al., 1999). This suggests that Dhh-Ptc signaling regulates maturation of the perineurium, but not early migration and sheath formation, which are regulated by Notch (Binari et al., 2013). There are likely many other signals that mediate perineurial development, and future studies are needed to help elucidate these.

iv. The role of glial-glial interactions

Peripheral nerve development requires all cells that form the nerve to precisely coordinate their migration and differentiation. This happens in the form of signaling between cells, and mechanisms of signaling between neurons and Schwann cells have been (and still are) studied extensively. Little is known about the interactions between other cell types, such as Schwann cells and perineurial glia, although several lines of evidence suggest these cell types signal reciprocally. Disrupting perineurial development

in zebrafish using the *nkx2.2a* MO leads to a failure of Schwann cells to wrap nerves, and perturbing Notch signaling in perineurial glia causes defects in Schwann cell myelination (Kucenas et al., 2008; Binari et al., 2013). Likewise, perineurial glia fail to wrap nerves in mutants lacking Schwann cells (Kucenas et al., 2008; Kucenas et al., 2009). These studies suggest that interactions between Schwann cells and perineurial glia are essential for motor nerve development, and future studies will likely reveal more specific signaling cues utilized by these cells.

v. Summary of motor nerve development

Recent studies of perineurial glia in zebrafish have led to the development of a new model of motor nerve development. In this model, nerve development begins as the axons of spinal motor neurons grow and exit the spinal cord through MEPs. Neural crest cells migrate ventrally along the neural tube and associate with the nascent axons. Perineurial glia originate in the spinal cord and migrate out through MEPs to associate with the outgrowing axons as well. Neural crest cells differentiate into SCPs, then ISCs, and finally into mature Schwann cells that wrap axons. Perineurial glia ensheath on top of the Schwann cell-axon complexes and eventually differentiate to form the mature perineurium (Figure 1-3).

Peripheral Nerve Regeneration

Damage to the PNS often results in a debilitating loss of sensation and motor control. Although peripheral nerves can regenerate, recovery from severe injuries is often poor. Past and present regeneration research has focused primarily on the study of axons,

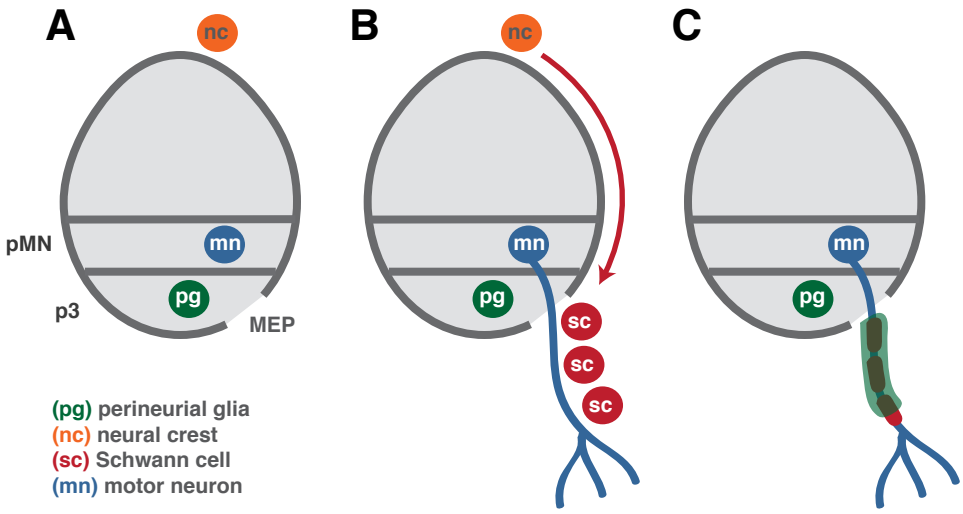

Figure 1-3: Zebrafish motor nerve development. (A) Motor neurons are specified in the pMN domain of the spinal cord. Perineurial glial precursors originate in the p3 domain. Neural crest cells arise from ectoderm dorsal to the neural tube. (B) Motor axons exit through motor exit points (MEPs). A subset of neural crest cells migrates ventrally and gives rise to Schwann cells that associate with the outgrowing motor axons. Perineurial glia exit the spinal cord and also associate with the axons. (C) Schwann cells wrap motor axons. Perineurial glia ensheath on top of the Schwann cells and axons and form the perineurium. mn, motor neuron; pg, perineurial glia; nc, neural crest; sc Schwann cell.

Schwann cells, and macrophages, with little emphasis put on the perineurium and other connective tissue sheaths. The goal of my work is to determine how perineurial glia respond to nerve injury and coordinate with other cell types during regeneration. This will ultimately help elucidate a more complete picture of the regenerative program. Nerve injuries vary widely in severity, and for simplicity, I will focus here primarily on the events that ensue following the most severe form of injury- complete transection or axotomy. This section will focus on what is known about PNS regeneration with regards to axons, Schwann cells, and macrophages, and will review the few studies describing changes occurring in the perineurium after injury.

i. Axon degeneration and regrowth

Peripheral nerve injuries that are severe enough to disrupt axon continuity induce a program of degeneration and regeneration within the neuron, whereby the distal axon degenerates, the cell body survives, and a new axon regrows. Transections divide a nerve or axon into a proximal and distal stump, with the proximal end being the portion that is still attached to the cell body, and the distal end being the portion that extends to targets. Elegant imaging studies along mouse sensory projections and the zebrafish PLLn have demonstrated that immediately following a transection, the axons closest to the injury site on both sides rapidly fragment and degenerate. This has been termed acute axonal degeneration (AAD) (Kerschensteiner et al., 2005; Villegas et al., 2012).

AAD is followed by Wallerian degeneration of the distal stump axons (Waller, 1850). Wallerian degeneration occurs in three distinct stages (Martin et al., 2010; Wang et al., 2012). The first is a latent period, where the axons have been severed but the distal

portion remains intact and is electrically excitable (Moldovan et al., 2008). The second is a fragmentation stage, where distal axons undergo a sudden and rapid fragmentation along their entire length (George et al., 1995; Rosenberg et al., 2012; Kerschensteiner et al., 2005; Martin et al., 2010). This stage is mediated in part by extracellular Ca^{2+} influx, which is necessary and sufficient to induce fragmentation (Wang et al., 2012). Importantly, fragmentation is an active process as opposed to a passive dying of the axon. This is evidenced by studies showing fragmentation can be delayed by expression of the gain-of-function protein Wallerian degeneration slow (Wlds) (Lunn et al., 1989; MacDonald et al., 2006; Adalbert et al., 2005; Martin et al., 2010). Although the mechanism of Wlds-mediated protection is still a subject of investigation, it is conserved across all model organisms tested thus far, and a recent study in *Drosophila* suggested Wlds may act to suppress injury induced Ca^{2+} elevation through effects on mitochondria (Avery et al., 2012). After fragmentation, the third and final stage of Wallerian degeneration is clearance, where phagocytes remove debris, clearing the way for new axon regrowth.

While the distal stump is degenerating, changes are also occurring on the proximal side of the injury. Within the neuron cell bodies, changes in gene expression act to downregulate constitutively active genes and upregulate regeneration genes associated with growth and survival. Near the injury site, the proximal ends of cut axons swell and forms endbulbs, which accumulate and secrete molecules that influence the local microenvironment. Sprouts containing new growth cones then arise from the proximal stump axons and regrow along the basal lamina of Schwann cells until targets are reached and re-innervated (Zochodne, 2012).

ii. The role of Schwann cells: changes in signaling and behavior

Schwann cells respond rapidly to nerve injury with a surprising level of plasticity. During this response, previously differentiated Schwann cells become activated and revert to a state reminiscent of ISCs. This accompanies dynamic changes in gene expression and behavior that are critical for the success of nerve regeneration. On the molecular level, axotomy induces Schwann cells to downregulate myelin genes and upregulate genes that support neuronal survival, axon regrowth, proliferation, and attraction of macrophages. Although similar to ISCs, the expression profile of these cells is distinctly different, suggesting that Schwann cells undergo a transdifferentiation to a new state that is dedicated to nerve repair (Arthur-Farraj et al., 2012). At the behavioral level, activated Schwann cells have several functions. Shortly after an injury, Schwann cells along the distal stump begin to degrade and phagocytize their own myelin (Perry et al., 1995; Stoll et al., 1989; Liu et al., 1995). These cells retain their basal lamina, proliferate, and organize into longitudinally oriented cellular columns called bands of Büngner, which serve as guidance tracts for axons re-growing through the distal stump. Along the proximal stump, Schwann cells become similarly activated and are intimately associated with new axon sprouts emerging from the proximal stump. In cases where there is a gap between the proximal and distal stump, axons and Schwann cell processes traverse the gap together, with Schwann cells slightly leading axons (McDonald et al., 2006). Later, Schwann cells differentiate again and remyelinate the new axons.

The signals governing Schwann cell activation and transdifferentiation are only beginning to be elucidated. Changes in expression appear to be driven in large part by the transcription factor c-Jun, and in nerves lacking c-Jun, Schwann cell transdifferentiation

is impaired and regeneration fails (Arthur-Farraj et al., 2012; Parkinson et al., 2008). Re-activation of Nrg1-Erbb signaling may also be important. Within minutes after sciatic nerve transection in rats, Erbb2 is phosphorylated, and blocking activation of Erbb2 inhibits Schwann cell demyelination and proliferation (Guertin et al., 2005; Kwon et al., 1997). Erbb2 and Erbb3 expression is also upregulated after injury (Carroll et al., 1997). As mentioned above, Erbb2/Erbb3 signaling is a potent activator of the ERK1/2 pathway (Birchmeier and Nave, 2008), and driving ERK1/2 signaling in Schwann cells of uninjured nerves induces demyelination and macrophage recruitment in a manner similar to what is seen after transection (Napoli et al., 2012). How Erbb2/Erbb3 signaling is activated after injury is not entirely clear. During development Erbb2/Erbb3 promotes differentiation and myelination, but after injury it appears to promote activation and demyelination. This could be due to differences in the source, concentration, or type of Nrg1 ligand that is available after injury. Although normally membrane tethered, Nrg1 type III can be cleaved to allow for paracrine signaling (Fleck et al., 2013). High doses of soluble Nrg1 type II and III induce ERK1/2 activation and c-Jun expression *in vitro* (Syed et al., 2010). Several studies have indicated that Nrg1 is upregulated in Schwann cells themselves during Wallerian degeneration, which could act through an autocrine mechanism to activate Erbb2/Erbb3 (Carroll et al., 1997). This non-axonal Nrg1 appears to be particularly important for remyelination (Stassart et al., 2012).

Although many questions remain regarding the molecular signals governing the Schwann cell injury response, it is clear they play an essential role in regeneration as a whole. Impairments in Schwann cell activation invariably lead to defects in axon regrowth. Additionally, activated Schwann cells secrete factors that contribute to the

breakdown of the BNB and the recruitment of macrophages after injury (Napoli et al., 2012). This places Schwann cells at the center of the coordinated cell-cell interactions that are critical to successful nerve regeneration.

iii. Inflammatory response: macrophage recruitment and debris clearance

Debris clearance is an essential component of PNS regeneration. The speed and efficiency with which this happens is likely a major reason why regeneration is more successful in the PNS than CNS (Vargas and Barres, 2007). In the PNS, nerve injury induces a breakdown of the BNB, which in turn allows the infiltration of immune cells such as macrophages. Macrophages are recruited to injured nerves by a wide variety of chemokines and cytokines thought to be released by Schwann cells, such as leukemia inhibitory factor (LIF) and monocyte chemoattractant protein-1 (MCP-1) (Tofaris et al., 2002; Leskovar et al., 2000; Toews et al., 1998). Once in the nerve, macrophages efficiently phagocytize myelin, axon, and other debris, clearing the way for new regrowth (Perry et al., 1987; Perry and Brown, 1992).

iv. Summary of peripheral nerve regeneration (axons, Schwann cells, and macrophages)

Vertebrate nerve regeneration has been studied intensely for over one hundred years. During that time, scientists have worked to develop a framework of regenerative events that occur following injury. Here, I will summarize the details presented above and present a simplified version of this framework with respect to axons, Schwann cells, and macrophages. In this model, transection divides the nerve into a proximal and distal stump, which quickly leads to AAD, where the axon ends closest to the injury site

fragment and slightly degenerate back. Schwann cells become activated and transdifferentiate into repair cells that are somewhat similar to ISCs. They demyelinate, phagocytize myelin debris, proliferate, and aid in the recruitment of macrophages and the stimulation of axon regrowth. Distal stump axons fragment and degenerate through Wallerian degeneration, and debris is cleared. Axon sprouts emerge from the proximal stump and are guided across the injury gap by Schwann cells. Schwann cells in the distal stump align into bands of Büngner, which provide a favorable environment for axon regrowth. Axons then re-innervate targets, Schwann cells remyelinate, and functional recovery is restored (Figure 1-4).

v. Changes in the perineurium

Notably, nerve sheath cells such as perineurial glia are absent from the paradigm presented above, owing to how little is known of their role. Whether or not regenerative events recapitulate developmental events is a subject of much debate. However, it stands to reason that because perineurial glia are essential for development, they may also play an important role in regeneration. Indeed, a few studies have described intriguing changes that occur in the perineurium after injury. Electron microscopy (EM) studies of divided mammalian sciatic nerves described that axons appeared to regrow through tracts that contained both Schwann cell and perineurial lamella, and that perineurial cells gradually surrounded the newly regenerated axon-Schwann cell complexes and bound them into many small mini-fascicles (Morris et al., 1972; Thomas and Jones, 1967). These observations are interesting in light of a recent study that showed cultured nerve fibroblasts, which were isolated from the perineurium, could induce Schwann cells to

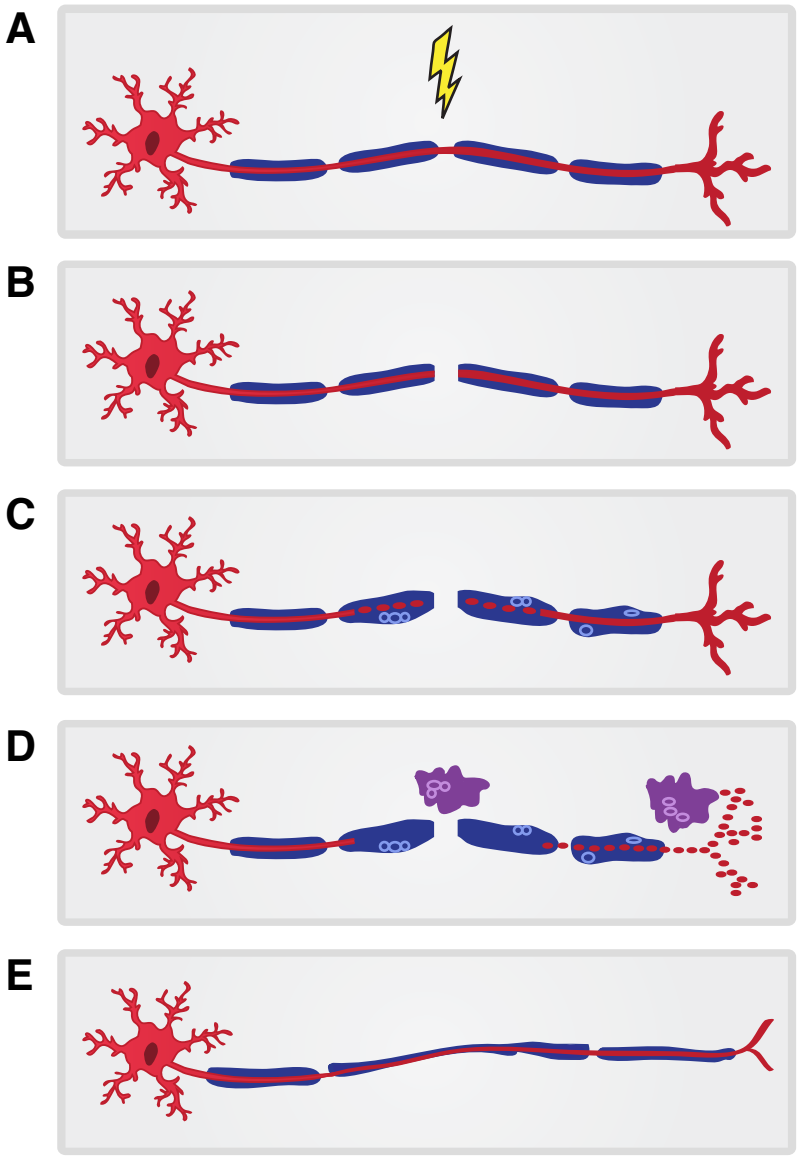

Figure 1-4: Peripheral nerve regeneration. (A) An intact myelinated peripheral neuron. Neuron and associated axon are red, myelinating Schwann cells are blue. (B) Transection divides the axon into a proximal and distal stump. (C) Axons near the injury site fragment and degenerate through AAD. Schwann cells become activated and phagocytic (light blue circles). (D) Distal axons fragment and degenerate through Wallerian degeneration. Macrophages (purple) are recruited and phagocytize debris (light purple circles). (E) New axon regrows along Schwann cell basal lamina.

organize into discrete cellular bands *in vitro*. This behavior was dependent on ephrin-B/EphB2 interactions between the fibroblasts and Schwann cells, and loss of this signaling *in vivo* resulted in impaired Schwann cell organization and misdirected axon regrowth (Parrinello et al., 2010). These studies suggest perineurial cells and Schwann cells are intimately associated during regeneration, and that interactions between these cells may be critical for their behavior.

The perineurium may also be involved in bridge formation. After a nerve transection, the divided stumps initially retract back due to elastin in the epineurial sheath, creating a gap. If the gap is small or stumps are rejoined by surgical anastomosis or conduits, a tissue bridge quickly forms between the stumps. The formation of this bridge precedes the ingrowth of axons and Schwann cells and serves as the first physical link between the proximal and distal stumps (McDonald and Zochodne, 2003; McDonald et al., 2006). An electron microscopy study by F. Scaravilli described that the earliest bridge was composed of fibrin, erythrocytes, and cells that were devoid of basal lamina and resembled fibroblasts. These fibroblast-like cells gradually acquired features of perineurial cells, developing a basal lamina, pinocytic vesicles, and elongated processes. Processes stretched longitudinally across the bridge and formed tight junctions with similar cells. Regenerating axons and Schwann cells grew between these flattened cells, which eventually surrounded them (Scaravilli, 1984). Others have reported similar findings (Hirasawa et al., 1994; Yamamoto et al., 2011). It has been suggested that the initial bridge cells are derived from the perineurium, although this has been difficult to ascertain by electron microscopy (Schroder et al., 1993; Scaravilli, 1984).

These studies are consistent with the hypothesis that the perineurium plays a significant role in regeneration, but there are still many questions. Regeneration is a dynamic process, and previous investigations of the perineurium have relied solely on fixed tissue specimens and *in vitro* cell culture. Currently, no study has provided a detailed description of perineurial cell behavior following injury in a live animal. Additionally, it is not known how perineurial cells coordinate with other cell types during regeneration, or whether they are essential for axon regrowth. In this dissertation, I address these knowledge gaps by coupling laser-mediated nerve transection with time-lapse imaging in live zebrafish. This work represents the first characterization of perineurial glial behavior after injury in a live animal and more fully elucidates the role of the perineurium in PNS regeneration.

The zebrafish (*Danio rerio*) and its use in nerve regeneration studies

In the work presented here, I use the zebrafish spinal motor nerve as a model to study the behavior of perineurial glia after nerve transection. Traditionally, vertebrate nerve regeneration has been predominantly studied in rodent systems. These studies have been vital to our understanding of ultrastructural changes that occur following injury. However, the lack of specific markers for the perineurium and the inability to visualize cellular behavior in the intact animal has impeded further study. Other model systems such as *Drosophila* and *C. elegans* have also provided valuable contributions to the regeneration field, but the peripheral glia in these models are somewhat different from those in vertebrates. By using zebrafish, I have been able to study vertebrate glia in an experimentally tractable system.

Zebrafish embryos develop externally and are optically transparent. This, coupled with the use of transgenes to fluorescently label cell populations, allows cell behavior to be visualized in in an intact living organism. This is powerful in nerve regeneration studies, where cells undergo rapid and dynamic changes. Indeed, zebrafish have recently gained traction as a model system for nerve regeneration, with several groups studying the dynamics of axon degeneration, macrophages, and Schwann cells (Martin et al., 2010; Villegas et al., 2012; Rosenberg et al., 2012; Rosenberg et al., 2014; Xiao et al., 2015; Ceci et al., 2014). As with development, nerve regeneration thus far appears to be markedly conserved between zebrafish and mammals.

In the following manuscript, I provide the first detailed description of perineurial glial behavior after nerve transection in a live animal. My data demonstrate that perineurial glia respond dynamically to nerve injury, coordinate with other cell types, and are essential for axon regrowth. In Chapter 3, I describe a novel assay that I developed to study glial behavior following nerve injury in zebrafish. In this assay, a MicroPoint laser ablation system is used to transect the spinal motor nerve in live, transgenic zebrafish, and the subsequent behavior of perineurial glia is visualized using time-lapse confocal microscopy. In Chapter 4, I use this assay to investigate the perineurial response to injury in depth. I show that perineurial glia respond rapidly and dynamically to motor nerve transection by phagocytizing debris and extending processes into the injury gap, eventually bridging it. Perineurial bridges form before Schwann cells or axons traverse the gap, and loss of bridging leads to impaired axon regrowth. Additionally, I show that perineurial glia respond to transections on adjacent unensheathed nerve tracts by extending membrane processes toward injury sites and phagocytizing debris. This

response is impaired in a mutant lacking Schwann cells, suggesting Schwann cells aid in the attraction of perineurial processes. In Chapter 5, I further investigate this relationship and show that the recruitment of perineurial processes by Schwann cells is dependent on Erbb signaling. Surprisingly, perineurial bridges formed even in the absence of Schwann cells, suggesting that perineurial glia are able to overcome the loss of a Schwann cell-derived attractive cue, and likely respond to signals from multiple cell types. The work presented here highlights perineurial glia as active and essential players in the regenerative process. This has led to a more complete understanding of how multiple cell types coordinate their actions to rebuild the nervous system and suggests these cells should be more carefully considered in future regeneration studies.

Chapter 2

Materials and Methods

Fish husbandry

All animal studies were approved by the University of Virginia Institutional Animal Care and Use Committee. Zebrafish strains used in this study included *Tg(nkx2.2a:megfp)*^{vu17} (Kirby et al., 2006; Kucenas et al., 2008), *Tg(olig2: dsred2)*^{vu19} (Kucenas et al., 2008), *Tg(mpeg1:EGFP)* (Ellett et al., 2011), *Tg(sox10:eos)* (Prendergast et al., 2012), *Tg(NBT:DsRed)* (Peri and Nüsslein-Volhard, 2008), *Tg(spi1:Gal4,UAS:EGFP)*^{zf149} (Peri and Nüsslein-Volhard, 2008), *Tg(mnx1:Mmu.Wlds-GFP)* (Rosenberg et al., 2012), *Tg(sox10(7.2):mrfp)*^{vu234} (Kucenas et al., 2008). Table 2-1 describes the expression and abbreviations of all transgenic lines. Mutant lines used in this study included *colourless*$^{m241-/-}$ (*sox10*$^{-/-}$) (Kelsh et al., 1996; Dutton et al., 2001), *erbb3b*$^{st48-/-}$ (Lyons et al., 2005), and *gpr126*$^{st49-/-}$ (Monk et al., 2009). Table 2-2 describes the abbreviations and lesions of mutant lines. Embryos were produced by pairwise matings, raised at 28.5 °C in egg water, staged according to hours or days post fertilization (hpf and dpf, respectively) and embryos of either sex were used for all experiments described below (Kimmel et al., 1995). Embryos used for immunohistochemistry and microscopy were treated with 0.003% phenylthiourea (PTU) in egg water to reduce pigmentation.

In vivo imaging

At 24 hpf, all embryos used for live imaging were manually dechorionated and transferred to egg water containing PTU to block pigment formation. At specified stages,

Table 2-1: Descriptions and abbreviations of transgenic lines

Transgene name	Abbreviation	Description of expression
Tg(nkx2.2a:megfp)^{vu17}	*nkx2.2a:gfp*	membrane EGFP in *nkx2.2a*$^{+}$ cells (perineurial glia, floorplate, OPCs)
Tg(olig2:dsred)^{vu19}	*olig2:dsred*	cytosolic DsRed in *olig2*$^{+}$ cells (motor neurons/axons, OPCs)
Tg(mpeg1:EGFP)	*mpeg1:gfp*	cytosolic EGFP in *mpeg1*$^{+}$ cells (macrophages)
Tg(sox10:Eos)	*sox10:eos*	cytosolic photoconvertable Eos in *sox10*$^{+}$ cells (Schwann cells)
Tg(NBT:DsRed)	*nbt:dsred*	cytosilic DsRed in *nbt*$^{+}$ cells(neurons/axons)
Tg(spi1:Gal4,UAS:EFP)^{zf149}	*spi1:gfp*	cytosolic EGFP in *spi1*$^{+}$ cells (Leukocytes, microglia)
Tg(mnx1:Mmu.Wlds-GFP)	*mnx1:wlds-gfp*	Wld^{s} and nuclear GFP in *mnx*$^{+}$ cells (motor neurons/axons)
Tg(sox10(7.2):mrfp)^{vu234}	*sox10:rfp*	membrane RFP in *sox10*+ cells (Schwann cells, OPCs)

All lines are stable, germline transgenics. Labeled cells listed are only those pertinant to this study.

Table 2-2: Mutant lines used in this study

Mutants Line	Abbreviation	Lesion	Effect
colourless$^{m241-/-}$	*cls*	unidentified lesion in *sox10*	disrupted *sox10* expression
erbb3b$^{st148-/-}$	*erbb3*	premature stop codon in *erbb3b*	truncates protein in the extracellular domain
gpr126$^{st149-/-}$	*gpr126*	premature stop codon in *gpr126*	truncates protein before the GPCR proteolytic site and 7 transmembrane domain

All lines are stable, germline mutantations.

embryos were anesthetized using 3-aminobenzoic acid ester (Tricaine), immersed in 0.8% low-melting point agarose and mounted on their sides in glass-bottomed 35 mm Petri dishes (Electron Microscopy Sciences). Images were captured using either 25x (NA 0.8) oil, 40x (NA 1.2) water, or 63x (NA 1.2) water immersion objectives mounted on a motorized Zeiss AxioObserver Z1 microscope equipped with a Quorum WaveFX-X1 spinning disc confocal system (Quorum Technologies Inc.). For time-lapse imaging, Z image stacks were collected every 5 min for 3-4 hours, and three-dimensional datasets were compiled using Sorenson 3 video compression (Sorenson Media) and exported to QuickTime (Apple) to create movies. Image adjustments were limited to contrast enhancement and level settings using MetaMorph software and ImageJ.

Nerve transection

Nerve transections were performed using the 'spinal motor axon and analysis of nerve glia' (SMAANG) technique as published and presented in Chapter 3 (Lewis and Kucenas, 2013; Binari et al., 2013). The MicroPoint (Andor Technology) was attached to a spinning disk confocal system (Quorum Technologies Inc.) consisting of a nitrogen-pumped dye laser (wavelength 435 nm) controlled by MetaMorph version 7.7. Ablation laser settings ranged from power 15 to 20 depending on the age of the larvae and nerve position. One to two motor nerves per larva in hemisegments 10–16 were transected in all experiments. To transect nerves, a thin elliptical ROI was drawn digitally in MetaMorph over the image of the nerve, and the nerve was laser pulsed precisely within the ROI until the nerve appeared transected, whereby fluorescence did not refill the ROI in >10 s. Successful transections with this protocol were independently confirmed by identifying

the presence of axonal degeneration in transgenic lines that label motor axons. *In vivo* imaging of transected nerves was performed as described above. For multi-day experiments, larvae were demounted immediately after injury, allowed to recover in PTU and remounted for imaging at 24 and/or 48 hours post injury.

Immunohistochemistry

Whole-mount

Larvae were fixed in AB Fix (4% paraformaldehyde, 0.1% TritonX-100, 1x PBS) for 3 hours at 23 °C, followed by a 5 minute wash with PBSTx (1% TritonX-100, 1x PBS), a 5 minute wash with DWTx (1% TritonX-100 in distilled water), a 5 minute wash with acetone at 23 °C and a 10 minute wash with acetone at -20 °C. Larvae were pre-blocked in 5% goat serum/PBSTx for 1 hour, then incubated in primary antibody for 1 hour at 23 °C and overnight at 4 °C. Larvae were washed extensively with 1x PBSTx and incubated in secondary antibody for 1 hour at 23 °C and overnight at 4 °C. Larvae were washed extensively with 1x PBSTx and stored in 50% glycerol/PBS at 4 °C until imaging. Larvae were mounted on their sides in 0.8% low-melting point agarose on glass-bottomed 35 mm Petri dishes and imaged using the confocal microscope described above. Image adjustments were limited to contrast enhancement and level settings using MetaMorph software and ImageJ.

Sections

20 dpf juveniles were fixed in AB Fix (4% paraformaldehyde, 8% sucrose, 1xPBS) for 4 hours at 23°C and 4°C overnight. >3 month adults were fixed in AB Fix for 3 days at

23°C and 4°C overnight. The anterior and posterior ends of juveniles and adults were removed, such that only an approximately 0.5 cm region of the trunk remained. Trunks were and embedded in 1.5% agar/30% sucrose. Agar blocks were frozen in 2-methylbutane chilled by immersion in liquid nitrogen. Coronal sections (20µm for juveniles, 50µm for adults) were collected using a cryostat microtome. Sections were rehydrated in 1x PBS for 60 min at 23°C and preblocked in 2% goat serum/BSA/1x PBS for 30 min. Sections were incubated in primary antibody overnight at 4°C. Sections were washed extensively with 1x PBS, incubated for 3 h at 23°C with secondary antibodies, and washed with 1x PBS for 30 min. Sections were mounted in Vectashield (Vector Laboratories) and imaged using the confocal microscope described above. Image adjustments were limited to contrast enhancement and level settings using MetaMorph software and ImageJ.

Antibodies

The primary antibodies used were mouse anti-acetylated tubulin (1:5,000, Sigma), rabbit anti-Sox10 (1:5000) (Binari et al., 2013), mouse anti-ZO-1 (zona occludins 1; 1:200, Invitrogen) and rabbit anti-MBP (myelin basic protein; 1:250) (Kucenas et al., 2009). Secondary antibodies used were Alexa Fluor 488 goat anti-rabbit, Alexa Fluor 568 goat anti-rabbit, or Alexa Fluor 568 goat anti-mouse, Alexa Fluor 647 goat anti-rabbit and Alexa Fluor 647 goat anti-mouse (Invitrogen).

LysoTracker staining

To label organelles with low pH, 4 day post fertilization (dpf) larvae were immersed in 20 μM LysoTracker Red DND-99 (Molecular Probes)/2% DMSO or 10 μM LysoTracker Deep Red (Molecular Probes)/1% DMSO in egg water for 2 hours at 23 °C. Larvae were then rinsed once with egg water and immediately mounted for imaging.

DAPT treatment

Stock solutions for DAPT (565784; N-[(3,5- difluorophenyl)acetyl]-L-alanyl-2-phenylglycine-1,1-dimethylethyl ester; EMD Chemicals) were made in DMSO and used at 100 μM as previously described (Binari et al., 2013). DAPT was diluted in PTU egg water plus DMSO to a final concentration of 1% DMSO and mixed by vortexing. Larvae were placed in 3 ml of PTU egg water containing DAPT in 35 mm Petri dishes from 48-72 hpf. Larvae were then washed in PTU egg water and moved to fresh PTU until 6 dpf for experiments. Control larvae were placed in 3 ml of PTU egg water containing 1% DMSO alone from 48-72 hpf, washed in PTU egg water, then moved to fresh PTU until 6 dpf for experiments.

AG1478 treatment

A 10mM InSolution^{TM} stock of AG1478 (CAS 175178-82-2) was received from Calbiochem and diluted in PTU egg water plus DMSO to a final concentration of to 6μM AG1478 and 1% DMSO. Larvae were placed in 3 ml of PTU egg water containing AG1478 or DMSO control in 35 mm Petri dishes beginning at 84 hpf. At approximately 96 hpf larvae were anesthetized by adding Tricane directly to conditioned PTU egg water

and mounted for live-imaging as described above. Mounted larvae were covered in AG1478 or DMSO control containing anesthetic and transection and imaging were performed as described above.

Transmission electron microscopy

Larvae were prepared for electron microscopy using microwave fixation (Panasonic Model #NNSD967S) and were kept on ice at approximately 15 °C throughout all microwave steps to prevent sample heating. 6 dpf larvae were euthanized with Tricaine and fixed in 2% glutaraldehyde/4% paraformaldehyde in 0.1 M PB. Samples were pulsed in the microwave then kept in fixative for 2 hours at 23 °C. Samples were washed in 0.1M PB for 30 min, transferred to 1% OsO4 in 0.1M PB, pulsed in the microwave then left for 1 hour at 23 °C. Samples were washed in 0.1M PB for 30 min, followed by 5 minute rinses in 50% and 70% EtOH. Preparations were stained en bloc with 4% uranyl acetate in 70% EtOH and pulsed in the microwave. Samples were then subjected to ethanol dehydration and pulsed in the microwave after each change in solution: 70% ethanol, 95% ethanol and 100% ethanol twice. Preparations were transferred to 100% acetone, pulsed in the microwave, changed to new 100% acetone and pulsed in the microwave again. Samples were put in a 1:1 acetone/EMBED mix and left overnight at 23 °C, then changed to 100% EMBED and left uncapped for 6 hours to allow evaporation of any remaining acetone. Finally, samples were placed into fresh EMBED and left to cure overnight in a 60 °C oven. Ultra-thin sections (70 nm) were obtained on a Leica UCT ultramicrotome, transferred to copper grids and counterstained with uranyl acetate.

Sections were visualized on a JEOL 1010 Transmission electron microscope and imaged with a 16 M pixel SIA-12C camera (Scientific Instruments and Applications).

Morpholino injections

The *spi1b* translation blocking morpholino oligonucleotide (MO) (5'-GATATACTGATACTCCATTGGTGGT-3') (Rhodes et al., 2005; Villegas et al., 2012) was purchased from Gene Tools. The MO was dissolved in water to create a stock solution of 2 mM and diluted in water and Phenol red to create a working injection concentration of 0.5 mM. We injected 2–4 nl into the yolk just below the single-cell of fertilized embryos. All MO-injected embryos were raised in PTU embryo medium at 28.5 °C.

Data quantification and statistical analysis

All graphically presented data represent the mean of the analyzed data. Statistical analyses and graphing were performed with GraphPad Prism software. Level of significance was determined by using an unpaired t test using a confidence interval of 95%. For Figure 4-5E, I ran a Z test to compare two proportions using independent samples, and compared the proportion of nerves exhibiting "no regrowth" between each group. I again used a confidence interval of 95% to determine significance. For Figure 5-4B, the number of nerves per fish with *nkx2.2a*$^{+}$ cells of each morphology were counted by eye under wide-field microscopy and compared between wild type and *erbb3* mutants. For Figure 5-7D, nerve roots of stained larvae were imaged by confocal microscopy with a 63x objective. The number of *sox10*$^{+}$ nuclei in each image were subsequently counted, followed by graphing and t test analysis as described above.

Chapter 3

Motor nerve transection and time-lapse imaging of glial behaviors in live zebrafish

Published as a video article in the Journal of Visualized Experiments (JOVE) 6/20/2013

Accessible at http://www.jove.com/video/50621/

Abstract

The nervous system is often described as a hard-wired component of the body even though it is a considerably fluid organ system that reacts to external stimuli in a consistent, stereotyped manner, while maintaining incredible flexibility and plasticity. Unlike the CNS, the PNS is capable of significant repair, but we have only just begun to understand the cellular and molecular mechanisms that govern this phenomenon. Using zebrafish as a model system, we have the unprecedented opportunity to couple regenerative studies with *in vivo* imaging and genetic manipulation. Peripheral nerves are composed of axons surrounded by layers of glia and connective tissue. Axons are ensheathed by myelinating or non-myelintaing Schwann cells, which are in turn wrapped into a fascicle by a cellular sheath called the perineurium. Following an injury, adult peripheral nerves have the remarkable capacity to remove damaged axonal debris and re-innervate targets. To investigate the roles of all peripheral glia in PNS regeneration, we describe here an axon transection assay that uses a commercially available MicroPoint laser (nitrogen-pumped dye laser- 435nm wavelength, Andor Technology) to axotomize motor nerves in live transgenic zebrafish. We further describe the methods to couple these experiments to time-lapse imaging of injured and control nerves. This experimental paradigm can be used to not only assess the role that glia play in nerve regeneration, but

can also be the platform for elucidating the molecular mechanisms that govern nervous system repair.

Introduction

Zebrafish have been used extensively to study development of the nervous system because of their optical transparence and ease of transgenesis, which when coupled, allows for spectacular imaging of dynamic cell behaviors in a living embryo. Additionally, because zebrafish and mammals share nearly all of the genes required for nervous system formation, cellular and molecular information collected in this model organism is directly relatable to other vertebrate species. Although incredibly powerful for neurodevelopmental studies, the zebrafish and its unique attributes have the potential to also elucidate the mechanisms that maintain and rebuild the nervous system after injury. Zebrafish larvae maintain their translucence into late larval stages and pigmentation can be effectively blocked with either the use of pharmacological inhibitors of melanin production or genetic mutants that lack pigment cells. Thus, using this model organism to study injury and regeneration in older animals is possible and offers the unique opportunity to directly investigate the cellular and molecular mechanisms that rebuild the nervous system. In this manuscript, we describe how to efficiently and reproducibly injure nerves in the PNS of zebrafish larvae. This injury paradigm lends itself to studying not only degeneration, but also the responses of peripheral glia and immune cells as well as the interactions between these populations during regeneration.

The PNS is a complex network of motor and sensory nerves that is necessary to pass information between the CNS and the skin, organs and muscle of the body, allowing

an organism to interact with its environment and survive. Along these nerves, peripheral glia, including myelinating and non-myelinating Schwann cells and perineurial glia, as well as connective tissue, encase the axons and ultimately form the mature nerve. Injury of these nerves initiates a process known as Wallerian degeneration (Waller, 1849). This mechanism of axonal fragmentation, immune recruitment, debris clearance and regeneration is very stereotyped and genetically regulated (Geuna et al., 2009). Previous studies in mammalian systems have described the roles of Schwann cells during nerve degeneration and regeneration (Stoll and Muller, 1999; Hirata and Kawabuchi, 2002; Geuna et al., 2009; Parrinello et al., 2010). In these studies of fixed tissue or cell culture, Schwann cells not only recruited macrophages to the injury site to aid in debris clearance, but also aided in myelin phagocytosis themselves. While these studies have been incredibly informative, we have never before visualized in real time, glial responses to peripheral axon injury in vivo, and no other studies have investigated the relationship between the different classes of peripheral glia during these events.

Recently, two labs have investigated Wallerian degeneration using zebrafish and laser mediated axon injury similar to what we describe here (O'Brien et al., 2009; Martin et al., 2010; Rosenberg et al., 2012; Villegas et al., 2012). In some of these studies, superficial sensory axons were axotomized in young larvae using a custom built, two-photon confocal microscope (O'Brien et al., 2009; Martin et al., 2010; Villegas et al., 2012). In another study, which is very similar to our own, deeper axons within the ventral motor nerve were transected in 5 day old larvae using a commercially available laser ablation system (Rosenberg et al., 2012). In both of these experimental set ups, the focus was on Wallerian degeneration and both axons and immune cells were imaged. To

expand on these studies, we describe injuring motor axons in older larvae with mature, myelinated nerves and assay the response of all nerve-associated peripheral glia during degeneration and regeneration.

To do this, we transect motor nerves in 6 and 7 day post fertilization (dpf) larvae and visualize the responses of individual glial populations as well as investigate the interactions between these populations along injured axons. Using double and triple transgenic lines that label peripheral glia, including Schwann cells and perineurial glia, as well as a marker for axons, we use a commercially available laser ablation system (MicroPoint, Andor Technology) consisting of a nitrogen-pumped dye laser (wavelength 435 nm) controlled by MetaMorph version 7.7 attached to a Quorum WaveFX-X1 spinning disc confocal system (Quorum Technologies) to create axon transections. This experimental set-up allows us to visualize live, larval zebrafish, injure specific peripheral motor axon tracts and time-lapse image the responses of distinct glial populations to axon injury and their relationship to one another. This protocol can be further adapted to create nerve injuries in zebrafish of different ages, with different transgenic lines or genetic mutants to address different scientific questions.

Protocol

1) Preparation and mounting of zebrafish embryos for ablation and live imaging

1.1) Prepare a stock of 0.8% low melt agarose in egg water. Aliquot into 13X100mm disposable culture tubes and store at 4 °C until needed.

1.2) Select adult zebrafish containing stably integrated transgenes to fluorescently label motor neurons and glial cell types of interest. Cross adult zebrafish to obtain embryos.

1.3) Collect zebrafish embryos in egg water and place in 28.5 °C incubator for correct staging later (Kimmel et al., 1995). At approximately 24 hours post fertilization (hpf), remove egg water and add 0.002% 1-phenyl 2-thiourea (PTU) in egg water. Return embryos to the incubator.

1.4) Between 24 and 96 hpf, embryos should be screened for the presence of desired transgenes on a fluorescent dissecting scope. Place selected embryos in fresh PTU egg water and return to the incubator.

1.5) When larvae have reached 6 days post fertilization (dpf) (or your desired age), remove them from the incubator, select a few larvae for mounting, and transfer them to a smaller dish. Remove the water and immediately replace with approximately 0.02% Tricane in PTU egg water. Allow larvae to sit in anesthetic approximately 5 minutes before mounting.

1.6) Prepare agarose for mounting. Obtain an aliquot of 0.8% low melt agarose from the refrigerator and place in a 250ml beaker filled with 50ml of tap water. Microwave for 30 seconds, or until the agarose is melted. Add some cold tap water to the beaker until the beaker water is no longer hot, but warm (the end goal being a beaker of warm water, with

a culture tube of melted agarose in it). Do not continue on to the next step however, until the agarose in the culture tube feels warm to the touch (not hot).

1.7) Mount larvae for injury/imaging. Select an anesthetized larva and transfer it to a single or multi-well 35mm glass bottom dish. Remove any water that was transferred with the larva, then immediately cover the larva with warm agarose. Add enough agarose to fill the glass-bottomed portion of the dish without creating a large dome. As the agarose hardens, use a dissecting needle to position the larva on its side at the bottom of the dish, then tilt the larva just slightly on its back. It is imperative for injury and subsequent imaging, that the mounted larva be touching the glass on the bottom of the dish. Use the dissecting needle to maintain the larva in this position until the agarose is solidified and the larva is immobilized (Figure 3-1A-C).

1.8) Once the agarose is fully hardened, slowly pipet enough Tricane water (this can be the same Tricane used for anesthesia) into the dish to completely cover the agarose and larva.

2) MicroPoint laser calibration and testing

2.1) Turn on all confocal microscope instrumentation, appropriate diode lasers for exciting zebrafish transgenes, and MicroPoint laser. Be sure the beamsplitter labeled "7240 blank" is in place, the laser attenuator is fully open, and the 435nm Coumarin dye cell is in place. On the computer, open MetaMorph software.

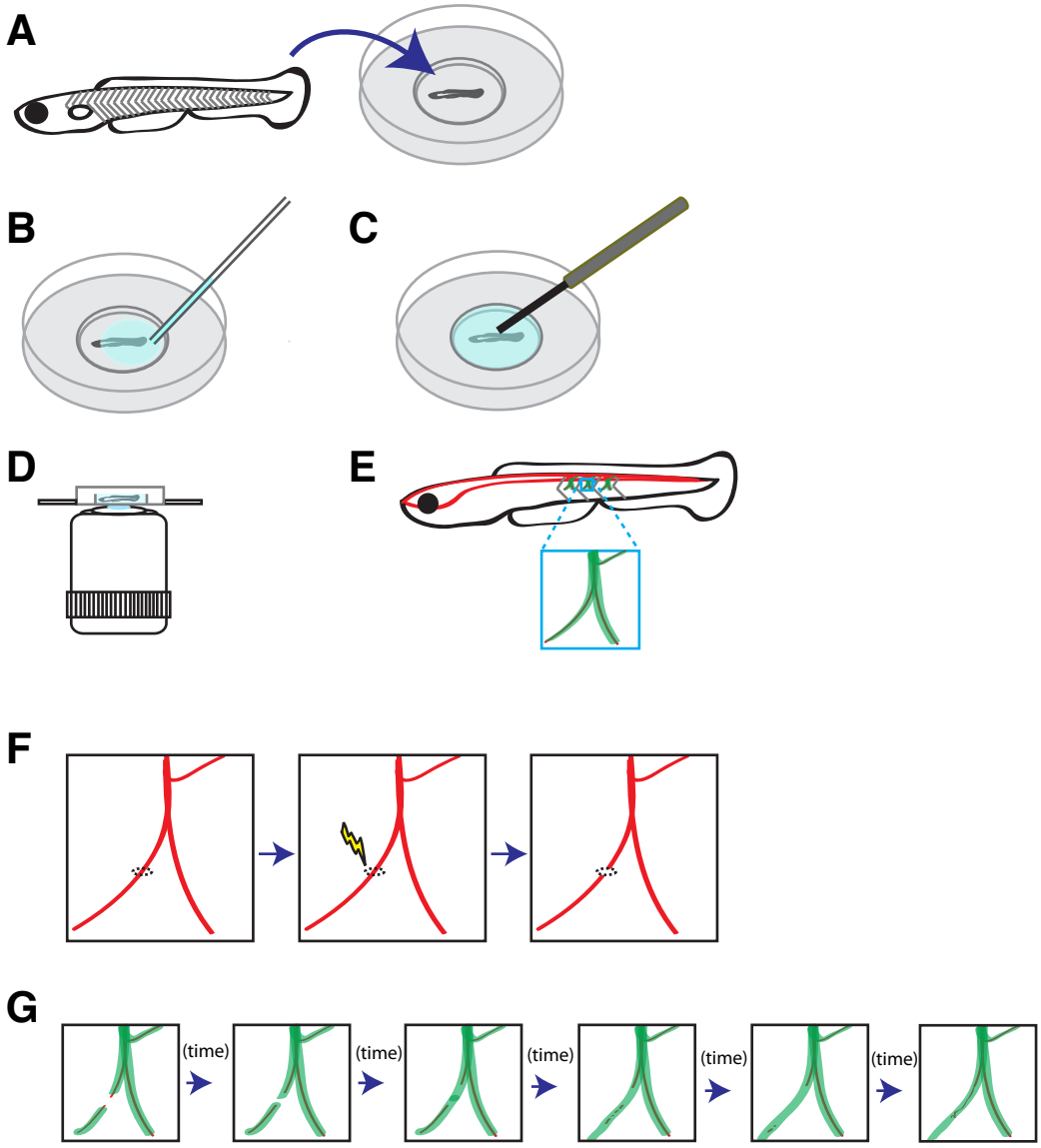

Figure 3-1: Motor nerve transection and time-lapse imaging of zebrafish larvae. Schematic illustrating a summary of the assay procedure. (A) Place anesthitized larva in a glass bottom dish. (B) Add 0.8% low-melt agarose. (C) Position the larva against the glass with a dissecting needle. (D) Place dish on confocal microscope. (E) Select a nerve and collect an image pre-abaltion. (F) Select a thin eliptical ROI along the rostral nerve and ablate to create a transection. (G) Collect time-lapse images of the axons and glial cells.

2.2) Move the 63x 1.2NA water immersion objective into position and apply a small drop of Immersol W 2010 onto the objective. Obtain a glass slide with one mirrored side to use for calibration of the MicroPoint laser. Place the slide, mirror side down, onto the microscope stage.

2.3) Using the eyepiece under brightfield illumination, find and focus on a scratch or etch in the mirror. The brightfield light will be shining down onto the glass slide, but will only pass through to the objective in places where the mirror has been scratched or etched away. This will cause the mirror to look black through the eyepiece, and the etchings to look like spots or lines of light.

2.4) Using the knob under the eyepiece, manually close the light path to the oculars. On the computer, switch to the confocal port to view and focus the etchings on the computer screen. Click “Targeted Illumination” to open the MicroPoint Targeted Illumination window that controls the MicroPoint laser calibration and power settings, and select the “configuration” tab. In the “intensity” box, set the number of pulses to “1” and the attenuation plate to “3” % transmission. Be sure the “coordinate system setting” drop-down box is set to the 63x 1.2NA water immersion objective.

2.5) Select the ellipse tool from the main toolbar, and click the image on the computer screen to create a single circular ROI. Do this 3 more times until there are 4 circular ROIs spaced randomly over the image. Click “frap” to fire the laser. This will create 4 small spot etchings, 1 within each circular ROI. If the laser does not fire, check to be sure the

MicroPoint is turned on and connected properly, and that the light path to the oculars is closed. If no etching is seen, check to be sure the “7240 blank “ beamsplitter is in place. If everything is in place, increase the laser power and “frap” until the etchings are visible. If a laser power setting greater than 10 is necessary to etch the glass, this may indicate the laser plasma cartridge needs to be replaced.

2.6) If the etched spots appear centered within the selected ROIs, no calibration is necessary (proceed to 2.8). If the spots are not centered, the calibration setting needs to be updated.

2.7) To calibrate, in the MicroPoint Targeted Illumination window, check the boxes by “manually click on calibration points” and “display images during calibration” and set the “range for calibration point” to “30”, then click “update setting”. The laser will fire and an image will appear along with a dialogue box with an option to cancel the calibration. The image should contain a single etched point. If the point does not appear, cancel the calibration, increase the laser power, and start the calibration again. If the point appears, click in the center of the spot. The laser will fire again, and another point will appear. Click that point, and repeat this process until the calibration is complete and 9 spots appear in a grid fashion. Repeat step 2.5 to check that the calibration was successful.

2.8) Remove the glass slide from the microscope stage and clean the objective. Open the light path to the oculars, and replace the beamsplitter labeled “7240 blank” replace with “7247 100%ILL”.

3) Nerve transection using MicroPoint laser ablation and time-lapse confocal imaging of glial cell behaviors

3.1) Remove the stage used to hold the glass slide and replace with a stage suitable for holding 35mm glass bottomed dishes. Continue to use the 63x 1.2NA water immersion objective.

3.2) Apply a small drop of Immersol W 2010 to the objective, and place the dish with mounted larva on the stage. Stabilize the dish with clips (Figure 3-1D).

3.3) Using the eyepiece and widefield illumination, focus the larva and locate the motor nerves. Scan the nerves in hemisegments 10-20 and select a motor nerve for transection.

3.4) Switch to the confocal port to live-view the nerve on the computer screen. Select Z planes to image and acquire an image of the uninjured nerve (Figure 3-1E).

3.5) Setup the time-lapse. It is best to create all necessary settings for the time-lapse before performing the ablation, so there is no delay in starting the time-lapse once the injury is complete. Settings should be in place to capture Z projections of all transgenes in 5-30 minute intervals, depending on the experiment.

3.6) Remove beamsplitter “7247 100%ILL” and replace with “7240 blank”. Close the light path to the oculars.

3.7) Return to the live-view of the nerve. Use the appropriate fluorescent channel to view the axon that will be transected.

3.8) Using the ellipse tool, create a thin elliptical ROI in the area to be ablated, then click "CreateROIsForLaserApp2" to create smaller ROIs within the selected region.

3.9) Adjust the laser power and ablate. In the "MicroPoint Targeted Illumination" window set the number of pulses to "2" and the attenuation plate to "20" % transmission. Click "frap" to fire the laser within the selected ROIs. If fluorescence remains within the ROIs, increase the attenuation plate transmission (laser power), wait approximately 10 seconds, and click "frap" again. Do this until you reach a setting that causes fluorescence to disappear within the ROIs. Wait 10 or more seconds and check the ablated area again for fluorescence. Beware that an ROI may initially appear ablated, when it is actually photobleached. If fluorescence returns, increase the laser power and click "frap" again. Repeat until florescence disappears within the ROIs and does not return within 10 seconds. It is best to start with a lesser laser power and increase to the necessary power. The necessary laser power may vary based on individual microscopy systems, age of Coumarin dye, specimen mounting, age of larvae, and thickness of the tissue. Once an ideal laser power has been established, this power setting may be used again on subsequent nerves in the same experiment (Figure 3-1F).

3.10) Begin the time-lapse. Once the ablation is completed, click "acquire" to begin time-lapse imaging (Figure 3-1G).

3.11) Analyze the data. When imaging is complete, use Metamorph software to compile data and create color composite Z projections for each time point. Create a QuickTime movie to analyze the behavior of axons and glial cells simultaneously**.**

Representative Results:

The assay described here can be used to assess the response of glial cells and other nerve-associated cell populations to axonal injury in vivo. Movie 3-1 (accessible at http://www.jove.com/video/50621/) shows an example of a nerve injury created using this method and the response of surrounding glial cells. This experiment was performed in *Tg(nkx2.2a:megfp);Tg(olig2:dsred)* zebrafish, in which perineurial glia express a membrane targeted EGFP and motor neurons express cytosolic DsRed. The injury was made along the rostral projection of a trunk motor nerve in a 6 dpf live zebrafish, and the nerve was subsequently time-lapse imaged in both the EGFP and DsRed channels. This allowed simultaneous visualization of axon and glial cell behaviors immediately following the injury.

Figure 3-2 shows still images of static time-points taken from Movie 3-1. The dotted ellipse shows the ROI that was ablated using the MicroPoint Laser. One minute post transection (mpt), the ablated area lacked fluorescence and the injury zone measured approximately 3.5 μm from the proximal to distal stump. The success of a transection can be confirmed by imaging the distal nerve stump and looking for signs of Wallerian degeneration, including distal axon fragmentation and rapid clearance. The absence of axonal fluorescence along the distal stump in Figure 3-2 at 2 hours post transection (hpt)

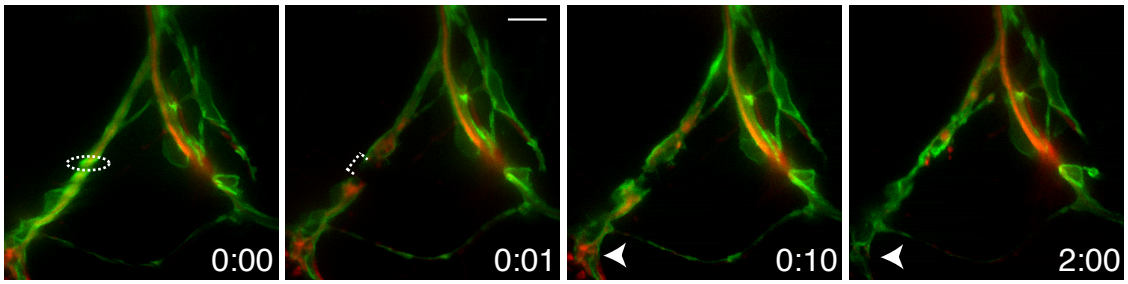

Figure 3-2: Motor nerve transection and still images of glial cell behavior. Panels are still images taken from Movie 3-1 (accessible at http://www.jove.com/video/50621/). The dotted elliptical area represents the ROI that was ablated, creating a transection injury denoted by the dotted line. Arrow-heads point to axonal fluorescence that is present at 10 mpt, but not at 2 hpt, indicating the distal axons degenerated. Scale bar 10μm.

indicates these axons have indeed undergone Wallerian degeneration and the transection was successful.

Adjusting the laser power to an ideal setting is critical when performing MicroPoint laser ablation experiments. Ideal laser power settings will cleanly ablate the nerve only within the selected ROI, and laser power settings that are either too low or too high will yield suboptimal results. Figure 3-3A shows an injury that was performed with a laser power that was too low. Fluorescence remained within the ROI after firing the laser, resulting in an incomplete transection. Figure 3-3B shows an injury that was performed with a laser power that was too high, resulting in an extremely large ablation.

Discussion:

The most critical steps of this experimental design are: 1) properly mounting larvae for injury and subsequent *in vivo* imaging and 2) focusing the MicroPoint laser and selecting the correct power settings in order to create a clean nerve transection that results in minimal extra-tissue damage. To help ensure a successful axotomy for *in vivo* imaging and subsequent analysis, mount multiple larvae in either individual glass bottom dishes or in a glass bottom dish with dividers. After focusing the laser, we recommend testing different power settings on a test larva to identify the optimal parameters for nerve transection. These settings are usually fairly consistent between experiments, but can change if: 1) larvae are not mounted properly, 2) larvae of different ages are used, 3) the laser isn't focused correctly or 4) the laser needs maintenance. An optimal nerve transection will create an injury along a nerve that is between 2 and 5 μm and doesn't disturb neighboring tissue.

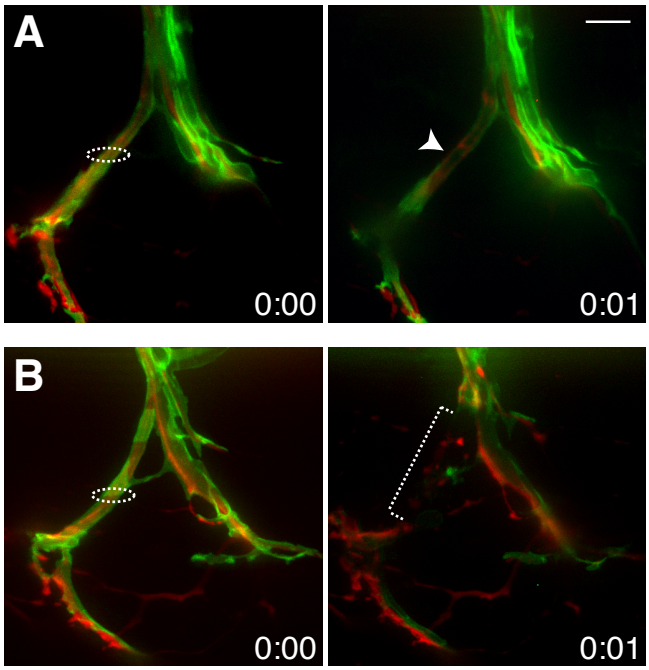

Figure 3-3: Suboptimal laser power settings leads to undesired results. (A) An attempted ablation performed with a laser power that is too low. The dotted ellipse denotes the selected ROI. 1 mpt the area has been slightly photobleached and not transected (arrowhead). (B) An ablation performed with a laser power that is too high. The dotted ellipse denoted the selected ROI. 1 mpt the ablated area is much larger than the selected ROI (dotted line). All images are taken from live 6 dpf *Tg(nkx2.2a:megfp);Tg(olig2:dsred)* zebrafish larvae with anterior to the left and dorsal to the top. Scale bar 10 µm.

When analyzing the response of any cell type to nervous system injury, we suggest conducting at least 2 types of controls. The first is selecting an area to injure that is immediately next to the nerve of interest, but is not touching any nerve tissue. This will allow you to determine if the cellular responses you see are due to damage in general, or to injury of axons. The second control is to image a nerve in the same fish that you have created a nerve injury. This type of control eliminates larva-to-larva variability due to staging and imaging parameters including confocal exposure times for imaging, etc.

In this protocol we also describe scenarios that create injuries that are too small or too large for our particular studies. Depending on the experimental question, these types of injuries can be used for analysis. The main limitations to this type of procedure would be the objectives available for creating the injury and subsequent time-lapse imaging. The older the larva you use, the longer working distance objective required.

The protocol we describe here allows the user to create focal nerve transections along deep nerves in mature larvae. We couple this technology to *in vivo*, time-lapse imaging and use a commercially available laser ablation system that reproducibly creates injuries each time used. This technology can be altered to use different transgenic lines or mutant larvae to test different hypotheses about the mechanisms that rebuild the nervous system after injury.

Chapter 4

Perineurial glia are essential for motor axon regrowth following nerve injury

Published in The Journal of Neuroscience September 17, 2014 34(38) 12762-12777

Article and supplemental movies accessible at

http://www.jneurosci.org/content/34/38/12762.long

Abstract

Development and maintenance of the peripheral nervous system (PNS) is essential for an organism to survive and reproduce, and damage to the PNS by disease or injury is often debilitating. Remarkably, the nerves of the PNS are capable of regenerating following trauma. However, full functional recovery after nerve injuries remains poor. Peripheral nerve regeneration has been studied extensively, with particular emphasis on elucidating the roles of Schwann cells and macrophages during degeneration and subsequent regeneration. In contrast, the roles of other essential nerve components, including perineurial glia, are poorly understood. Here, we utilize laser nerve transection and *in vivo* time-lapse imaging in zebrafish to investigate the role and requirement of perineurial glia following nerve injury. We show that perineurial glia respond rapidly and dynamically to nerve transections by extending processes into injury sites and phagocytizing debris. Perineurial glia also bridge injury gaps before Schwann cells and axons, and we demonstrate that these bridges are essential for axon regrowth. Additionally, we show that perineurial glia and macrophages spatially coordinate early debris clearance, and that perineurial glia require Schwann cells for their attraction to

injury sites. This work highlights the complex nature of cell-cell interactions following injury and introduces perineurial glia as integral players in the regenerative process.

Introduction

In all vertebrate peripheral nerves, axon-Schwann cell complexes are bundled into fascicles by the perineurium (Figure 4-1A). The mature perineurium is a cellular sheath formed by concentrically arranged layers of flattened, interdigitated perineurial cells that originate in the CNS as glia (Akert et al., 1976; Schmidt et al., 1997; Kucenas et al., 2008; Clark et al., 2014). These cells function to protect the nerve and regulate the transport of material between the interior and exterior of the fascicle (Akert et al., 1976; Bourne, 1968; Burkel, 1967; Kristensson and Olsson, 1971). Previously, we showed that perineurial glia play an essential role in nerve development (Binari et al., 2013; Kucenas et al., 2008; Clark et al., 2014). However, how they respond to nerve injury and participate in regeneration is poorly understood.

Immediately following a nerve transection, proximal and distal stump axons begin to fragment and degenerate back from the injury site in a process called acute axonal degeneration (AAD) (Kerschensteiner et al., 2005). Distal stump axons then begin Wallerian degeneration, which is characterized by a latent period followed by distal axon fragmentation (Waller, 1850; George et al., 1995; Villegas et al., 2012). During these degenerative processes, Schwann cells rapidly transdifferentiate, phagocytize their own myelin and recruit macrophages to clear debris (Perry et al., 1995; Arthur-Farraj et al., 2012). As regeneration begins, a tissue bridge forms to connect the proximal and distal stumps. Schwann cells then infiltrate this bridge, organize into cellular columns and help

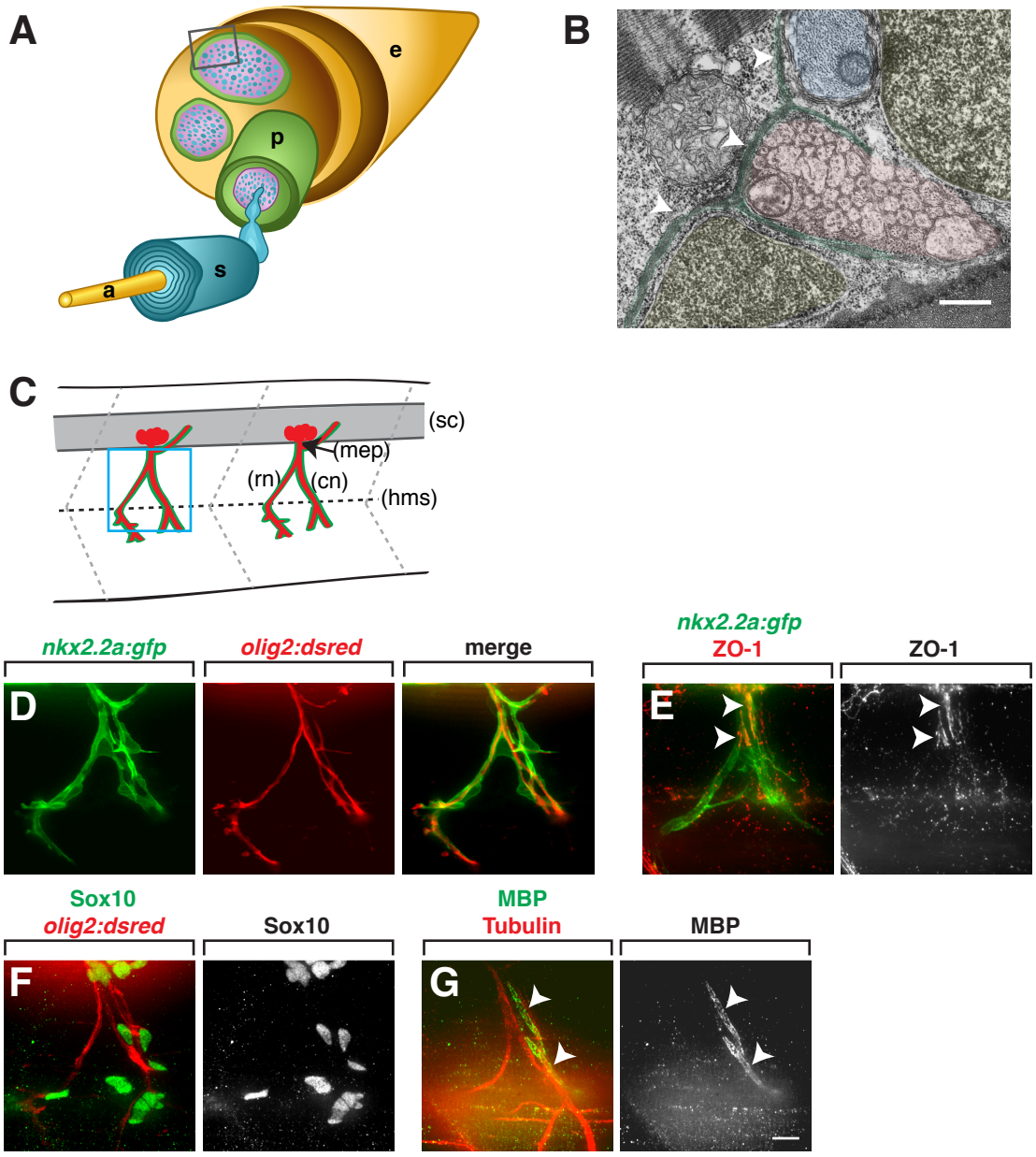

Figure 4-1: Anatomy of the 6 dpf zebrafish spinal motor nerve root. (A) Diagrammatic representation of a cross section through an adult peripheral nerve shows axons (a) are wrapped by Schwann cells (s), and bundled into a fascicle by the perineurium (p). Several fascicles are encased by the epineurium (e). Gray box denotes approximate area represented in B. (B) Transmission electron micrograph of a transverse section through the spinal motor nerve root of a wild-type 6 dpf larva. Yellow shading denotes Schwann cell nuclei, pink denotes a bundle of unmyelinated axons and blue denotes a myelinated axon. Arrowheads point to a single layer of perineurium, which is shaded green. (C) Diagrammatic representation of a 6 dpf larvae with dorsal to the top and anterior to the left. Blue box denotes the imaging field used throughout experiments. (sc) spinal cord, (hms) horizontal myoseptum, (mep) motor exit point, (rn) rostral nerve, (cn) caudal nerve. (D) In a 6 dpf *nkx2.2a:gfp;olig2:dsred* larva, *nkx2.2a*$^{+}$ perineurial glia fully ensheath *olig2*$^{+}$ motor axons. (E) ZO-1 staining in a *nkx2.2a:gfp* larva shows concentrated expression near the motor exit point (arrowheads) at 6 dpf. (F) Sox10 labeling is present along *olig2*$^{+}$ motor axons at 6 dpf. (G) MBP staining is present along the caudal but not rostral motor nerve bundle. Scale bars: 0.5 µm for (B) 10 µm for (D-G).

guide newly regrowing axons across the gap and back to their original targets (Nguyen et al., 2002; McDonald et al., 2006; McDonald and Zochodne, 2003; Parrinello et al., 2010) (for review see Vargas and Barres, 2007; Chen et al., 2007; Wang et al., 2012). The role of the perineurium throughout these processes is poorly understood, though several studies have hypothesized that the initial tissue bridge could be perineurial in origin (Schroder et al., 1993; Scaravilli, 1984). In support of this hypothesis, electron microscopy studies show that axons re-grow through tracts containing both Schwann cell and perineurial lamellae (Morris et al., 1972; Thomas and Jones, 1967). However, no study has ever focused on perineurial glial behavior following injury and it is not known how these cells coordinate with other cell types, or whether they are required for axon regrowth.

Here we use laser axotomy and *in vivo*, time-lapse confocal imaging to transect spinal motor nerves in live transgenic zebrafish and visualize perineurial glial responses after injury. We show that perineurial glia respond immediately to nerve transection by extending processes toward the injury site and phagocytizing debris. Perineurial processes bridge the proximal and distal stumps, and in the absence of these bridges, axon regrowth is impaired. Additionally, we show that debris clearance appears to be coordinated between perineurial glia, macrophages and Schwann cells, and that perineurial glial attraction to injury sites is dependent on Schwann cells. These data reveal an essential role for perineurial glia during regeneration and demonstrate the importance of Schwann cell-perineurial glial interactions after injury.

Results

The zebrafish spinal motor nerve as a model for studying glial behaviors during regeneration

To investigate the role and requirement of perineurial glia during degeneration and subsequent regeneration, we used the spinal motor nerve of 6 day post fertilization (dpf) zebrafish larvae as a model. Zebrafish have recently become a common model system in which to study nerve degeneration and regeneration (Villegas et al., 2012; O'Donnell et al., 2013; Martin et al., 2010; O'Brien et al., 2009; Rosenberg et al., 2012), and previous work has shown that by 5-6 dpf, both motor axons and their associated glia are differentiating and forming mature spinal motor nerves (Rosenberg et al., 2012; Binari et al., 2013). This makes regeneration studies feasible in a relatively mature, yet tractable system.

Prior to performing nerve transections, we sought to further characterize spinal motor nerve ultrastructure in 6 dpf zebrafish larvae. Using electron microscopy, we observed that by this stage, motor axons were sorted with large caliber axons associated with myelinating Schwann cells and small diameter axons encased within immature Schwann cells, and both were bundled into a fascicle by a single layer of perineurial cells (Figure 4-1B). Using *nkx2.2a:gfp;olig2:dsred* larvae, where *nkx2.2a* regulatory sequences drive expression of membrane tethered EGFP in perineurial glia and *olig2* regulatory sequences drive expression of DsRed in motor neurons/axons, we assayed the extent of perineurial ensheathment along motor nerves. At 6 dpf, spinal motor root axons were fully ensheathed by *nkx2.2a*$^{+}$ perineurial glia from the motor exit point (MEP) to the horizontal myoseptum (hms), and perineurial processes frequently extended along

axons well beyond the hms (Figure 4-1C,D). In the mature perineurium, differentiated perineurial cells express tight junction proteins, including zona occludins 1 (ZO-1), which connect individual cells together and give this nerve component its blood-nerve-barrier function. To investigate the extent of perineurial glial maturity and differentiation at 6 dpf, we labeled larvae with an antibody specific to ZO-1. Consistent with previous findings (Binari et al., 2013), we observed ZO-1 labeling along *nkx2.2a*$^{+}$ perineurial sheaths with the highest concentration near the MEP (Figure 4-1E). To confirm that Schwann cells were present along motor nerves and at a similar stage of differentiation, we labeled 6 dpf larvae with antibodies specific to Sox10, a transcription factor expressed by all Schwann cells, and myelin basic protein (MBP), to label mature, myelinating glia. At this stage, we observed Sox10^{+} cells along both rostral and caudal nerve roots, and MBP immunoreactivity was present along the caudal motor root and absent from the rostral motor root (Figure 4-1F,G). This MBP profile persisted out to approximately 20 dpf (data not shown) and therefore, we concluded that rostral motor root axons are associated with non-myelinating Sox10^{+} glia while caudal motor root axons are ensheathed by myelinating glia. Taken together, these data show that Sox10^{+} glia and perineurial glia are differentiating and forming mature structures along spinal motor nerve roots at 6 dpf. Therefore, these nerves are an ideal model to study the role of perineurial glia during nerve degeneration and regeneration.

In order to investigate the role of perineurial glia during motor nerve degeneration and subsequent regeneration, we developed an injury-response assay in live, 6 dpf larvae. For this assay, we used a nitrogen pumped dye laser (MicroPoint, Andor Technology) to transect the rostral spinal motor nerve root, resulting in a complete axotomy of this nerve

bundle (Lewis and Kucenas, 2013) (Figure 4-2A,B). This assay is highly reproducible and similar to other published nerve transection assays (Rosenberg et al., 2012). Given that this method of transection relies on the use of a UV laser, we sought to confirm that motor axons were fully cut and not simply photobleached after injury. To investigate this possibility, we fixed 6 dpf larvae after transection and labeled them with an antibody specific to acetylated tubulin to label all spinal motor axons. In these larvae, we consistently observed clear breaks in tubulin expression along rostral motor nerves where we had previously transected the nerve, but DIC imaging did not show any obvious tissue damage surrounding the lesions (Figure 4-2B,C). From these data, we are confident that our nerve injury assay produces full and reproducible transections with no obvious damage to neighboring tissue.

To determine if our injury assay produced similar axonal degeneration dynamics to previously published studies (Rosenberg et al., 2012; Villegas et al., 2012; Martin et al., 2010), we sought to characterize these events more carefully. Following transection of the rostral motor nerve, we observed that proximal and distal stump axons appeared to die back, gradually causing a widening of the injury gap (Figure 4-2D). The phenomenon of axon die back, or acute axonal degeneration (AAD), is well established in mammalian systems (Kerschensteiner et al., 2005; Wang et al., 2012; Zochodne, 2012) and has been reported in zebrafish as well (Villegas et al., 2012). In our assay, we observed that AAD began along both stumps immediately after injury, increasing the distance between stumps by an average of 16.6 μm over the first 2 hours post transection (hpt) (SD=6.0, n=10). Interestingly, during our temporal analysis, we noticed that proximal stump AAD occurred earlier and at a faster rate than distal stump AAD (Figure 4-2E). Ultimately,

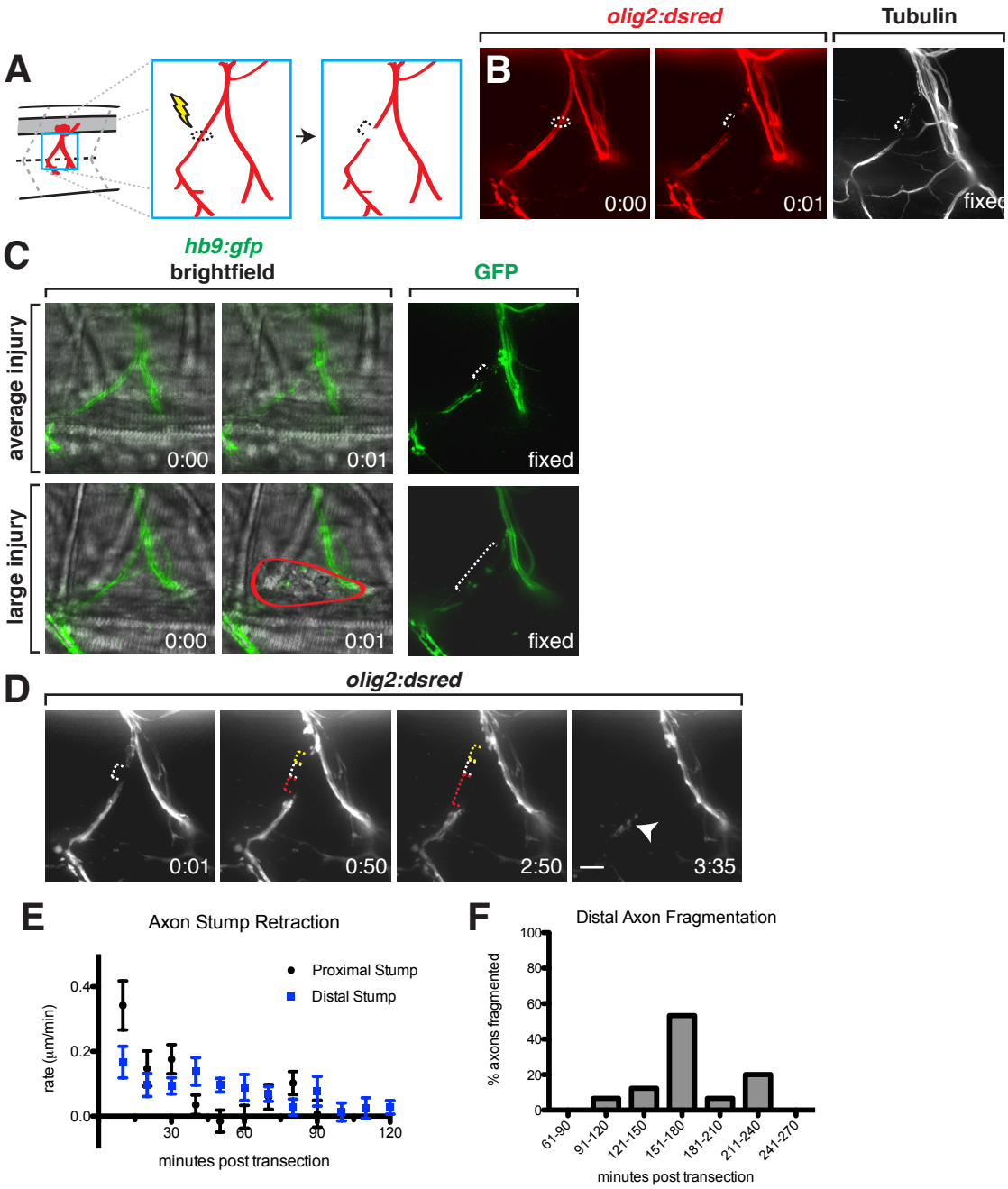

Figure 4-2: Motor nerve transection induces acute and Wallerian degeneration of axons. (A) Diagrammatic representation of the rostral spinal motor nerve root transection assay we use in these studies. (B) Rostral motor nerve transection in a 6 dpf *olig2:dsred* larva. Dotted ellipse denotes ablated ROI and dotted bracket denotes injury gap. Tubulin staining is not present in the injury gap of the transected nerve. (C) Average size injury in *hb9:gfp* larvae is not detectable by brightfield microscopy, but a large size injury is. GFP staining is not present in the injury gap after transection. (D) After transection at 6 dpf in a *olig2:dsred* larva, *olig2*$^{+}$ axons degenerate. White dotted line denotes initial injury gap, yellow dotted line denotes proximal stump AAD, red dotted line denotes distal stump AAD and arrowhead points to debris following distal stump Wallerian degeneration. (E) Graphical representation of rate of proximal and distal stump AAD over time. (F) Graph of the onset of distal axon degeneration in n=15 nerves. Time in bottom right corners denotes minutes post transection. Scale bar: 10 µm.

within a few hours, AAD along the distal stump gave way to Wallerian degeneration of distal axons, with individual axons fragmenting all at once, usually between 151-180 minutes post transection (mpt) (Figure 4-2F), which is consistent with previous findings in zebrafish (Rosenberg et al., 2012; Martin et al., 2010; Villegas et al., 2012). From these studies, we conclude that our nerve injury assay is highly reproducible with axon degeneration dynamics similar to previously reported models of axon injury in zebrafish (Rosenberg et al., 2012; Martin et al., 2010; Villegas et al., 2012), and therefore, provides an ideal model to investigate the role of perineurial glia in nerve degeneration and regeneration.

Perineurial glia respond to spinal motor nerve root injury

Although many studies have investigated the mechanisms that govern peripheral axon degeneration and regeneration, the role of perineurial glia during these processes is still poorly understood. Studies on fixed tissue preparations have hypothesized that: 1) perineurial cells may be the first cellular component to traverse injury gaps and connect proximal and distal stumps after nerve transection (Scaravilli, 1984; Schroder et al., 1993), and 2) that axons regrow through tracks that contain both Schwann cell and perineurial lamella (Thomas and Jones, 1967; Morris et al., 1972). However, despite these indications that perineurial glia may be important for regeneration, perineurial glial behavior following injury has never been formally investigated.

To this end, we transected the rostral spinal motor nerve root in 6 dpf *nkx2.2a:gfp;olig2:dsred* larvae (n=11) using the assay we describe above coupled with *in vivo*, time-lapse imaging. These transections severed both motor axons and their

ensheathing perineurial glial membranes and resulted in an average injury gap of 4.9 μm (SD = 1.9, n=11) between the proximal and distal stumps at 1 mpt. We began time-lapse imaging immediately after the injury, and by 15 mpt, we observed that perineurial glia extended highly motile membrane processes toward the injury site from both the proximal and distal stumps. Around this same time, vesicles formed in perineurial glial membranes near the transection site. Interestingly, these vesicle-like structures appeared along both stumps during the period of AAD, and were particularly numerous along the proximal stump, which degenerates more rapidly. During the imaging window (3 hours) after nerve injury, perineurial glia eventually bridged the injury site, connecting the proximal and distal stumps, and remained along the distal stump after distal axons degenerated and were cleared (Figure 4-3A and Movie 4-1 available at http://www.jneurosci.org/content/34/38/12762.long).

To determine if the size of the initial injury gap was correlated to the time it took perineurial glia to form bridges, we measured the size of the injury gap at 1 mpt and plotted it against the time it took perineurial cells to extend processes into the injury site and bridge the gap. We found that regardless of the size of the injury, perineurial glia always extended highly motile membrane processes towards the injury gap within 20 mpt. However, as injury size increased, the time to bridge formation increased linearly, indicating that larger injuries take perineurial glia respectively longer to bridge (Figure 4-3B). Interestingly, perineurial glia did not routinely bridge large injuries (>10 μm) during the imaging window, which is led us to hypothesize that the bridging behavior may be mediated by perineurial-perineurial interactions.

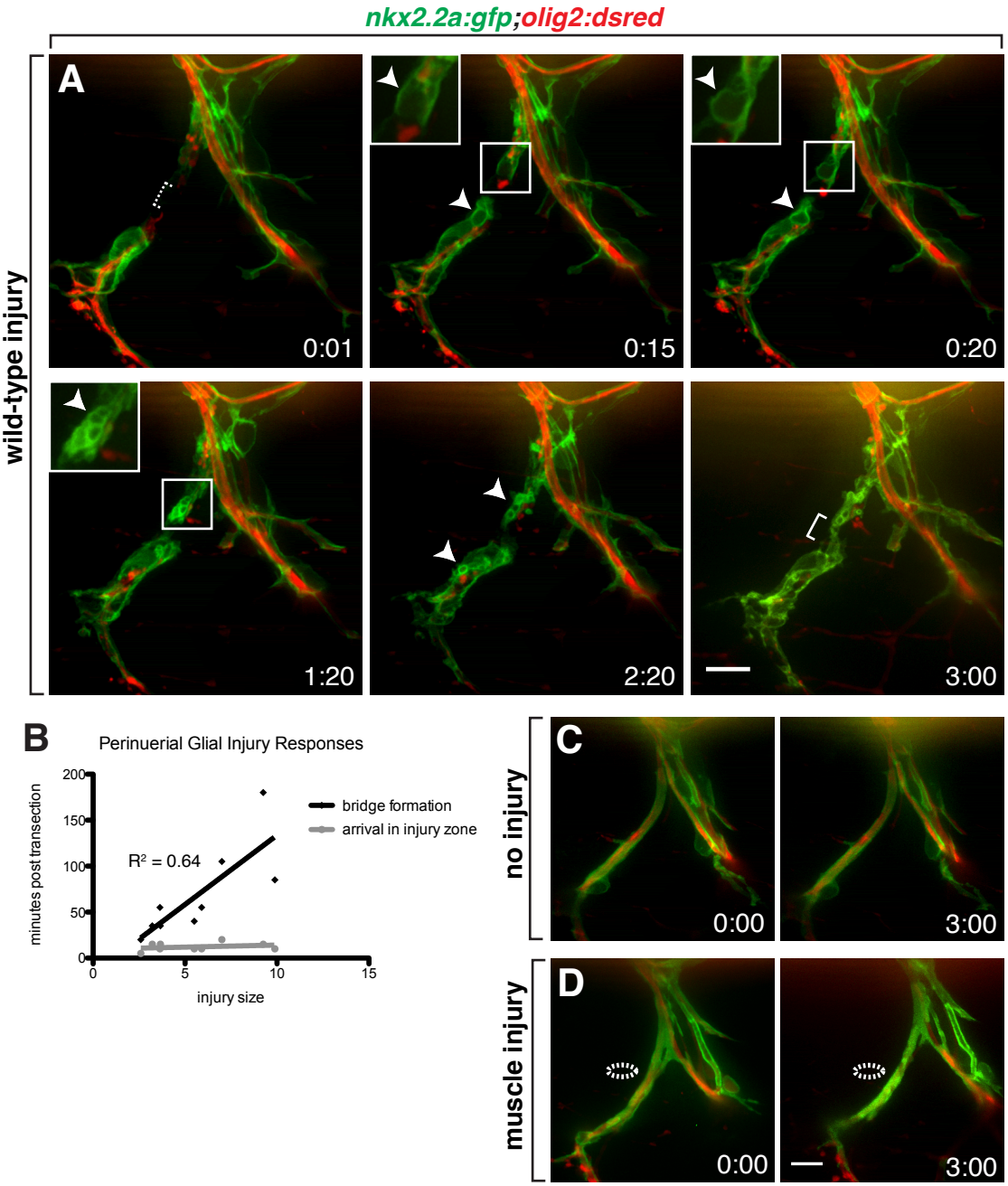

Figure 4-3: Perineurial glia respond to rostral motor nerve injury. Frames captured from a 3 hr time-lapse movie of a 6 dpf *nkx2.2a:gfp;olig2:dsred* larva beginning at 1 mpt with dorsal to the top and anterior to the left. Mpt is denoted in bottom right corner of each image. (A) Perineurial glia respond to rostral spinal motor nerve root transection by extending processes into the injury site, forming vesicles (insets and arrowheads), and bridging the injury gap (bracket). (B) Graphical representation of the time it took perineurial glia to bridge the injury gap plotted against the initial injury size. (C&D) Perineurial glial membranes are stable in both (C) the absence of injury and (D) after injury to tissue adjacent to the nerve. Dotted ellipse denotes ablated ROI. Scale bar: 10 μm.

To verify that the perineurial glial behaviors we observed were a response to nerve injury and not general damage or heat created by the laser, we created focal lesions in the muscle tissue less than 10 μm from rostral motor axons (n=3) and assayed the perineurial glial response with time-lapse imaging. In the three hours after injury, this type of damage did not elicit any changes in nearby perineurial glia when compared to uninjured control larvae (Figure 4-3C,D). Taken together, these data are consistent with the hypothesis that cues derived specifically from nerve damage induce a rapid change in perineurial glial behavior that results in perineurial glia extending processes towards the injury site, developing vesicles and ultimately bridging the injury gap.

Perineurial glia phagocytize debris after nerve injury

While characterizing the response of perineurial glia to spinal motor nerve root injury, we noticed that the formation and temporal dynamics of perineurial glial vesicles coincided with periods of axonal degeneration (Figures 4-2 and 4-3 and Movie 4-1). Many vesicles formed along the proximal stump as it was rapidly degenerating during the first 45 mpt, and vesicles frequently formed along the distal stump during acute and Wallerian degeneration (Figure 4-3A and Movie 4-1). However, we never observed perineurial vesicles along uninjured nerves or during normal nerve development prior to 6 dpf (Figure 4-3C and data not shown). This led us to hypothesize that perineurial glia may be phagocytic and aid in debris clearance after injury. To investigate this hypothesis, we transected nerves in 6 dpf *nkx2.2a:gfp;olig2:dsred* larvae and looked for the presence of axonal fluorescence within perineurial glial vesicles. Single z-planes taken from time-lapse images showed $DsRed^{+}$ axonal fluorescence was frequently present inside GFP^{+}

perineurial membrane vesicles during both AAD and Wallerian degeneration (Figure 4-4A,B**,**C). Additionally, orthogonal views demonstrated that the GFP^{+} perineurial vesicles were indeed spherical in nature, and therefore, morphologically consistent with phagocytic vesicles (Figure 4-4D). Notably, not all vesicles contained axonal fluorescence, and it is possible these vesicles contained debris derived from other nerve components, including myelin, Schwann cells or extracellular matrix.

As an independent method of testing the phagocytic ability of perineurial glia, we used LysoTracker dye. LysoTracker is a membrane permeable dye that fluoresces at acidic pH and this dye has previously been used in zebrafish to label phagosomes as they fuse with lysosomes and acidify (Peri and Nüsslein-Volhard, 2008). To confirm that the vesicle-like structures we observed after injury represent phagosomes or phagolysosomes, we treated 4 dpf *nkx2.2a:gfp* larvae with 20 μM LysoTracker Red, transected nerves and followed individual perineurial glial vesicles with time-lapse imaging. After injury, we observed that perineurial vesicles became LysoTracker positive over time (Figure 4-4E), suggesting these vesicles were acidifying. LysoTracker staining was present pre-injury and in uninjured controls, however this staining never occurred within clearly defined perineurial vesicles and was likely due to staining of lysosomes (data not shown) (Chazotte, 2011). These data demonstrate that after nerve damage, perineurial glia form phagocytic vesicles, many of which contain axonal debris. In our previous time-lapse imaging (Figure 4-3A), we noticed that perineurial vesicles were most numerous along the proximal stump as those axons underwent AAD. Therefore, we conclude that perineurial glia initially focus their phagocytic activity along the proximal

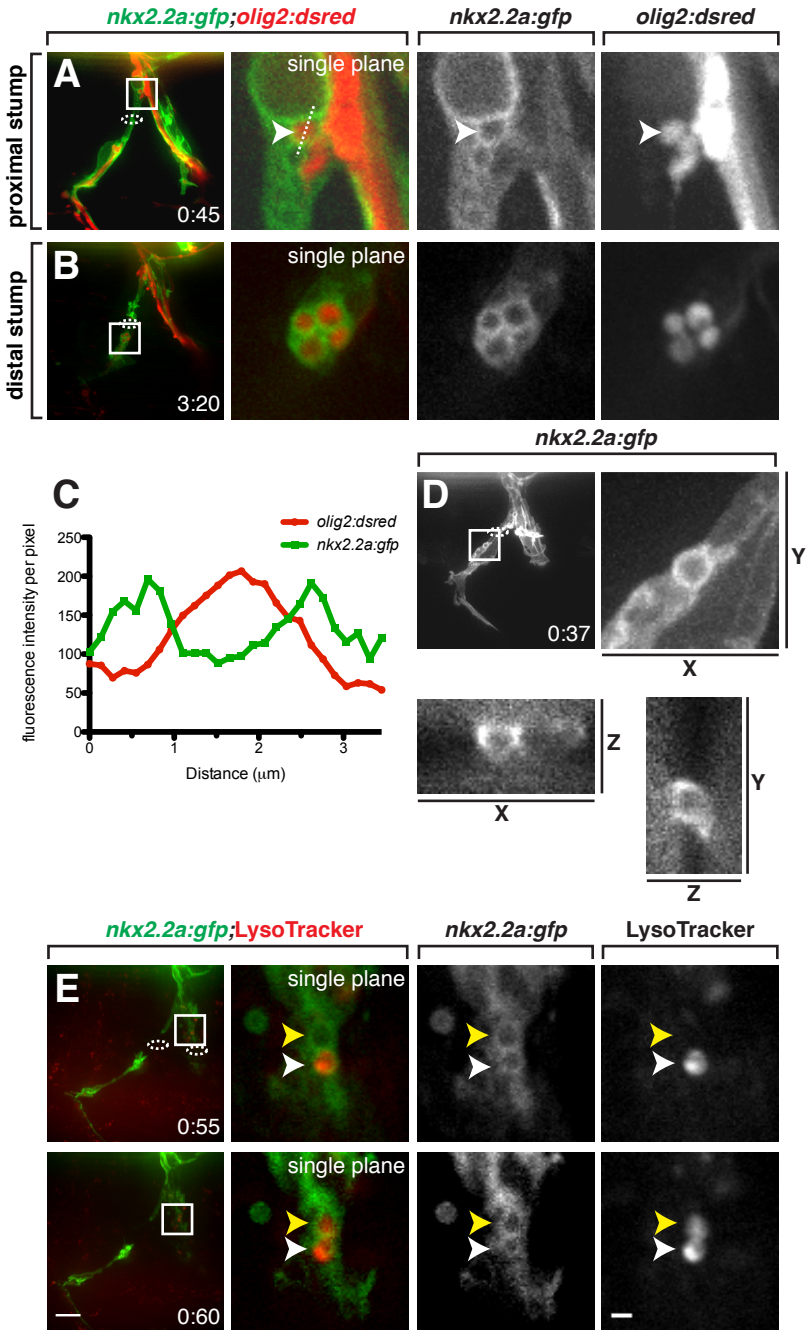

Figure 4-4: Perineurial glia phagocytize debris following nerve injury. Frames captured from a time-lapse movie of a 6 dpf *nkx2.2a:gfp;olig2:dsred* larva beginning at 1 mpt with dorsal to the top and anterior to the left. Mpt is denoted in bottom right corner of each image and dotted ellipses denote ablated ROIs. Magnified regions (white boxes) are single z planes where denoted. (A,B) Rostral nerve transections in 6 dpf *nkx2.2a:gfp;olig2:dsred* larvae show *olig2*$^{+}$ axon fragments (arrowheads) within *nkx2.2a*$^{+}$ perineurial membranes along the proximal stump during AAD (A) and distal stump during Wallerian degeneration (B). (C) Fluorescence intensity of *nkx2.2a:gfp* and *olig2:dsred* along the white dashed line ROI drawn in A shows an increase in *olig2:dsred* fluorescence within the *nkx2.2a:gfp* fluorescing vesicle. (D) A perineurial vesicle shown with accompanying orthogonal views. (E) Rostral and caudal nerve transections of a 4 dpf *nkx2.2a:gfp* larva stained with LysoTracker. At 55 mpt, Lysotracker staining is visible within an *nkx2.2a*$^{+}$ perineurial vesicle (white arrowhead) and by 60 mpt, staining is visible within a second, adjacent vesicle (yellow arrowhead). Scale bars: 10 μm for full images, 1.5 μm for magnified insets.

stump. This sets forth an interesting hypothesis, where debris clearance may be spatially coordinated between different cell types after nerve injury.

Perineurial glial bridges are required for axon regrowth

Above, we show that perineurial glia bridge the injury gap between proximal and distal nerve stumps following transection, with timing that is dependent on the size of the injury (Figure 4-3). Importantly, these bridges formed before new axons began to regenerate and remained intact after distal axons degenerated. Previous studies of sciatic nerve regeneration in rats showed that a tissue bridge forms to connect the proximal and distal stumps shortly after transection and that this bridge precedes the ingrowth of axons and Schwann cells (McDonald and Zochodne, 2003; McDonald et al., 2006; Parrinello et al., 2010; Schroder et al., 1993). Collectively, these data are consistent with the hypothesis that perineurial glia provide an essential tissue bridge that helps guide regenerating axons across the injury gap and back to their original targets.

To investigate this hypothesis, we assessed the ability of axons to regrow in the absence of perineurial glial bridges. Using 6 dpf *nkx2.2a:gfp;olig2:dsred* larvae, we deliberately created rostral spinal motor nerve transections that resulted in gaps of varying sizes, ranging from 3.5 to 20 μm. We then let the larvae recover and imaged them at 48 hours post transection (hpt) to assess the presence or absence of perineurial bridges and the extent of axon regrowth. Previous studies in zebrafish demonstrate that motor axons begin to regrow after injury by 24 hpt, with full functional recovery achieved by 48 hpt (Rosenberg et al., 2012), rendering 48 hpt a suitable time point to assay axon regrowth.

In our studies, we defined full regrowth as the presence of an axon bundle at 48 hpt that was approximately the same thickness and followed a similar path as the original, uninjured nerve (Figure 4-5A). Moderate regrowth was defined as the presence of an axon bundle that was significantly thinner than the original nerve, but followed a similar path (Figure 4-5B). Finally, no regrowth was characterized as exhibiting either no axon regrowth from the proximal stump, or sprouting that did not extend beyond the horizontal myoseptum (Figure 4-5C). When we created transections that resulted in injury gaps that were less than 7 μm (n=9) and imaged at 48 hpt, perineurial glia always bridged injury sites and axons successfully regrew along these bridges following the original path (Figure 4A,B). Of these nerves, 33% exhibited full regrowth and 66% exhibited moderate regrowth (Figure 4-5E), which is consistent with clinical data describing that peripheral regeneration results in variable and often imperfect outcomes (Zochodne, 2012; Witzel et al., 2005). In contrast, when injury gaps ranged between 7 and 10 μm (n=6), only 17% of nerves exhibited full axon regrowth at 48 hpt, 50% exhibited moderate regrowth and 33% exhibited no regrowth (Figure 4-5E). In the cases of full and moderate regrowth, perineurial glia bridged the injury site in all but one instance. In this situation, axons appeared to re-route around the injury site and make their way to back to a perineurial glial cell along the distal stump. Once meeting with the distal perineurial glia, axons then followed the glia along what appeared to be their original path (data not shown). In all cases of no regrowth, perineurial bridges were never present, and although we often observed axon sprouts from the proximal stump, they did not follow along any defined path and perineurial ensheathment of these sprouts was variable (Figure 4-5C). Finally, when we created transections that resulted in injury gaps that were greater than 10 μm

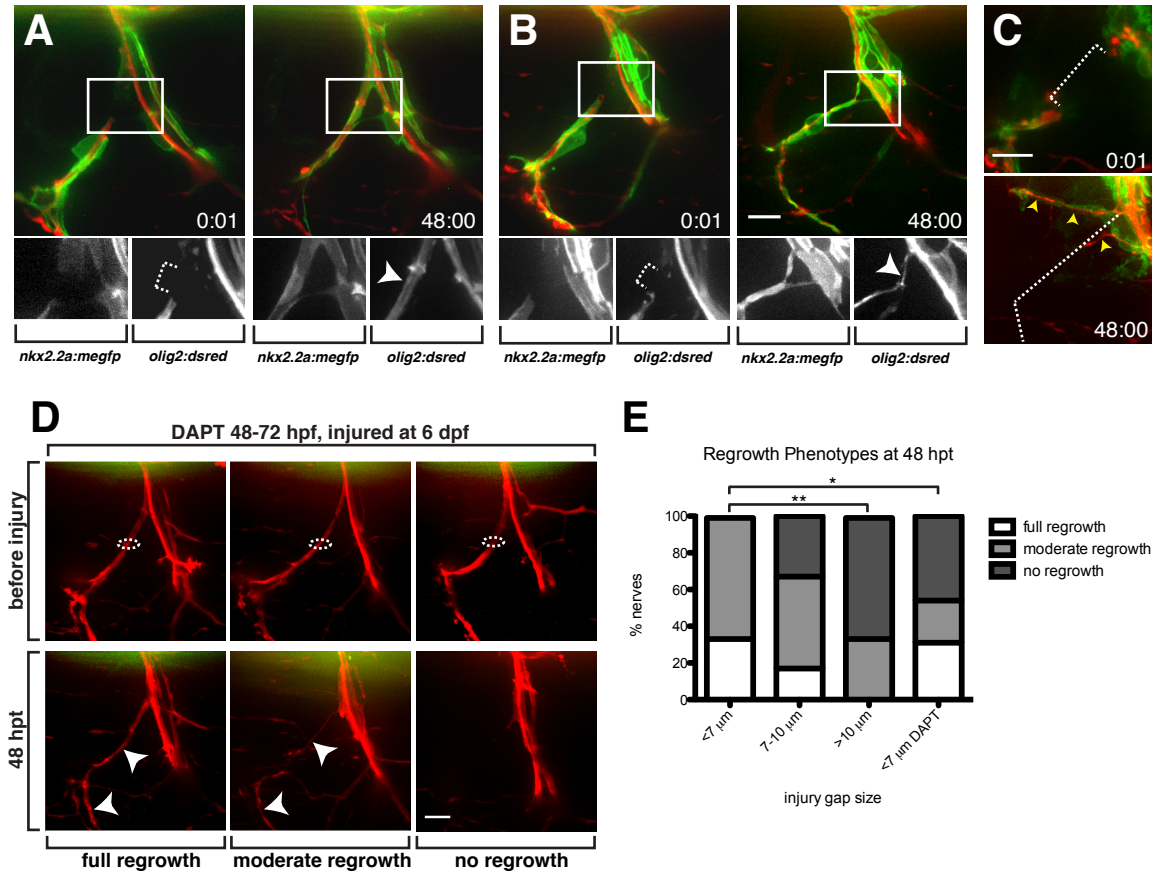

Figure 4-5: Perineurial bridges are essential for axon regrowth. All frames are live images taken from transected, 6 dpf *nkx2.2a:gfp;olig2:dsred* larvae with dorsal to the top and anterior to the left. Mpt is denoted in bottom right corner of each image and dotted ellipses denote ablated ROIs. White boxes denote magnified images below and dashed brackets label the injury. (A) A representative example of a transection that resulted in a <7 µm injury gap at 1 mpt where axons exhibited full regrowth with a tight perineurial sheath by 48 hpt. (B) A representative example of a transection that resulted in a <7 µm injury gap at 1 mpt and had moderate axon regrowth by 48 hpt. (C) When a >10 µm injury gap at 1 mpt was created, we observed no axon regrowth and aberrant axon sprouting (yellow arrowheads) at 48 hpt. (D) DAPT treatment from 48-72 hpf resulted in the absence of perineurial glia along motor nerves at 6 dpf. Rostral nerve transections in these larvae resulted in a mix of full, moderate and no regrowth phenotypes at 48 hpt. (E) Graphical representation of data in panels A-D. The number of nerves analyzed for each condition is as follows: <7 µm n = 9, 7-10 µm n= 6, >10 µm n= 6, <7 µm DAPT n=13. Significance presented represents the difference in the proportion of nerves with a "no regrowth" outcome. The difference in "no regrowth" between the <7 µm and >10 µm conditions was significant with p = 0.00424. The difference in "no regrowth" between the <7 µm and <7 µm DAPT conditions was significant with p = 0.01684. Scale bars: 10 µm.

(n=6), we never observed full regrowth, 33% of cases had moderate regrowth with perineurial bridges and 67% had no regrowth and no perineurial bridges (Figure 4-5C,E). Importantly, regardless of injury size, in 20 of 21 cases, the presence of a perineurial bridge was associated with axon regrowth and the absence of a bridge was associated with no regrowth. We interpret this to mean that as the size of the injury increased, the ability of perineurial glia to bridge became impaired, and when bridges did not form, axons were not able to regrow. Taken together, these data are consistent with the hypothesis that perineurial glial bridge formation is required for axon regrowth after injury.

To more directly test the requirement of perineurial glia for axonal regeneration, we assessed the ability of axons to regrow in the absence of perineurial glia. In a previous study, we show that Notch signaling is required during a distinct temporal window (48-72 hpf) for perineurial glial development (Binari et al., 2013). During this window, treating embryos with either DAPT, a gamma secretase inhibitor, or genetically blocking Notch signaling via a dominant-negative form of the Notch intracellular domain (NICD) cofactor, suppressor of hairless (Su(H)), led to a complete failure of perineurial glial migration into the PNS (Binari et al., 2013). Importantly, even though perineurial glia failed to exit the spinal cord, Schwann cells were still present along motor nerves after Notch perturbation, although they failed to myelinate axons (Binari et al., 2013). Therefore, this experimental paradigm allowed us to remove perineurial glia from motor nerves but leave Schwann cells intact. For these studies, we treated *nkx2.2a:gfp;olig2:dsred* embryos with DAPT from 48-72 hpf, then transferred larvae to fresh medium without drug until 6 dpf. We used DAPT treatment to block perineurial

glial migration from the spinal cord as opposed to genetic manipulation because the heat shock required for genetic manipulation resulted in larvae that were extremely unhealthy by 6 dpf (data not shown). Similar to our previous studies (Binari et al., 2013), we observed that perineurial glia were completely absent from spinal motor nerves at 6 dpf in larvae that had been previously treated with DAPT (Figure 4-5D). We then transected rostral motor nerves in these larvae and imaged at 48 hpt to assess axon regrowth. All transections created injury gaps that were less than 7 μm, which in vehicle control animals, always resulted in the formation of perineurial bridges and either full or moderate regrowth (Figure 4-5A,B,E). In contrast, in DAPT-treated larvae that lacked perineurial glia along motor axons, and therefore perineurial bridges (n=13), we observed that nearly half (46%) of all transections resulted in no axon regrowth (Figure 4-5D,E). Collectively, these data demonstrate that axon re-growth is hindered in the absence of perineurial glial bridges, and we conclude that this is consistent with the hypothesis that perineurial glial bridges are essential for full axon regrowth.

Perineurial glia, Schwann cells and macrophages appear to coordinate their behaviors during axon degeneration

Successful peripheral nerve regeneration requires the efforts of multiple cell types, including macrophages and Schwann cells. Because perineurial glia play a role during injury as well, we sought to investigate if they coordinated their injury response with these other cell types. Previous studies demonstrate that shortly after nerve damage, macrophages are recruited to injured lesions and play a major role in debris clearance (Griffin et al., 1992; Perry et al., 1987; Vargas and Barres, 2007; Rosenberg et al., 2012). To view macrophage activity after injury, we transected and time-lapse imaged the rostral

nerve in 6 dpf *mpeg1:gfp;olig2:dsred* larvae (n=12), in which *mpeg1* regulatory sequences drive cytosolic EGFP specifically in macrophages (Ellett et al., 2011). In 10 of 12 cases, macrophages were recruited to injured nerves within 4 hpt (the end of the imaging time period), and vesicles were observed within these macrophages at both the injury site, and along the distal stump (Figure 4-6A,B). Axonal debris was often present within vesicles along the distal stump as axons underwent Wallerian degeneration (Figure 5B), and LysoTracker staining indicated that these vesicles represent phagocytic activity (Figure 4-6C). When we tracked the migration of individual macrophages over time, we found that along 12 nerves, 21 total cells responded to the injuries. Interestingly, these cells appeared to clear debris primarily at the injury site and along the distal stump (Figure 4-6A,B,D), and rarely extended processes along the proximal stump (Figure 4-6D). Given our earlier data that showed perineurial glia phagocytize debris along the proximal stump, these data led us to hypothesize that macrophage and perineurial clearing activity may be spatially coordinated after injury.

To investigate how perineurial glia and macrophages coordinate their behaviors after injury, we transected nerves and time-lapse imaged 6 dpf *nkx2.2a:gfp;olig2:dsred;mpeg1:gfp* larvae (n=4), which allowed us to visualize axons, perineurial glia and macrophages, simultaneously. Although perineurial glia and macrophages were both labeled with GFP, they were readily distinguishable based on fluorescent protein localization (membrane vs. cytosolic), morphology and behavior. As described above (Figure 4-3 and 4-4 and Movie 4-1), our time-lapse imaging data revealed that transection induced perineurial glia to extend highly motile membrane processes toward injury sites and form phagocytic vesicles (Figure 4-7). These

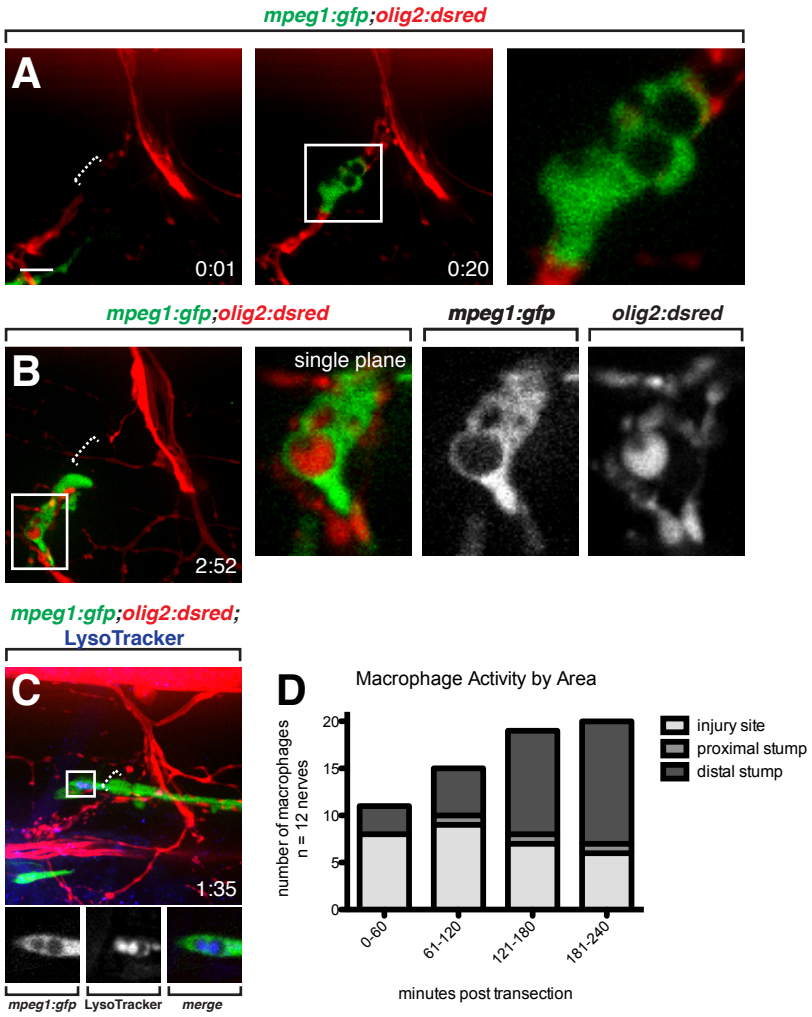

Figure 4-6: Macrophages phagocytize debris primarily at the injury site and along the distal stump after transection. Frames captured from time-lapse movies beginning at 1 mpt with dorsal to the top and anterior to the left. Mpt is denoted in bottom right corner of each image and dotted brackets denote the injury gaps. (A,B) Representative frames captured from time-lapse movies of 6 dpf *mpeg1:gfp;olig2:dsred* larvae show a macrophage containing vesicles at the injury gap (A) and a macrophage with vesicles containing axonal debris along the distal stump (B). (C) Frame captured from a time-lapse movie of a 4 dpf *mpeg1:gfp;olig2:dsred* larva stained with LysoTracker Deep Red dye shows LysoTracker staining within macrophage vesicles near the injury gap. (D) Quantification of macrophage activity along various areas of the nerve. Data was taken from time-lapse movies of 6 dpf *mpeg1:gfp;olig2:dsred* larvae. 21 macrophages from 12 nerves were individually tracked, and the total number of cells in each area was assessed over 240 mpt and binned by time. White boxes denote region of magnified inset. Scale bar: 10 μm.

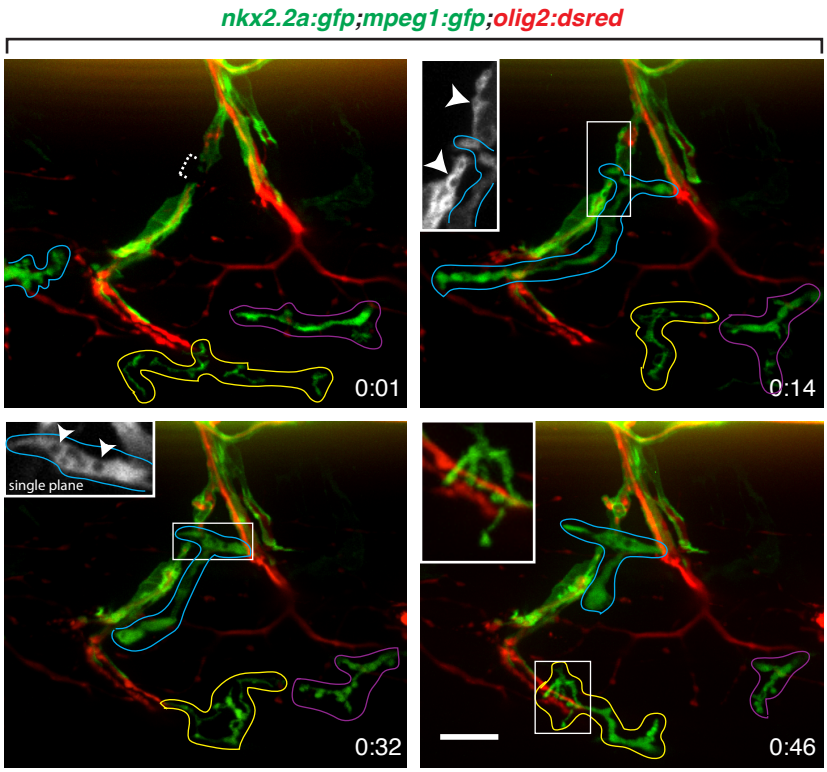

Figure 4-7: Perineurial glia spatially coordinate early debris clearance with macrophages. Representative frames captured from a time-lapse movie of a 6 dpf *nkx2.2a:gfp;mpeg1:gfp;olig2:dsred* larvae. Individual macrophages are outlined to distinguish from perineurial glia and to allow tracking throughout the sequence. By 14 mpt, perineurial glia began to phagocytize debris along the degenerating stumps and a macrophage (blue outline) arrived at the injury gap. At 32 mpt, vesicles (arrowheads) appeared within the macrophage and by 46 mpt, an additional macrophage (yellow outline) appeared to contact distal stump axons. A third macrophage (purple outline) did not respond to the injury during the imaging window. White boxes denote region of magnified inset. Scale bar: 10 μm.

phagocytic vesicles populated perineurial glial membranes along both stumps immediately adjacent to the injury site and were particularly numerous along the proximal stump, which undergoes rapid AAD immediately after injury (Figure 4-7). Interestingly, these perineurial responses were usually observed before the arrival of macrophages, and the mean response time for perineurial glia was significantly shorter and less variable than for macrophages (perineurial glial mean response time: 8.636 mpt ±0.09749, n = 11, macrophage mean arrival time: 45.0 mpt ±14.43, n = 9, p = 0.0120). While perineurial glial vesicles appeared along the stumps undergoing AAD, macrophages were usually attracted directly to the injury gap, and vesicles within these macrophages indicated they were clearing debris primarily in the gap zone (Figure 4-7). We also observed that additional macrophages were often recruited to the distal stump as axons fragmented during Wallerian degeneration (Figure 4-7) and we frequently observed vesicles in perineurial glia along the distal stump around this time as well (Figure 4-4). This data demonstrates that perineurial glia respond to transections and begin debris clearance more quickly than macrophages. It also shows that these two cell types initially focus on clearing debris within distinct zones, with perineurial glia focusing on the degenerating stumps, and macrophages focusing on the injury gap, but work together in similar areas during later stages of degeneration. This is consistent with the hypothesis that perineurial glia and macrophages spatially coordinate debris clearance.

In addition to macrophages, Schwann cells also play an important role in peripheral degeneration and regeneration by phagocytizing myelin and forming cellular columns that span injury gaps to help guide regenerating axons (Parrinello et al., 2010;

Gaudet et al., 2011; Webber and Zochodne, 2010; Lutz and Barres, 2014; Perry et al., 1995). Because Schwann cells and perineurial glia coordinate their behaviors and require each other during development (Kucenas et al., 2008; Binari et al., 2013; Clark et al., 2014), we hypothesized that these cell types may coordinate again following nerve injury. To test this hypothesis, we transected nerves and time-lapse imaged *nkx2.2a:gfp;sox10:eos* larvae, which allowed visualization of perineurial glia and Schwann cells simultaneously. The *sox10:eos* transgene uses regulatory elements from the *sox10* gene to drive expression a cytosolic, photo-convertible Eos protein in Schwann cells. Mature Eos protein, when exposed to ultraviolet (UV) light, shifts its emission from a green fluorescent state (516 nm) to a red fluorescent state (581 nm). By exposing these larvae to UV light, we can easily distinguish Schwann cells (red after UV light exposure) from perineurial glia (green after UV light exposure). For these studies, we exposed larvae to UV light prior to time-lapse imaging and subsequently re-exposed the larvae every 20 minutes throughout the course of imaging to convert any newly produced green Eos so that Schwann cells would remain completely red. Similar to our results above (Figure 4-3), we observed several phagocytic vesicles within perineurial membranes along the proximal stump within 15 to 20 mpt (data not shown). We also observed vesicles within *sox10*$^{+}$ cells on the proximal stump (data not shown), and later along the distal stump (Figure 4-8A). Importantly, these vesicles could be labeled with LysoTracker, suggesting they represent phagocytic activity (Figure 4-8A). These data indicate that Schwann cells were phagocytizing debris with similar temporal and spatial dynamics as perineurial glia. As we continued imaging, perineurial glia bridged the injury gap during the 4 hour imaging window we used after transection (Figure 4-8B,C).

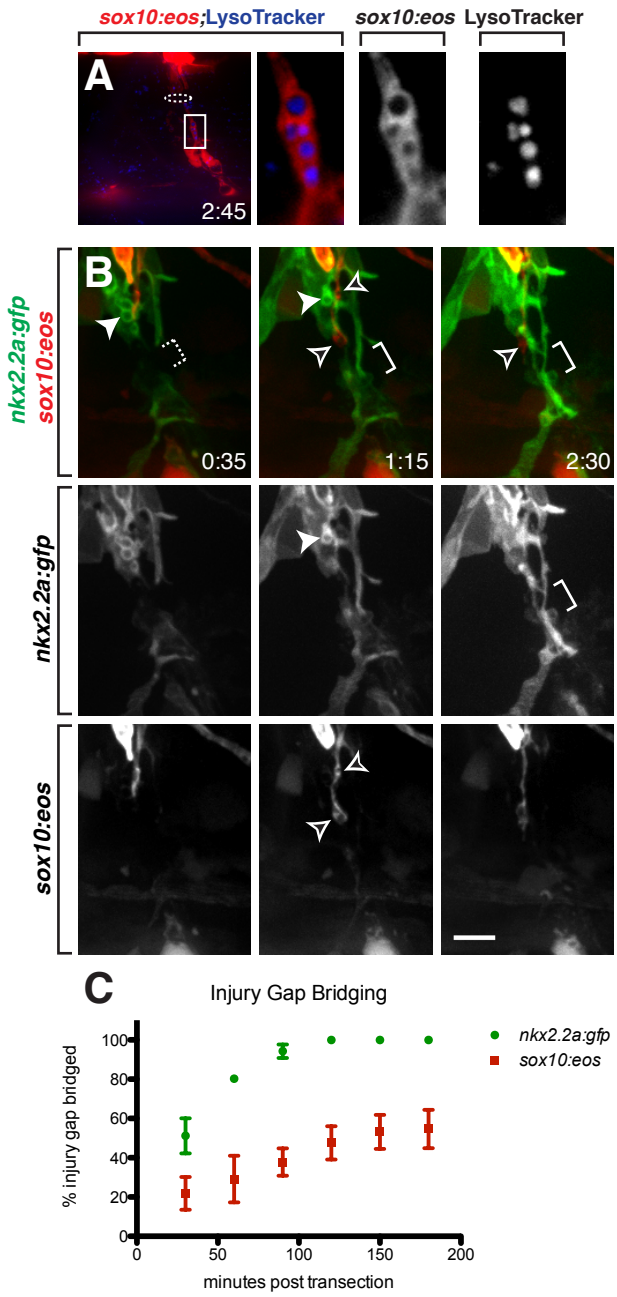

Figure 4-8: Perineurial glia bridge injury gaps before Schwann cells. Frames captured from time-lapse movies are displayed with dorsal to the top and anterior to the left. Mpt is denoted in bottom right corner of each image. Dotted ellipse denotes ablated ROI and dotted bracket denotes injury gap. (A) Frames captured from a time-lapse movie of a 4 dpf *sox10:eos* larva stained with LysoTracker Deep Red shows LysoTracker staining within *sox10:eos*$^{+}$ vesicles. (B) Frames captured from a time-lapse movie of a 6 dpf *nkx202a:gfp;sox10:eos* larva. By 35 mpt, perineurial glia had phagocytic vesicles (arrowheads) but had not yet bridged the entire injury gap (dotted bracket). At 1 hr 15 mpt, vesicles were present within both Schwann cells (open arrowheads) and perineurial glia and perineurial glia had bridged the injury gap (solid bracket). At 2 hr 30 mpt, perineurial glia remained across the injury gap but the Schwann cell never bridged. (C) Quantification of injury gap bridging by *nkx2.2a*$^{+}$ and *sox10:eos*$^{+}$ processes (n=4). The % of the initial injury gap that was bridged by each type of process was measured every 30 minutes. *nkx2.2a*$^{+}$ processes bridged 100% of the injury gap (a complete bridge) by 120 mpt, where as *sox10:eos*$^{+}$ processes did not. Scale bar: 5 µm.

Schwann cells however, extended processes slightly towards the injury site, but never bridged the injury gap during the imaging time-period (n=4) (Figure 4-8B,C). These data demonstrate that perineurial glia and Schwann cells both phagocytize debris after injury, and that perineurial glia bridge injury gaps before Schwann cells. This is consistent with the idea that perineurial glia form an initial tissue bridge across the injury gap, with Schwann cells and axons traversing the gap later.

Perineurial glia require Schwann cells following nerve injury

Interactions between cell types are critical for ultrastructural and functional nerve regeneration (Parrinello et al., 2010; Napoli et al., 2012). Therefore, we sought to identify which cell types, if any, were required for the perineurial glial response to injury. To investigate this, we used a combination of time-lapse imaging, mutant analysis and cell-type specific perturbation. We first considered the possibility that perineurial glia respond to signals released from neighboring, damaged perineurial glial cells. To test this hypothesis, we transected motor axon tracts in *nkx2.2a:gfp;ntb:dsred* larvae that were not ensheathed by perineurial glia and assessed the response of nearby perineurial glial cells. These experiments were performed in 4 dpf larvae, as not all spinal motor axon tracts have become fully ensheathed by *nkx2.2a*$^{+}$ perineurial glia yet at this stage, providing an ideal situation to test this hypothesis. Additionally, perineurial glia respond to nerve transection by phagocytizing debris and bridging injury gaps in a manner similar to what we describe at 6 dpf (compare Figure 4-9A to Figure 4-3). Therefore, using 4 dpf larvae, we transected unensheathed axons approximately 10-15 μm away from neighboring perineurial glia and assessed the response of these neighbors to the injury (n=7).

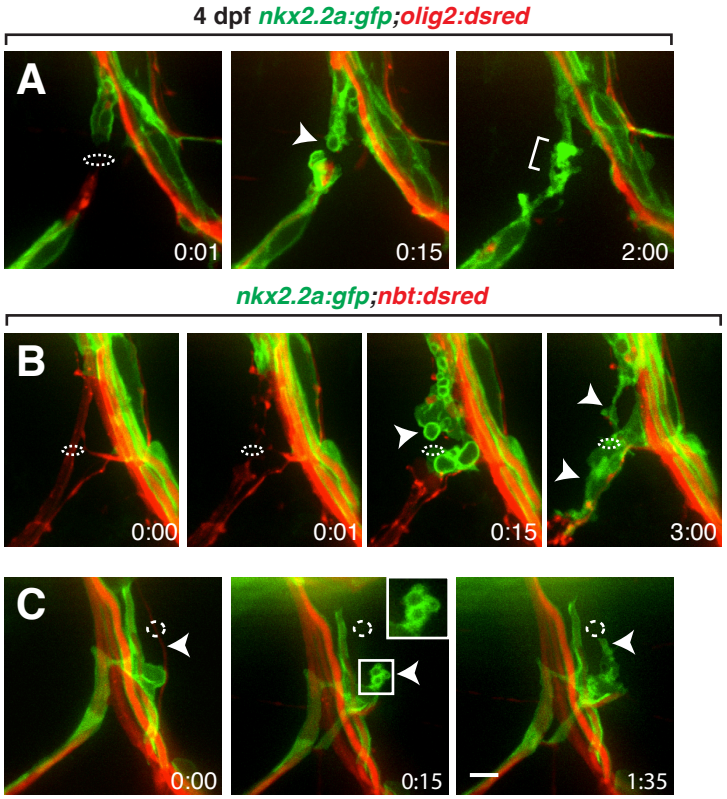

Figure 4-9: Perineurial glia respond to transections along unensheathed axons. All images are frames captured from time-lapse movies of larvae beginning at 1 mpt with dorsal to the top and anterior to the left. Mpt is denoted in bottom right corner of each image. Ablated ROIs are denoted by dotted ellipses. (A) The rostral motor nerve was transected in 4 dpf *nkx2.2a:gfp;olig2:dsred* larvae. Perineurial glia responded by phagocytizing debris (arrowhead) and bridging the injury gap (bracket) similarly as in 6 dpf larvae. (B,C) Unensheathed nerve tracts were transected in 4 and 6 dpf *nkx2.2a:gfp;nbt:dsred* larvae, respectively. Perineurial glia phagocytized debris (arrowheads) and extended processes toward injury sites along (B) unensheathed motor nerves and (C) sensory nerves in a manner indistinguishable from fully ensheathed nerves. Scale bar: 5 μm.

Immediately after injury, we observed that perineurial cells along neighboring, uninjured axon tracts rapidly extended processes toward the injury site and formed phagocytic vesicles by 15 mpt (Figure 4-9B**,**and Movie 4-2). This response time was similar to our previous findings along fully ensheathed tracts in 6 dpf larvae (mean response time for 4 dpf, 9.286 mpt ±2.296 n=7, 6 dpf, 8.636 mpt ±0.9749 n=11), suggesting perineurial glia respond to injuries with similar temporal dynamics regardless of ensheathment. To independently test the possibility that perineurial glia do not simply respond to axotomies because they sense damage in neighboring cells, we transected dorsal root ganglia sensory axons in 6 dpf *nkx2.2a:gfp;ntb:dsred* larvae, as they are not ensheathed by *nkx2.2a*$^{+}$ perineurial glia (unpublished data). In these instances, we again observed neighboring perineurial glia extend processes onto the unensheathed sensory axons and phagocytize debris (Figure 4-9C). Collectively, these data are consistent with the hypothesis that the perineurial glia do not respond to nerve injury using an autocrine mechanism. Instead, we hypothesize that perineurial glial activation after injury requires non-perineurial-derived cues. Interestingly, this is distinct from their bridging behavior, which we hypothesize is mediated by perineurial-perineurial interactions.

Another potential source of factors that could elicit perineurial behavior after injury is macrophages. Macrophages that respond to injury sites release a variety of cytokines (Leskovar et al., 2000), which could play a role in recruiting perineurial glia to injury sites or stimulating their phagocytic activity. To test this hypothesis, we transected nerves in larvae that lacked macrophages and assessed the perineurial glial response. To create larvae that completely lacked macrophages, we prevented macrophage specification by injecting single-cell embryos with a morpholino oligonucleotide (MO)

against the *spi1b* gene, which encodes a transcription factor essential for myeloid differentiation in zebrafish (Bukrinsky et al., 2009). As previously described, *spi1b* MO-injected fish lacked myeloid cells (Rhodes et al., 2005; Villegas et al., 2012) and were morphologically indistinguishable from control larvae at 6 dpf (Figure 4-10A,B). We performed our nerve transections in *nkx2.2a:gfp;olig2:dsred;spi1b:gfp* larvae. The *spi1b:gfp* transgene, which labels leukocytes, allowed us to verify that no macrophages were present during our studies. Following transection in *spi1b* morphant larvae (n=5), we observed that axonal debris created during AAD of the stumps appeared to be cleared normally, while debris generated by Wallerian degenerating axons along the distal stump was cleared more slowly, and often remained at the end of the 4-hour imaging window. This is in contrast to control larvae, where the majority of axonal debris was cleared almost immediately after fragmentation (prior to 4 hpt) (Figure 4-10C). Interestingly, the perineurial glial response to transection in *spi1b* morphants was indistinguishable from non-injected control larvae and perineurial cells extended processes towards the injury site, phagocytized debris and bridged the injury gap with the same temporal dynamics we describe above (compare Figure 4-10D to Figure 4-3). We interpret this data to mean that perineurial glia do not require signals from macrophages for their response to injury, and this is consistent with our earlier data which showed that perineurial glia usually respond to injuries before the arrival of macrophages. This data also demonstrates that perineurial glia and other phagocytes, such as Schwann cells, are sufficient to clear debris created during AAD, but not Wallerian degeneration of the distal stump.

Given that perineurial glia respond normally to transections along unensheathed axons and in larvae lacking macrophages, we next investigated the possibility that axon

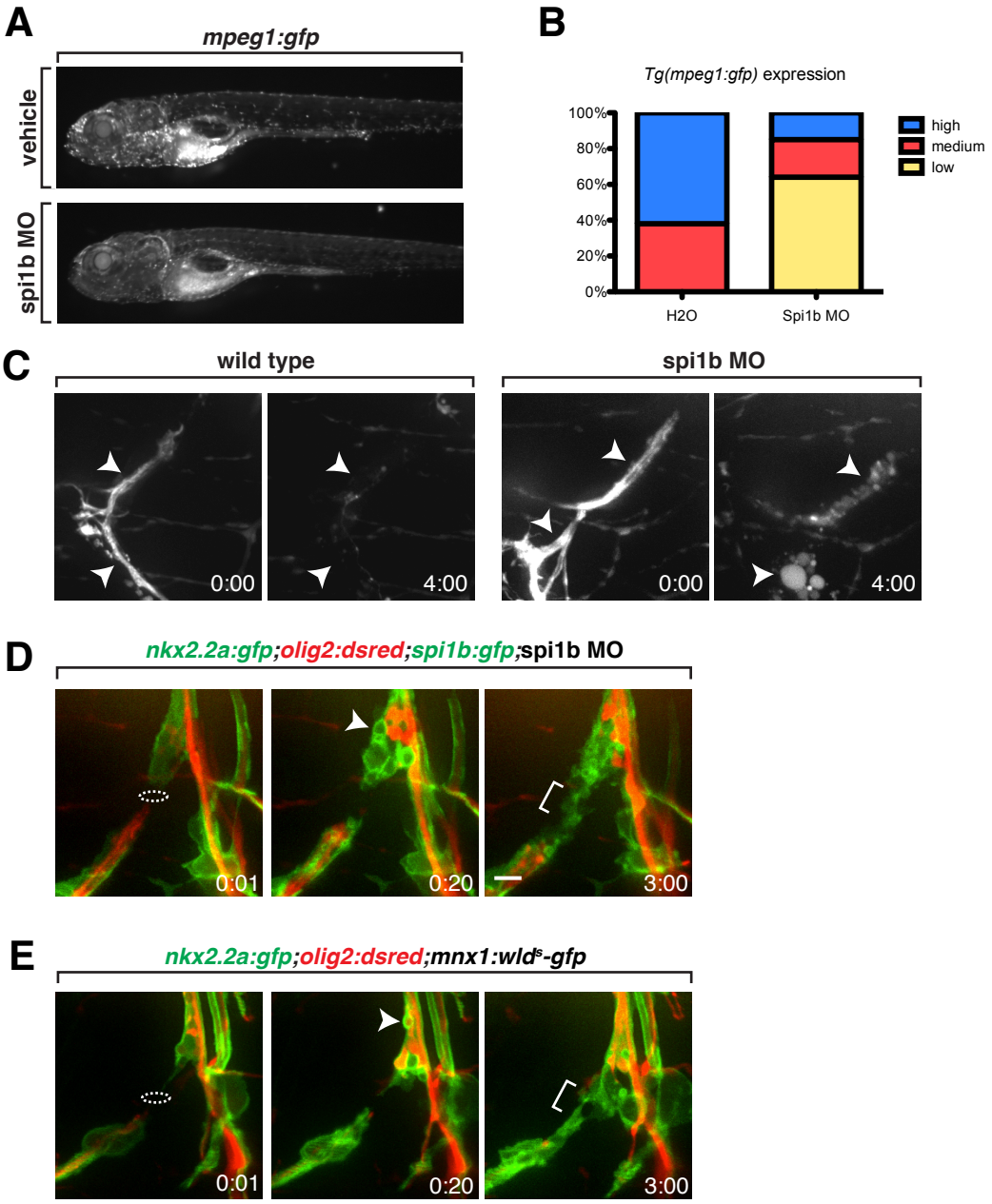

Figure 4-10: Perineurial glia respond normally to transections in the absence of macrophages or Wallerian degeneration. (A) 6 dpf larvae that were injected with spi1b MO are morphologically similar to vehicle control (water) injected larvae, but have decreased *mpeg1:gfp* expression. (B) % of larvae with low, medium, or high expression shows *mpeg1:gfp* was decreased in spi1b morphants. H2O injected n=29 larvae, MO injected n=53 larvae. (C) Frames taken from time-lapse movies of *olig2:dsred* expression in distal stump axons shows more debris is present at 4 hpt in spi1b morphants then in wild type. (D) Rostral motor nerves were transected in a 6 dpf *nkx2.2a:gfp;olig2:dsred;s-pi1b:gfp spi1b* MO-injected larva that lacked macrophages. Perineurial glia responded similarly to non-injected controls by phagocytizing debris (arrowhead) and bridging the injury gap (bracket). (E) Rostral motor nerves were transected in a 6 dpf *nkx2.2a:gfp;olig2:dsred;mnx1-wlds:gfp* larva where Wallerian degeneration was significantly delayed. Again, perineurial glia responded similarly to controls by phagocytizing debris (arrowhead) and bridging the injury gap (bracket). Scale bar: 5 μm.

fragmentation and degeneration is responsible for eliciting perineurial glial activity after injury. To test this hypothesis, we transected nerves in *mnx:Wld^{s}-gfp* larvae, in which motor neurons express the Wallerian degeneration Slow (Wld^{s}) protein (Rosenberg et al., 2012). Expression of Wld^{s} significantly delays Wallerian degeneration through a conserved axon-intrinsic mechanism (Lunn et al., 1989; Martin et al., 2010; MacDonald et al., 2006; Adalbert et al., 2005; Rosenberg et al., 2012) and has been shown to suppress aspects of glial activation in mouse and *Drosophila* (Lunn et al., 1989; MacDonald et al., 2006). Surprisingly, after axotomy in these mutants (n=6), perineurial glia phagocytized debris and bridged injuries in a manner that was indistinguishable from control larvae (compare Figure 4-10E to Figure 4-3), suggesting that Wallerian degeneration is not necessary for perineurial glia to respond to injuries in our assay.

Finally, we investigated the possibility that Schwann cells are required for the perineurial glial injury response. Nerve injury induces Schwann cells to release cytokines and growth factors that are responsible for recruiting macrophages and promoting axon regrowth (Chen et al., 2007; Vargas and Barres, 2007; Lutz and Barres, 2014; Napoli et al., 2012). Additionally, previous studies demonstrate that Schwann cells communicate reciprocally with perineurial glia during development, and that development of either cell type is disrupted in the absence of the other (Kucenas et al., 2008; Binari et al., 2013). This raised the intriguing possibility that signals released by Schwann cells could be responsible for eliciting perineurial glial responses after injury. To investigate this hypothesis, we transected nerves in 4 dpf *nkx2.2a:gfp;ntb:dsred;colourless^{m241} (cls)* mutant larvae, which are deficient for *sox10* and lack motor nerve-associated Schwann cells (Table 2-2) (Dutton et al., 2001). Although oligodendrocyte precursor cells (OPCs)

exit the spinal cord in *cls* larvae, they do not ensheath axons and die before 4 dpf (Kucenas et al., 2009). However, even in the absence of all other peripheral glia, we found that some perineurial glial cells still migrated from the spinal cord into the periphery and remained associated with motor nerves after OPCs died (Figure 4-11A). Although perineurial glia were present, they were sparse and did not form contiguous sheaths (Figure 4-11A). Therefore, we transected unensheathed axons to test the ability of neighboring perineurial glial cells in 4 dpf *cls* larvae to respond to injury (n=8). As in wild-type, transections were made approximately 10-15 μm away from the nearest perineurial glial cell (average distance between perineurial glia and transection site was 12.43 ±0.9436, n=7 in wild type and 10.89 ±1.144 n=8 for *cls*, not significant), and there was no relationship between the distance from transection site and the perineurial response time for either genotype (Figure 4-11B). Unlike wild-type larvae (Figure 4-9B and Movie 4-2), we observed that transection in *cls* larvae induced only minimal extension of perineurial processes toward injury sites (Figure 4-11A,C and Movie 4-3). However we still observed phagocytic vesicles along the proximal stump as it degenerated in all cases for both *cls* (n=8) and wild-type larvae (n=7) (Figures 4-9B and 4-11A and Movies 4-2 and 4-3). These data demonstrate that perineurial glia are significantly less attracted to injury sites in the absence of Schwann cells, but remain competent to phagocytize debris. Taken together, these studies are consistent with the hypothesis that perineurial glial behaviors after nerve injury are not dependent on signals from macrophages or degenerating axons. Instead, they appear to require interactions with Schwann cells, much like they do during development.

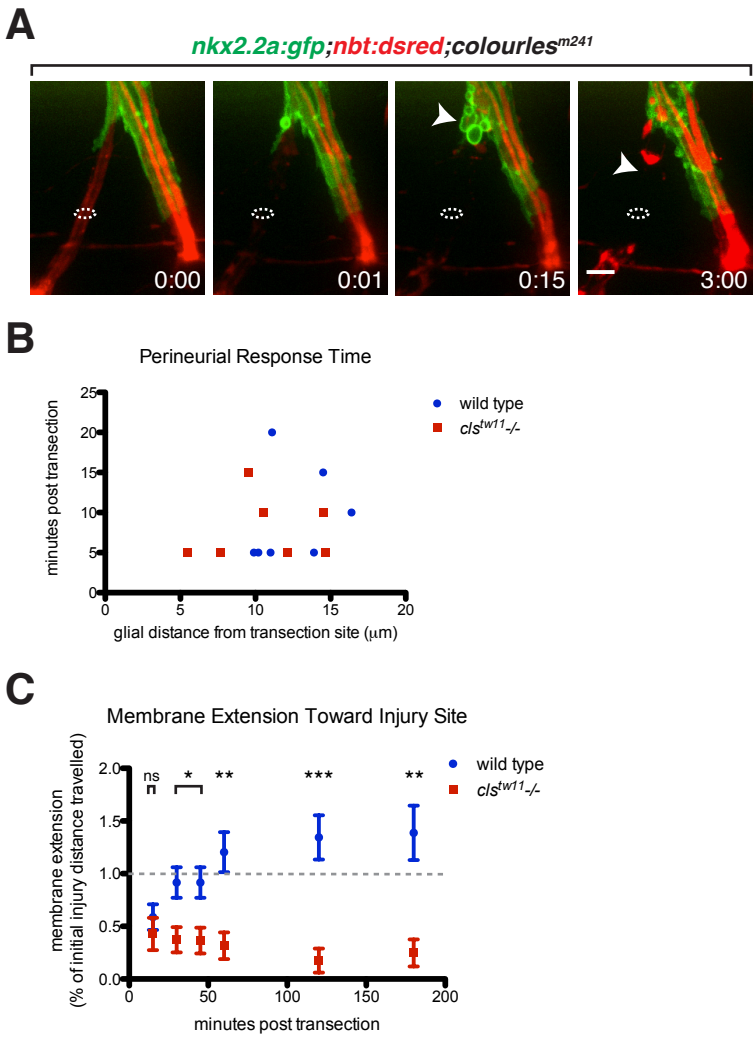

Figure 4-11: Perineurial glia require Schwan cells for their response to injury. (A) Perineurial glia phagocytized debris (arrowhead) but did not extend processes towards the injury site in a 4 dpf *nkx2.2a:gfp;nbt:dsred;colourless* mutant larva (compare to Figure 4-9B). (B) Graphical representation of the perineurial response time in wild type and *cls* larvae shows there is no relationship between the distance of glial cells from the transection site and response time in these experiments. The number of minutes post transection it took perineurial glia to begin extending processes toward injuries or phagocytize debris was plotted by the initial distance between the glial cells and the transection site. (C) Quantification of the extension of perineurial processes toward transection sites in wild type and *cls* larvae shows perineurial glia extend processes significantly further in wild type. Because the initial distance between the injury site and glial cells varied slightly with each trial, membrane extension was plotted as a percentage of the initial injury distance traveled, where values greater than 1 represent processes that have extended beyond the initial injury site. P values for each time point assessed are as follows: 15 mpt, p = 0.43966 (ns); 30 mpt, p = 0.01204 (*); 45 mpt, p = 0.02885 (*); 60 mpt p = 0.00159 (**); 120 mpt, p = 0.00037 (***); 180 mpt, p = 0.00268 (**). Scale bar: 5 μm.

Discussion

Peripheral nerve regeneration has long been a subject of intense study. However, the role of perineurial glia in this process has remained somewhat elusive. Some have hypothesized that perineurial cells may be responsible for creating the first bridge across the injury gap (Scaravilli, 1984; Schroder et al., 1993) and others have shown that the perineurium dramatically changes its structure along proximal and distal stumps after transection (Morris et al., 1972; Thomas and Jones, 1967). Here, we provide the first detailed account of dynamic perineurial glial behaviors after nerve transection. We show that spinal motor root axon transection induces rapid changes in the membrane activity of perineurial glia, with cells immediately adjacent to the injury extending highly motile processes towards the transected area and phagocytizing debris. Perineurial glial membranes then bridge injury gaps, and we demonstrate that these bridges are essential for guiding axon regrowth (Figure 4-12). We also show that perineurial glia do not require signals from other perineurial glia or macrophages for this response, and they respond normally even in the absence of Wallerian degeneration. Interestingly, perineurial glia do require Schwann cells for specific aspects of their injury response, much like they do during development. These data shed light on novel behaviors of perineurial glia after motor nerve injury and raise the intriguing possibility that they may be involved in other degenerative diseases of the PNS as well.

Perineurial glial phagocytic behavior

Macrophages and Schwann cells are the primary cells involved in debris clearance after nerve injury in the PNS. Schwann cells begin phagocytosis of myelin immediately after

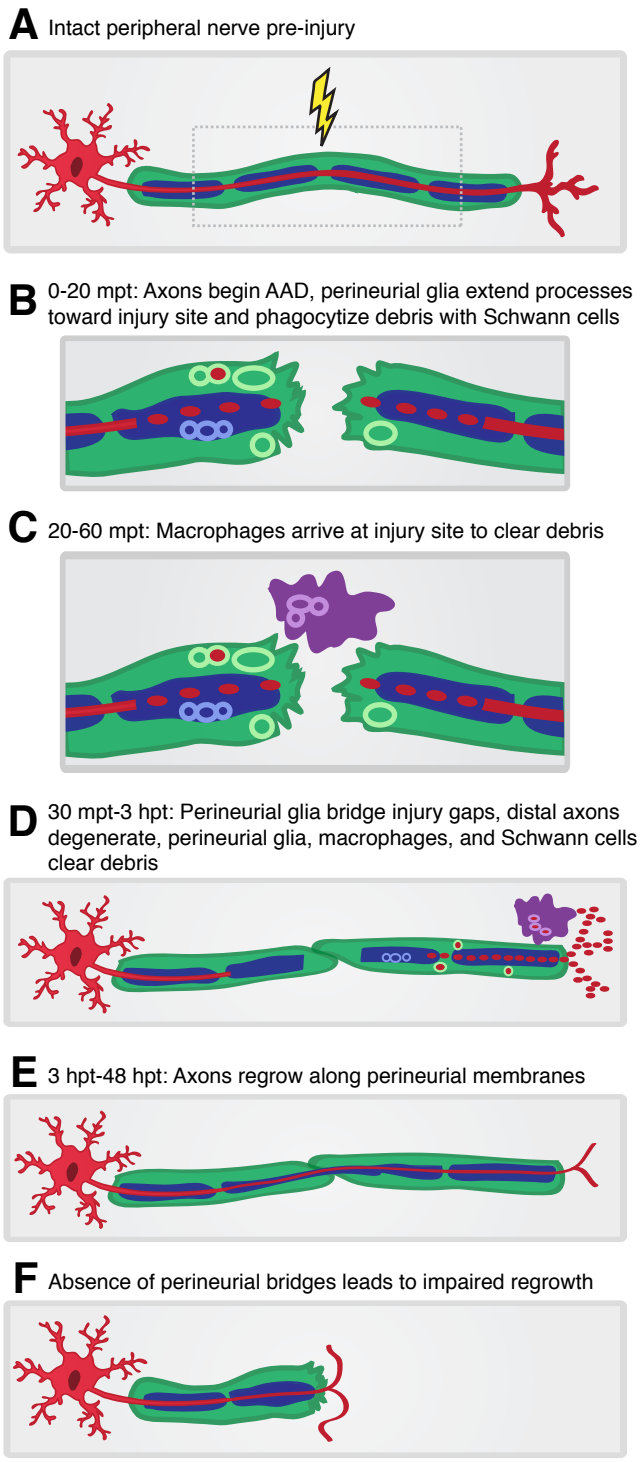

Figure 4-12: Model of perineurial glial response to motor nerve injury. Depicted timeline is an approximation based on data collected for this manuscript and highlights typical perineurial behaviors. Precise behaviors and response times vary for individual transections. Motor neurons are red, Schwann cells are blue, perineurial glia are green, macrophages are purple. Light circles are phagocytic vesicles.

injury and macrophages infiltrate nerves soon after (Perry et al., 1995; Liu et al., 1995) (Hirata and Kawabuchi, 2002; Vargas and Barres, 2007). Our data support these findings and demonstrate that perineurial glia are phagocytic and aid in debris clearance as well. This data is fitting with several electron microscopy studies that noted the presence of vesicles within perineurial cells along the proximal stump of transected mouse sciatic nerves (Morris et al., 1972; Roytta et al., 1987), and within the cells that form the initial bridge between transected stumps (Scaravilli, 1984). However, despite these observations, the authors stopped short of concluding that perineurial glia are phagocytic, as it is very difficult to determine the identity and origin of individual cells by electron microscopy after transection. Using *in vivo* imaging in a live system that allows for the specific and continuous visualization of perineurial glia, we demonstrate that perineurial glia are phagocytic.

Temporally, our data reveal that perineurial glial phagocytic vesicles are particularly abundant along the proximal stump immediately after injury, which is consistent with our data showing that proximal stump AAD occurs more rapidly than distal stump AAD. This is in contrast to mammalian systems, where AAD is reported to occur symmetrically along both stumps (Kerschensteiner et al., 2005). Spatially, our studies reveal that while perineurial glia focus on clearing debris along the degenerating stumps immediately after injury, macrophages tend to focus initially on the injury gap. These data are consistent with the hypothesis that macrophages and perineurial glia may coordinate debris clearance in different areas and raises the intriguing possibility that distinct phagocytic populations may selectively clear specific debris. In contrast, our studies showed that Schwann cell vesicles formed along the proximal stump shortly after

injury, and later along the distal stump, similar to perineurial glia. However, it is still possible that perineurial glia and Schwann cells phagocytize different types of debris in these regions. In the future, investigations into: 1) how debris clearance is coordinated between perineurial glia, Schwann cells and macrophages and 2) the molecular mechanisms that drive perineurial glial phagocytosis, will produce a more complete picture of nerve degeneration.

Perineurial glial bridges are required for regeneration

Previous studies in mammalian systems demonstrate that after sciatic nerve transection, a tissue bridge forms connecting the proximal and distal stumps, which axons and Schwann cells use while regenerating (McDonald and Zochodne, 2003; McDonald et al., 2006). The precise importance of this initial tissue bridge and the origin of the cells that construct it are not well understood, though several studies have proposed that this bridge is formed by perineurial cells (Scaravilli, 1984; Schroder et al., 1993). A study by Parrinello et al. in 2010 described that fibroblasts within this bridge are required to direct the formation of Schwann cell bands, and therefor affect axon regrowth (Parrinello et al., 2010). In a recent study (Clark et al., 2014) we demonstrated that a subset of mammalian perineurial cells express *Nkx2.2* and are CNS derived, similar to zebrafish, raising the intriguing possibility that the fibroblasts described by Parrinello et al. may be perineurial glia.

Our data unequivocally show that perineurial glia bridge injury gaps within the first few hours after transection, and this behavior occurs well before regenerating axons or Schwann cells are found in this region. When we tested the requirement of perineurial

glial bridges by either eliminating perineurial glia or creating injuries too large to be bridged, axon regrowth was impaired, frequently resulting in no regrowth and aberrant sprouting. Collectively, this data is consistent with the hypothesis that axons regrow along perineurial glial bridges and that these bridges are required for efficient regeneration of the nerve. In our DAPT treatment studies, we did observe some cases where axons regrew in the absence of perineurial bridges, and it is possible that Schwann cells and/or remaining axon guidance cues were sufficient to direct axon regrowth. We did not assay Schwann cells in these studies because previous work in the lab has demonstrated that a lack of perineurial glia due to Notch perturbation results in a deficit of peripheral myelin along spinal motor nerves (Binari et al., 2013). While we cannot rule out that reduced or improperly differentiated Schwann cells are a factor in our conclusions, there is currently no method available to eliminate perineurial glia without affecting Schwann cell development. Together, our data demonstrate that axon regrowth is most successful when perineurial bridges are formed.

What are the signals that drive perineurial glial behavior after nerve injury?

Nerve regeneration is a precisely coordinated process requiring communication between multiple cell types and previous studies have shown that axons, Schwann cells and macrophages are all capable of releasing factors that affect neighboring cells (Klimaschewski et al., 2013; Chen et al., 2007; Zochodne, 2012). Because we never observed extensive motility in perineurial processes or phagocytosis in the absence of nerve injury, we reasoned perineurial activation had to be a result of changes to the nerve environment due to transection. Our studies reveal that the initial perineurial glial

response to injury is independent of macrophages, degenerating axons and other perineurial glia. However, although distal axon fragmentation is not required for perineurial responses, we cannot rule out the possibility that signals released by fragmenting axons undergoing AAD, or damaged axons at the injury site, may elicit perineurial behavior.

We have previously demonstrated that perineurial glia and Schwann cells communicate reciprocally during development (Kucenas et al., 2008; Binari et al., 2013), and Schwann cells are known to release a variety of factors in response to injury that effect surrounding cells, including NGF, BDNF, LIF, MCP-1, and TNFα (Jessen and Mirsky, 2008; Vargas and Barres, 2007). Therefore, we hypothesized that these cell populations may communicate following nerve injury. Using mutants where all motor Schwann cells are absent, we observed that perineurial glia were less attracted to injury sites. While we cannot rule out the possibility that changes in perineurial behavior are due to disrupted perineurial glial differentiation in these mutants, there is currently no alternative approach to eliminate Schwann cells without perturbing perineurial glia.

Our data are consistent with the hypothesis that Schwann cells may be involved in either attracting perineurial glia to injury sites or that their damage during injury releases factors that lead to perineurial invasion into the injury gap. Interestingly, perineurial glia did form phagocytic vesicles in these studies, suggesting that perineurial attraction and phagocytic behavior are independent activities. This is reminiscent of what is seen in *Drosophila*, where different signaling pathways mediate glial activation and phagocytosis of debris (Ziegenfuss et al., 2012). This is also consistent with our data showing perineurial glia do not routinely bridge large injury gaps, which suggests that while

perineurial glia can be activated in the absence of perineurial-derived cues, they may still coordinate during bridging. Future studies will focus on elucidating the precise mechanisms by which perineurial glia communicate with other cell types after nerve injury, and determine if Schwann cell-perineurial glial signaling is reciprocal as it is during development.

In summary, we demonstrate that perineurial glia are essential for motor nerve regeneration. Immediately after injury, perineurial processes are rapidly attracted to nerve injuries and aid Schwann cells and macrophages in phagocytizing debris. Perineurial glia then bridge injury gaps before axons and Schwann cells and these bridges are essential for axon regrowth. Collectively, our work highlights the essential function of perineurial glia in nerve regeneration and provides insight into how these cells can be utilized to promote better regeneration in nerve injury patients.

Chapter 5

Perineurial glia require Schwann cells for their differentiation and response to injury

(Pertinent findings that are not my own are cited as Morris et al., in prep)

Abstract

Development and regeneration of vertebrate peripheral nerves requires the coordinated efforts of several distinct cell populations, including axons, Schwann cells and perineurial glia. The interactions between Schwann cells and axons are continuous and have been studied extensively, but how and if Schwann cells communicate with perineurial glia is poorly understood. Here, I have used multiple genetic and pharmaceutical perturbations in zebrafish to investigate how disrupting Schwann cells affects the ability of perineurial glia to develop and respond to injury. I show that in *gpr126* and *erbb3* mutants, which lack myelin and Schwann cells respectively, perineurial glia are present along motor nerves but fail to properly differentiate, suggesting that Schwann cells help mediate perineurial development. I also demonstrate that the recruitment of perineurial processes to nerve injury sites is impaired in *erbb3* mutants and when Erbb signaling is inhibited, suggesting that Schwann cells help attract perineurial glia to injury sites using signals downstream of Erbb activation. Interestingly, other aspects of the perineurial injury response were intact in *erbb3* mutants, suggesting signals from multiple cell types mediate different aspects of perineurial glial injury behavior. Collectively, these data show that Schwann cells and perineurial glia communicate during both peripheral nerve development and regeneration, and shed new light on the poorly understood role of glial-glial interactions in the PNS.

Introduction

The vertebrate PNS is composed of a complex network of nerves responsible for transmitting vital information to and from the CNS. The ability to develop, maintain and regenerate these nerves is essential for an organism's survival. As described Chapter 1, peripheral nerves are composed of axons that are myelinated by Schwann cells and bundled into fascicles by the perineurium, which is a protective sheath formed by several layers of perineurial glial cells (Burkel, 1967; Bourne, 1968; Krisrensson and Olsson, 1971; Akert et al., 1976; Kucenas et al., 2008; Clark et al., 2014). Previous work from the lab and the data presented in Chapter 4 suggest that Schwann cells and perineurial glia communicate and coordinate their behavior during both nerve development and regeneration (Kucenas et al., 2008; Lewis and Kucenas, 2014). However, the timing and nature of these interactions is not well understood.

Nerve development requires all cells within the nerve to precisely coordinate their migration and differentiation. This process begins when motor neurons project axons out of the spinal cord and into the periphery through MEPs. Meanwhile, a subset of neural crest cells migrates ventrally along the spinal cord and associates with the outgrowing axons. These cells migrate, proliferate, sort and ensheath axons while undergoing sequential differentiation from neural crest, to SCPs, to ISCs, and finally to mature Schwann cells (for review see (Jessen and Mirsky, 2005 and Chapter 1). Activation of the heterodimeric receptor complex Erbb2/Erbb3 on Schwann cells by axonal Neuregulin1 type III (Nrg1-III) is required continuously throughout this differentiation process (Birchmeier, 2009). Perineurial glia migrate into the periphery through MEPs shortly after the association of Schwann cells and eventually ensheath on top of motor axons and Schwann cells, differentiating into the mature perineurium (Kucenas et al., 2008). Schwann cells and perineurial glia both play

essential roles in motor nerve assembly, and evidence suggests these cells signal reciprocally during development. (Kucenas et al., 2008; Binari et al., 2013 and Chapter 1). However, precisely what aspects of perineurial development require signals from Schwann cells is not known.

Peripheral nerves have the remarkable capacity to regenerate after injury, which again requires the precise coordination of multiple cell types. As reviewed in Chapter 1, nerve transection induces a regenerative program whereby distal axons degenerate, debris is cleared, and new axons regrow from the proximal stump back to peripheral targets. Schwann cells aid in this process by phagocytizing myelin debris, recruiting macrophages, and helping to guide regrowing axons (Arthur-Farraj et al., 2012; Rosenberg et al., 2014). In Chapter 4 I showed that perineurial glia respond to injury by extending processes toward injury sites, phagocytizing debris, and forming the first tissue bridge across the injury gap. I also showed that the recruitment of perineurial processes to injury sites is impaired in the zebrafish *cls* mutant, which lacks Schwann cells (Chapter 4 and Lewis and Kucenas, 2014). This suggests that Schwann cells may signal to perineurial glia during regeneration as they do during development, but I did not investigate this extensively, and a mechanism for this is still unknown.

Here I shed light on the precise role that Schwann cell-perineurial glial interactions play in nerve development and regeneration. By characterizing the perineurial phenotype in multiple zebrafish mutants that affect Schwann cells, I demonstrate that Schwann cells are not required for perineurial glial migration during development. However, they are essential for proper perineurial differentiation. Additionally, using *erbb3* mutants that lack Schwann cells along motor nerves, I present further evidence that Schwann cells aid in the attraction of

perineurial processes to injury sites after nerve transection. Interestingly, pharmaceutical inhibition of Erbb receptor activation mimics the response seen in *erbb3*, suggesting that Schwann cells re-activate Erbb signaling after injury, and that this activation is upstream of signaling to perineurial glia. This work highlights the importance of glial-glial interactions during nerve development and regeneration.

Results

Perineurial glia migrate into the periphery in the absence of myelin and Schwann cells

Previous experiments performed during early zebrafish development concluded that Schwann cells were required for perineurial glia to exit the spinal cord (Kucenas et al., 2008; 2009b). In *colourless (cls)* mutants, which harbor a mutation in the transcription factor *sox10* (Dutton et al., 2001), Schwann cells migrate to motor roots, but do not wrap axons and eventually die (Kucenas et al., 2008; 2009b). Double mutant *mont blanc (mob)* (Barrallo-Gimeno, 2004) and *mother superior (mos)* (Montero-Balaguer et al., 2006) embryos, which have mutations that disrupt *tfap2a* and *foxd3* respectively, lack all neural crest and subsequently, lack Schwann cells along motor axons (Arduini et al., 2009; Kucenas et al., 2009b; Wang et al., 2011). Early time-lapse imaging experiments (3 dpf and before) suggested that perineurial glia did not exit the spinal cord or ensheath motor axons in either of these mutant lines (Kucenas et al., 2008; 2009b). However, subsequent imaging of *cls* larvae at later stages (4 and 6 dpf) revealed that some perineurial cells still exited the spinal cord and ensheathed motor axons, although they appeared sparse and did not form contiguous sheaths (Lewis and Kucenas, 2014). This led me to hypothesize that perineurial

glia may not in fact require Schwann cells to exit the spinal cord, but may require them for other aspects of their development.

To investigate further how perineurial migration is affected by Schwann cells, I began by looking for the presence or absence of perineurium in two additional zebrafish mutants that affect Schwann cell development: *gpr126* and *erbb3* (Table 2-2). This was done using live imaging in double transgenic *nkx2.2a:gfp*;*sox10:rfp* larvae to label perineurial glia and Schwann cells respectively (Table 2-1). I assessed the perineurium at 4 dpf, as previous work has shown that perineurial glia have finished migrating from the CNS into the periphery, and have begun wrapping on top of Schwann cells and motor axons by this time point (Kucenas et al., 2008; Lewis and Kucenas, 2014) (Figure 5-1A). Consistent with this, I observed *nkx2.2a*$^{+}$ perineurial glia in the periphery in 4 dpf wild type *nkx2.2a:gfp*;*sox10:rfp* larvae, which appeared to wrap on top of *sox10*$^{+}$ Schwann cells (Figure 5-1B).

To determine if perineurial glial exit is affected by Schwann cell differentiation, I used *gpr126* mutants. As described in Chapter 1, Gpr126 encodes a G protein-coupled receptor that is required autonomously in Schwann cells to initiate myelination. Previous studies showed that Schwann cells are present in *gpr126* zebrafish, but they fail to terminally differentiate, stall in the pro-myelinating phase, and lack expression of myelin associated genes (Monk et al., 2009). In accordance with this, I observed that *sox10*$^{+}$ Schwann cells were present along motor nerves in *gpr126* larvae at 4 dpf (Figure 5-1C). Interestingly, perineurial glia were also present along motor nerves and appeared morphologically similar to wild type (Figure 5-1C), suggesting that myelinating Schwann cells are not required for perineurial migration into the periphery.

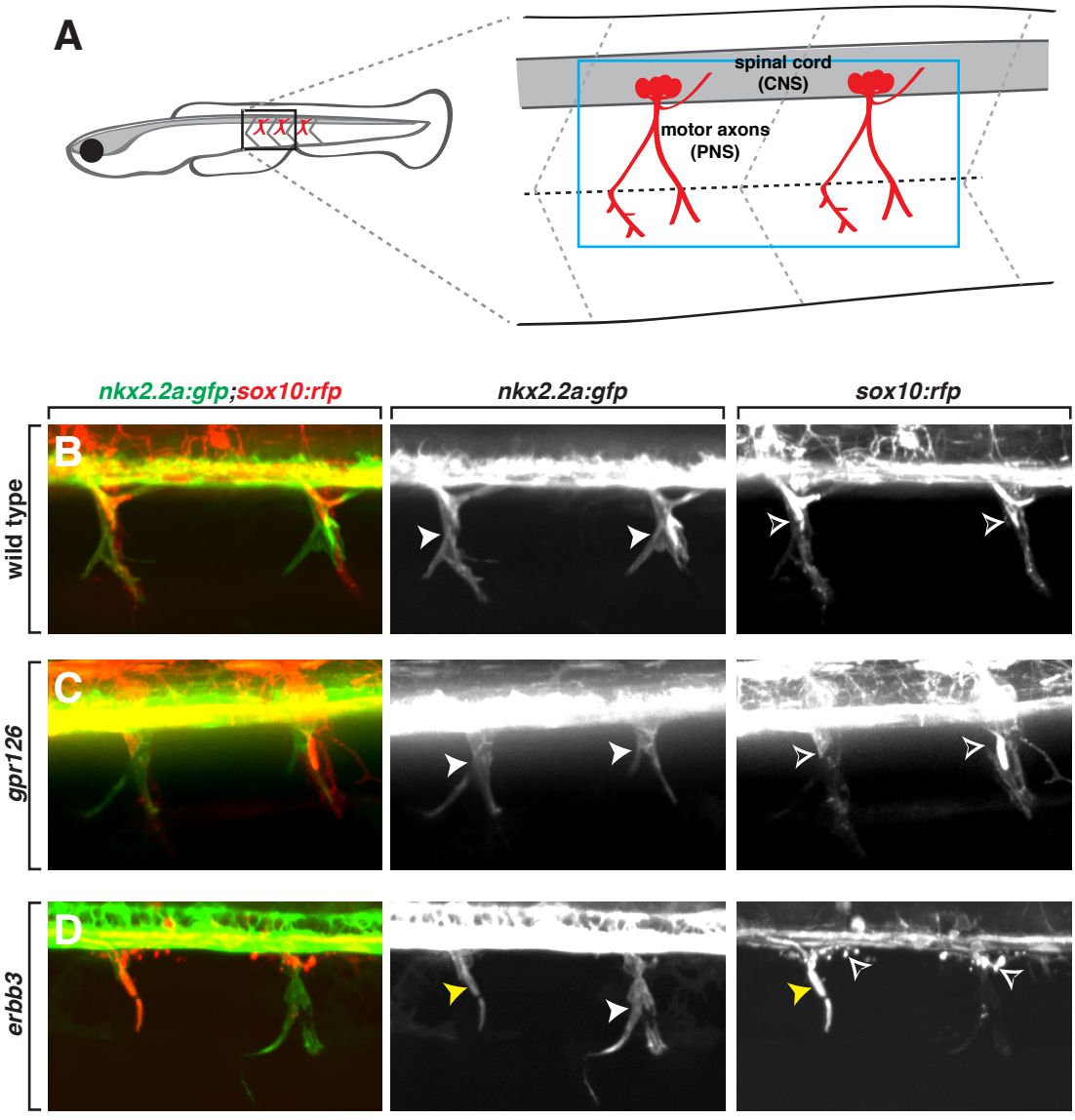

Figure 5-1: Perineurial glia are present in the periphery of *gpr126* and *erbb3* larvae. (A) Diagram depicts a 4 day post fertilization (dpf) zebrafish larva and blue box denotes the approximate area that was imaged in subsequent frames. (B-D) are live images from 4 dpf *nkx2.2a:gfp;sox10:rfp* larvae with anterior to left and dorsal to top. (B) *nkx2.2a*$^{+}$ perineural glia and *sox10*$^{+}$ Schwann cells were present in the periphery in wild type. (C) *nkx2.2a*$^{+}$ perineural glia and *sox10*$^{+}$ Schwann cells were also present in the periphery in *gpr126* larvae. (D) *nkx2.2a*$^{+}$ perineural glia were in the periphery in *erbb3*, along with s*ox10*$^{+}$ Schwann cell debris and double *nkx2.2a*$^{+}$*;sox10*$^{+}$ wrapping cells. White arrowheads denote *nkx2.2a*$^{+}$ perineurial glia, filled arrowheads denote *sox10*$^{+}$ Schwann cells and yellow arrowheads denote double *nkx2.2a*$^{+}$*;sox10*$^{+}$ cells.

To determine if perineurial glia can migrate into the periphery in the absence of Schwann cells, I used *erbb3* mutants. As described in Chapter 1, signaling through the Erbb2/Erbb3 tyrosine kinase receptor complex is required continuously throughout Schwann cell development (Riethmacher et al., 1997; Lyons et al., 2005; for review see Birchmeier, 2009), and Schwann cells are absent along peripheral nerves in both mouse and zebrafish *erbb3* mutants (Riethmacher et al., 1997; Lyons et al., 2005; Smith et al., 2014). This provided an additional avenue to test whether perineurial glia would be able to migrate into the periphery in the absence of Schwann cells. Consistent with previous reports, when I live imaged 4 dpf *nkx2.2a:gfp*;*sox10:rfp erbb3* embryos, I did not observe intact *sox10*$^{+}$ Schwann cells along motor nerves (Smith et al., 2014). However, I did observe bright puncta of *sox10*$^{+}$ debris near motor roots (Figure 5-1D), indicating neural crest cells had migrated to the motor root, but were unable to proceed further and died. I also observed cells that appeared to be ensheathing motor axons and were double positive for both *sox10* and *nkx2.2a*. I hypothesize these cells are oligodendrocytes or their precursors, which myelinate exclusively in the CNS of wild type embryos. Oligodendrocyte precursor cells (OPCs) express both *sox10* and *nkx2.2a* (Kucenas et al., 2009a; 2009b), and a previous study from the lab demonstrated that these cells aberrantly exited the spinal cord and myelinated motor nerves in *erbb3* embryos (Smith et al., 2014). Interestingly, even in the absence of Schwann cells and the presence of oligodendrocytes, *nkx2.2a*$^{+}$ perineurial glia were still observed in the periphery (Figure 5-1D and unpublished data from Morris et al., in prep). Collectively, these data suggest that perineurial glia are able to migrate into the periphery regardless of whether Schwann cells are present and differentiated.

Perineurial glia form minifascicles in the absence of differentiated Schwann cells

I demonstrated above that perineurial glia are able to migrate into the periphery in *gpr126* mutants, in which Schwann cells are present but do not myelinate. This is not entirely surprising in light of the fact that most perineurial glia exit the spinal cord by 48 hpf (Kucenas et al., 2008), which is before the onset of myelination in zebrafish. This raised the possibility that although initial migration is normal, later stages of perineurial development may be affected in these mutants. In support of this, a previous study showed fasciculation defects in the perineurium of *Gpr126* mouse sciatic nerves (Monk et al., 2011). To determine if perineurial defects are present in *gpr126* zebrafish, I began by live imaging the spinal motor nerve root in 6 dpf *nkx2.2a:gfp*;*sox10:rfp* wild type and *gpr126* larvae. Consistent with my previous reports (Chapter 4 and Lewis and Kucenas, 2014), I observed that the perineurial membrane usually appeared to ensheath the entire motor nerve root in wild type larvae (Figure 5-2A), which contains approximately 70 motor axons (Westerfield et al., 1986). This sheath was presumed to encase the entire axon bundle and nerve associated Schwann cells, as has been shown previously (Kucenas et al., 2008; Lewis and Kucenas, 2014). My initial assessment of perineurial ensheathment in *gpr126* larvae was that it appeared indistinguishable from wild type (Figure 5-2B). However, upon further inspection, I was able to identify several instances where the *nkx2.2a*$^{+}$ perineurial membrane appeared to ensheath directly on top of the *sox10*$^{+}$ Schwann cell sheath, as opposed to ensheathing around the perimeter of the entire axon bundle (Figure 5-2C). This abnormally tight ensheathment of Schwann cells was never observed in wild type larvae. This led me to hypothesize that perineurial glia were in the beginning stages of exhibiting fasciculation defects in *gpr126* larvae, and that these defects may be more evident at later stages.

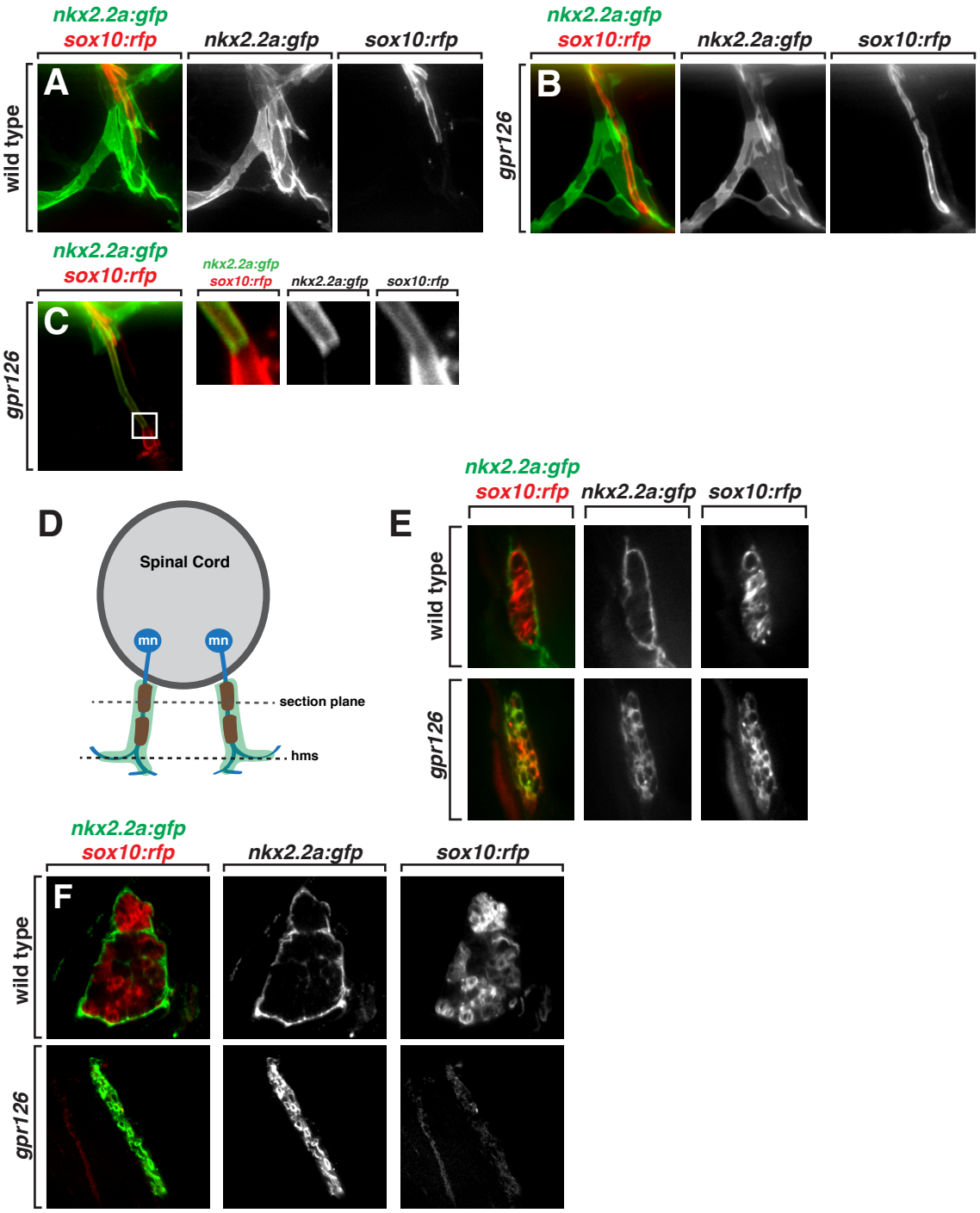

Figure 5-2: The perineurium forms minifascicles in *gpr126* mutants. All images are from *nkx2.2a:gfp;sox10:rfp* zebrafish. (A-C) are live images from 6 dpf larvae with dorsal to top and anterior to left. (A) Perineurial and Schwann cell ensheathment of the spinal motor nerve root in wild type. (B) Most perineurial and Schwann cell ensheathment in *gpr126* looked similar to wild type. (C) Perineurium was wrapped abnromally tightly on top of Schwann cells in some *gpr126* larvae. (D) Diagram of a transverse section through a zebrafish showing the section plane used in (E and F). (E) Cross section through the motor nerve in a 20 dpf jouvenile showed perineurium at the outter edge of 1 large fascicle in wild type and perineurial minifascicles in *gpr126*. (F) Cross section through an adult motor nerve showed perineurium lined the outter edge of fascicles in wild type and formed small minifascicles in *gpr126*. (mn) motor neuron, (hms) horizontal myoseptum.

To investigate perineurial fasciculation at later stages, I fixed intact 20 dpf and adult zebrafish and sectioned them through a coronal plane (Figure 5-2D). This allowed me to visualize cross sections through the motor nerves and assess perineurial fasciculation during late stages of development (20 dpf) and adulthood (>3 months). In wild type 20 dpf larvae, I observed that the *nkx2.2a*$^{+}$ perineurium was restricted to the exterior of the fascicle, and surrounded many *sox10*$^{+}$ Schwann cells. *sox10* expression generally appeared as rings, representing their wrapping of axons (Figure 5-2E). Interestingly, in *gpr126* larvae, *nkx2.2a*$^{+}$ perineurium was no longer restricted the exterior of the fascicle, and instead appeared as numerous smaller rings or minifasicles. The expression pattern of *sox10* was markedly similar to the expression pattern to *nkx2.2a*, appearing almost colocalized (Figure 5-2E). I believe this represents perineurial glia that ensheathed abnormally tightly on top of Schwann cells, similar to what I visualized at 6 dpf by live imaging (Figure 5-2C), and that I lacked the spatial resolution to distinguish the 2 membranes in these sections. Adult nerves exhibited similar perineurial phenotypes as 20 dpf nerves. In wild type adults, I often observed several larger fascicles, each with perineurium surrounding many *sox10*$^{+}$ Schwann cell rings. In *gpr126* adults, I again saw perineurial invasion into the nerve and the formation of many smaller minifasicles. *sox10* expression was now markedly reduced. I do not believe this represents an absence of Schwann cells, as evidence of Schwann cell death has never been reported at any age in either zebrafish or mouse *Gpr126* mutants. Rather, this likely indicates that signaling through Gpr126 is necessary to maintain *sox10* expression in Schwann cells through adulthood. Importantly, Gpr126 is required autonomously in Schwann cells during nerve development (Monk et al., 2009), thus the presence of perineurial minifasicles in both 20 dpf and adult *gpr126* zebrafish suggests that Schwann cells communicate with perineurial

glia during late stages of development, using signals generated downstream of Gpr126. Combined with earlier data (Figure 5-1), this is also consistent with the hypothesis that perineurial glia do not require Schwann cells to migrate from the spinal cord and ensheath nerves, but do need signals from Schwann cells to properly differentiate and fasciculate the nerve.

Perineurial glia exhibit differentiation defects in the absence of Schwann cells

Signaling though Erbb receptors is essential for many aspects of Schwann cell development, and previous studies have shown that Schwann cells are not present along peripheral nerves in mouse or zebrafish *Erbb3* mutants (Riethmacher et al., 1997; Lyons et al., 2005). My data above showing *sox10*$^{+}$ debris, which is indicative of cell death, near the motor root of *erbb3* embryos is consistent with this. Previous studies in the lab demonstrated that OPCs, which are usually restricted to the CNS, are present in the periphery in *erbb3* embryos (Smith et al., 2014). Oligodendrocytes aberrantly migrate into the periphery in *cls* mutants as well, but do not myelinate motor nerves and eventually die (Kucenas et al., 2009b). Central myelin proteins are expressed along the motor nerves in 8 dpf *erbb3* larvae (Smith et al., 2014), suggesting that unlike in *cls*, OPCs survive and go on to ensheath and myelinate motor nerves. However, this has yet to be visualized by live imaging, and the temporal dynamics of OPC myelination in the periphery are not known. To this end, I live imaged the motor nerve in double transgenic *nkx2.2a:gfp;olig2:dsred erbb3* zebrafish larvae at various stages. The *olig2:dsred* transgene uses regulatory sequences from *olig2* to drive expression of cytosolic DsRed. This can be used to label both motor axons and OPCs (Table 2-1). A subset of OPCs also expresses *nkx2.2a*, and inclusion of the *nkx2.2a:gfp* transgene allowed me to distinguish

OPCs from motor axons. Imaging of wild type *nkx2.2a:gfp;olig2:dsred* embryos at 57 hpf revealed that as expected, *nkx2.2a*$^{+}$ perineurial glia had migrated into the periphery and were already ensheathing motor roots near the MEP (Figure 5-3A). Subsequent imaging of wild type larvae over the next several days revealed that perineurial glia progressively ensheathed more of the nerve, such that the entire root was ensheathed between the MEP and the horizontal myoseptum by 6 dpf (Figure 5-3A). In contrast, when I imaged *nkx2.2a:gfp;olig2:dsred erbb3* embryos at 55 hpf, I observed *nkx2.2a*$^{+}$*;olig2*$^{+}$ OPCs along motor axons (Figure 5-3B). Over the next several days, OPCs ensheathed motor axons, adopted a tube-like morphology, and began expressing central myelin proteins (Figure 5-3B, unpublished data from Morris et al., in prep and Smith et al., 2014). This is consistent with the idea that OPCs in *erbb3* mutants remain on the nerve and myelinate motor axons.

I demonstrated above that perineurial glia were able to exit the spinal cord in both *gpr126* and *erbb3* mutants and that the motor nerve was abnormally fasciculated in *gpr126* mutants, in which Schwann cells are present but do not myelinate. Because *erbb3* mutants lack Schwann cells along the motor nerve entirely, I hypothesized that perineurial development would be affected in these mutants as well. To investigate this, I used live imaging in 6 dpf *nkx2.2a:gfp;olig2:dsred* wild type and *erbb3* larvae and characterized the phenotypes of *nkx2.2a*$^{+}$ cells. The majority of *nkx2.2a*$^{+}$ cells in wild type larvae appeared in an "ensheathing" morphology (Figure 5-4A,B) that is characteristic of perineurial glia (n=12 larvae). Cells were classified as "ensheathing" if their membrane appeared to ensheath over the entire axon bundle of a given axon tract. In contrast, *nkx2.2a*$^{+}$ cells appeared in 3 distinct morphologies in *erbb3* larvae at 6 dpf. The first and most prominent was "tubular" (Figure 5-4C), which I hypothesized represented OPCs wrapping axons as described above (Figure 5-

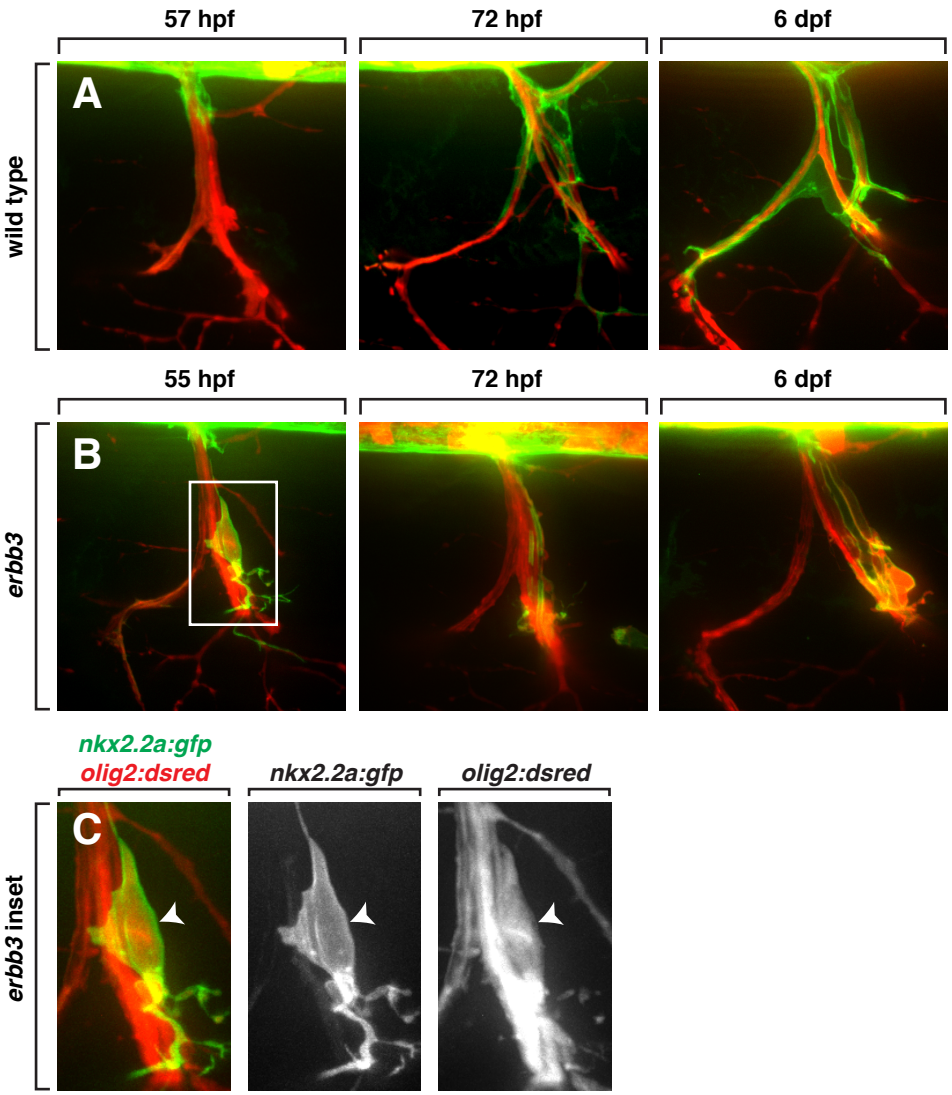

Figure 5-3: Oligodendrocytes wrap peripheral motor axons in *erbb3* larvae. All frames are live images from *nkx2.2a:gfp;olig2:dsred* larvae with dorsal to top and anterior to left. (A) Perineurium progressively ensheathed the motor nerve from 57 hpf to 6 dpf in wild type. (B) OPCs were present along the motor nerves at 55 hpf and wrapped motor axons by 72 hpf and 6 dpf in *erbb3.* (C) Inset from (B), OPC is double labeled with *nkx2.2a:gfp* (membrane tethered GFP) and *olig2:dsred* (cytosilc DsRed).

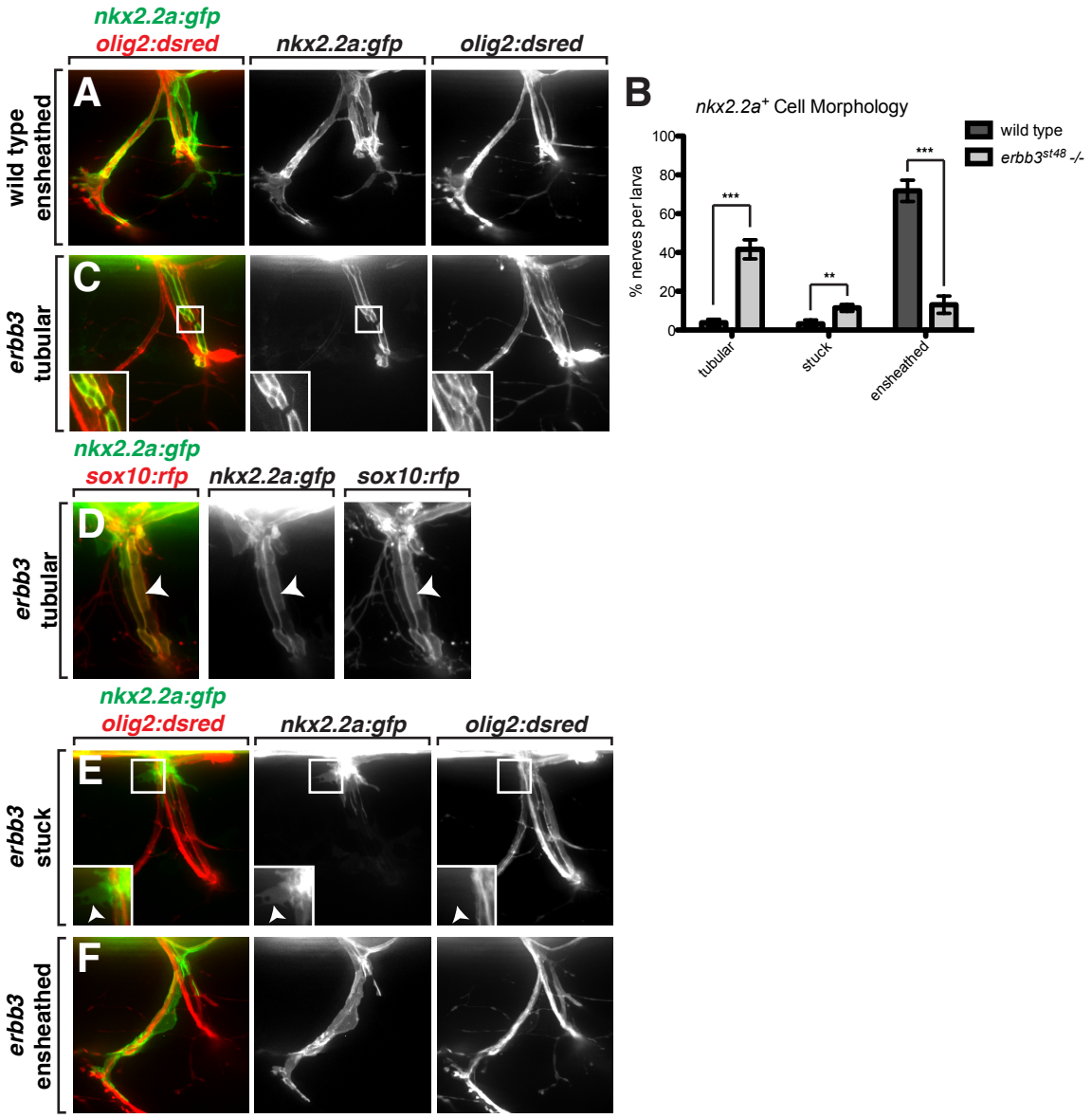

Figure 5-4: *nkx2.2a*⁺ cells appear in 3 distinct morphologies in *erbb3* larvae. All frames are live images from 6 dpf larvae with dorsal to top and anterior to left. (A) Perineurial glia ensheathed spinal motor root axons in wild type. (B) Quantification of *nkx2.2a*⁺ cell morphologies in wild type vs. *erbb3* larvae showed mutants had more nerves with tubular and stuck morphology cells and less nerves with ensheathed morphology cells (tubular $p < 0.0001$, wt = 3.8 ± 1.6, n=12; *erbb3* = 41.6 ± 4.9, n=20) (stuck $p = 0.0057$ wt = 3.2 ± 1.9, n=12; *erbb3* = 11.5 ± 1.8, n=20) (ensheathed $p < 0.0001$ wt = 71.8 ± 5.5, n=12; *erbb3* =13.1 ± 4.5, n=20). (C-F) are from *erbb3* larvae. (C) Tubular morphology on the caudal axon tract. Nodes appear as breaks in *nkx2.2a*⁺ fluorescence. (D) Some tubes are double labeled *nkx2.2a*⁺;*sox10*⁺ indicating they are OPCs. (E) Cells in stuck morphology were not *olig2*⁺ inidcating they are perineurial glia. (F) Ensheathed morphology cells looked similar to wild type perineurial glia, but rarely ensheathed the entire nerve root.

3B). This morphology was present in all mutant larvae examined (n=20 larvae), and was clearly visible along an average of 41.6 ± 4.9% of nerves per larva (Figure 5-4B). Upon closer inspection, I was able to identify breaks in the *nkx2.2a*$^{+}$ tubes, which are characteristic of the Nodes of Ranvier created between myelinated segments (Figure 5-4C). As an additional method to verify that these tubes represented wrapped OPCs, I live imaged 6 dpf *nkx2.2a:gfp;sox10:rfp* wild type and *erbb3* larvae. OPCs and Schwann cells both express *sox10*, but a subset of OPCs also expresses *nkx2.2a*. In wild type larvae, I observed single labeled *sox10*$^{+}$ tubes, which represented wrapped Schwann cells. In *erbb3* larvae, I observed both single labeled *sox10*$^{+}$ tubes and double labeled *nkx2.2a*$^{+}$*;sox10*$^{+}$ tubes; an expression pattern characteristic of OPCs (Figure 5-4D). The second *nkx2.2a*$^{+}$ cell morphology observed in *erbb3* larvae was classified as "stuck" and occurred much less frequently (Figure 5-4B,C). Cells that were "stuck" were located near the MEP and had wispy processes that extended in all directions. Notably, these cells did not express *olig2*, suggesting they were perineurial glia and not OPCs (Figure 5-4E). The third *nkx2.2a*$^{+}$ morphology observed in 6 dpf *erbb3* mutants was "ensheathing". These cells appeared to ensheath the axon bundle in a manner that was very similar to wild type perineurial glia (Figure 5-4F). However, they were observed less frequently in mutants (Figure 5-4B) and rarely covered the entire nerve from the MEP to the horizontal myoseptum. Taken together, these data strongly suggest that the "tubular" morphology is representative of OPCs, while the "stuck" and "ensheathing" morphologies are representative of perineurial glia. It also indicates that perineurial glia are able to migrate from the CNS in *erbb3* mutants, but by 6 dpf, their morphology is varied and often appears abnormal.

Based on the irregular perineurial morphologies I observed in *erbb3* larvae at 6 dpf, I hypothesized that perineurial glia do not differentiate properly in these mutants. To investigate this further, I fixed and sectioned adult *nkx2.2a:gfp;sox10:rfp* wild type and *erbb3* zebrafish to observe cross sections through the motor nerves. I then sought to identify any perineurial abnormalities in the mutants. Surprisingly, I did not see notable differences between wild type and *erbb3* adult nerves based on transgene expression. In wild type, *sox10*$^{+}$ Schwann cell rings were surrounded by an outer *nkx2.2a*$^{+}$ perineurium. Some perineurium was also present within the nerve, dividing it into several large fascicles (Figure 5-5A). A similar pattern of expression was observed in *erbb3* larvae (Figure 5-5B), except that *sox10*$^{+}$ rings were presumed to be oligodendrocytes and not Schwann cells (Figure 5-4D). I did not observe any double labeled *nkx2.2a*$^{+}$*;sox10*$^{+}$ rings within the nerve, suggesting that oligodendrocytes turned down expression of *nkx2.2a* between 6 dpf and adulthood. Interestingly, the appearance of normal perineurial ensheathment and fasciculation of adult *erbb3* nerves suggests that the morphological defects in the perineurium seen at 6 dpf do not persist into adulthood. As an additional way to investigate perineurial differentiation, I performed immunohistochemistry with an antibody to the tight junction protein ZO-1, which is a marker or perineurial differentiation. Consistent with this, I observed small puncta of ZO-1 labeling along the perineurium of adult wild type nerves (Figure 5-5A). ZO-1 labeling was also seen within the fascicles, which may represent junctions between axons and Schwann cells, as has been reported previously (Parmantier et al., 1999). When I stained *erbb3* adult nerves, I observed ZO-1 within the perineurium, but it appeared in abnormally large deposits (Figure 5-5B). This phenomenon was also observed by whole-mount immunohistochemistry at 8 dpf (unpublished data from Morris et al., in prep). Collectively,

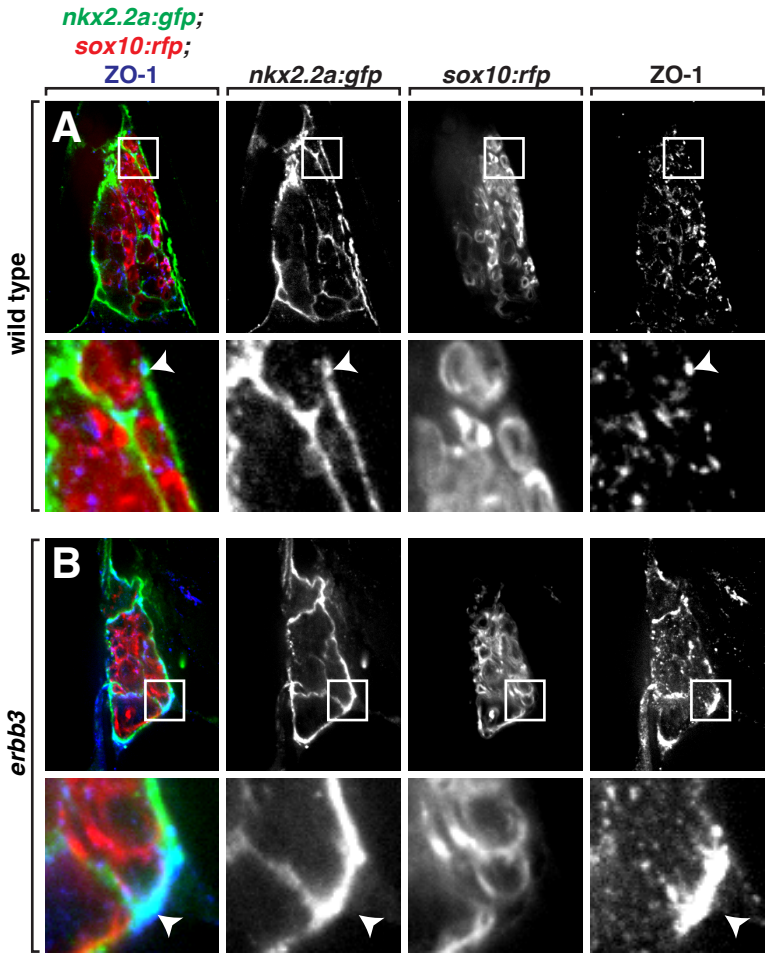

Figure 5-5: The perineurium ensheaths normally but contains large deposits of ZO-1 in *erbb3* adults. All frames are cross sections through the motor nerve root of adult *nkx2.2a:gfp;sox10:rfp* zebrafish. (A) Punctate ZO-1 expression is present along the perineurium and within the fascicle of wild type. (B) Large deposits of ZO-1 expression are present in the perineurium of *erbb3*. Arrowheads point to perineurial ZO-1.

these data demonstrate that perineurial differentiation is disrupted in *erbb3* zebrafish. Taken with the previous findings that perineurial glia aberrantly fasciculate in the absence of Gpr126 (Figure 5-2), this data is consistent with the idea that Schwann cells communicate with perineurial glia throughout development and are necessary to direct their proper differentiation.

The perineurial injury response is impaired in the absence of Erbb signaling

From the data presented above, I hypothesize that Schwann cells signal to perineurial glia during development, and my previous work suggests perineurial glia also require signals from Schwann cells during regeneration. In Chapter 4, I showed that perineurial glia extend dynamic and highly motile processes into injury sites and phagocytize debris. Additionally, I found that the recruitment of perineurial processes to transections along unensheathed axons is impaired in the absence of Schwann cells in *cls* mutants (Chapter 4 and Lewis and Kucenas, 2014). This suggests that Schwann cells may have a role in attracting perineurial processes to injury sites, and led me to hypothesize that recruitment of perineurial processes would be similarly impaired in *erbb3*.

To investigate the perineurial injury response in *erbb3*, I used my previously described assay of motor nerve transection and time-lapse imaging (Chapter 3,4; Lewis and Kucenas, 2013; 2014). Using either *nkx2.2a:gfp;olig2:dsred* or *nkx2.2a:gfp;nbt:dsred* larvae to label perineurial glia and motor axons, I identified motor nerves in 4 dpf larvae that were only partially ensheathed by perineurial glia (Figure 5-6A). I then transected an unensheathed area of the nerve, approximately 10-15μm from the closest perineurial glia, and used time-lapse confocal imaging to visualize the response of the nearby cells. The extent to which

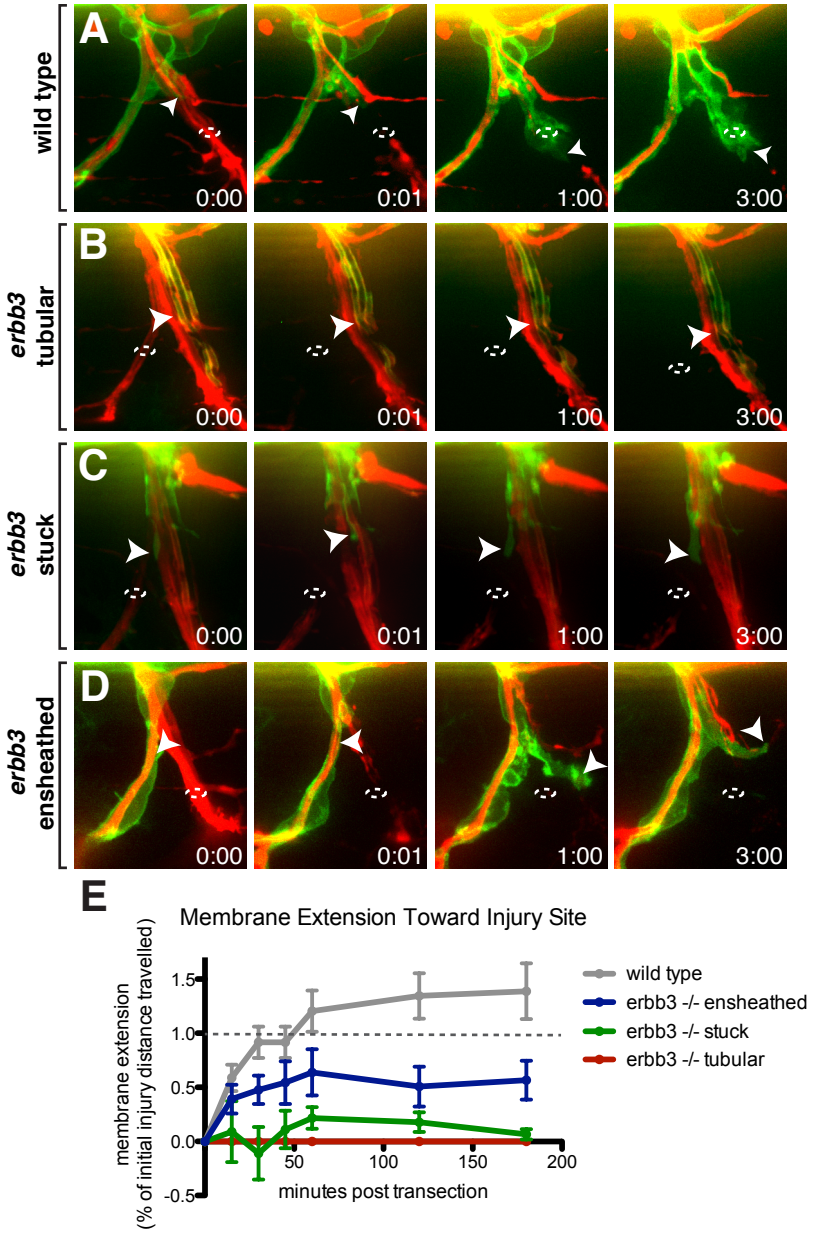

Figure 5-6: Recruitment of perineurial processes to transection sites is impaired in *erbb3* larvae. All images are frames taken from time-lapse movies in 4 dpf *nkx2.2a:gfp;nbt:dsred* (A) *or nkx2.2a:gfp;olig2:dsred erbb3* (B-D) larvae . (A) In wild type, a perineurial glia sent processes toward and beyond the transection site along an unensheathed axon tract. (B) In *erbb3,* a *nkx2.2a*$^{+}$ tubular cell did not respond to transection. (C) A *nkx2.2a*$^{+}$ stuck cell did not send substantial processes toward the transection. (D) A *nkx2.2a*$^{+}$ enstheathed cell sent a process toward the transection site, but it eventually became misdirected. (E) Quantification of the perineurial response to transections along unensheathed axon tracts. A value of 1 represents processes that have reached the original injury site, >1 have extended beyond the injury site, and <1 have not reached the injuty site. Dotted elipse denotes approximate ablated ROI.

perineurial processes extended toward the injury site was measured over the course of the next 3 hours. As I reported previously, wild type perineurial glia rapidly extended highly motile membrane processes toward the injury site in the minutes following transection. By 3 hpt, the processes had extended beyond the initial injury and stretched toward the distal stump (Figure 5-6A,B). I then sought to test the response of perineurial glia in *erbb3* larvae. Because I observed 3 distinct morphologies of *nkx2.2a*$^{+}$ cells in this mutant (tubular, stuck, and ensheathing), I tested the response of these cells separately. First, I transected axons that were nearby "tubular" cells, which I interpreted to be oligodendrocytes. Interestingly, I saw no apparent response by these cells, which remained wrapped on axons of the adjacent tract for the entire imaging period (Figure 5-6B,C). Next I transected axons that were near perineurial glia in the "stuck" morphology. These cells responded by extending thin processes in the direction of transection, but they did not reach the injury site by 3 hpt, and often retracted back (Figure 5-6B,D). Finally, I transected axons near perineurial glia in the "ensheathed" morphology, which were morphologically very similar to wild type perineurial glia. These cells initially extended robust processes toward the injury site. However, these processes eventually stalled, retracted, or became misdirected, and did not reach the injury (Figure 5-6B,E). Collectively, these data suggest that perineurial glia are less attracted to transection sites in the absence of Schwann cells, and further strengthen my previous conclusion that signals from Schwann cells help recruit perineurial glia to sites of nerve damage.

Schwann cells quickly become activated in response to nerve injury, and it is possible that these changes lead to the release of a paracrine signal that is attractive to perineurial glia. Indeed, Schwann cells have been shown to recruit macrophages to injured nerves through the

release of MCP-1 and other cytokines (Tofaris et al., 2002; Napoli et al., 2012). Precisely how Schwann cells become activated is not known, but Erbb receptors and their downstream signaling components (primarily ERK1/2) have been implicated (reviewed in Chapter 1). Thus, I hypothesized that Erbb signaling may be important for the ability of Schwann cells to recruit perineurial processes to injury sites. To test this, I treated wild type *nkx2.2a:gfp;olig2:dsred* larvae with the Erbb inhibitor AG1478 and measured the recruitment of perineurial processes to transection sites as described above. AG1478 is a potent inhibitor of Erbb receptor activation (Levitzki and Gazit, 1995; Busse et al., 2000), and treatment of zebrafish embryos early in development phenocopies *erbb3* mutants (Lyons et al., 2005). To inhibit Erbb activation in this assay, I treated larvae with 6μM AG1478 beginning at 84 hpf, and performed transections in drug at 4 dpf (96-100 hpf). Perineurial glia in DMSO control treated larvae responded similarly to wild type; extending processes to injury sites by 3 hpt (Figure 5-7A,B). Interestingly, when I transected nerves in AG1478 treated larvae, I observed that perineurial processes initially extended toward the transection site, but eventually stalled or retracted, and did not reach the injury by 3 hpt, although the difference in process extension was not significant (Figure 5-7B,C). This defect was remarkably similar to what was observed by "ensheathed" perineurial glia in *erbb3* mutants (Figure 5-6B,E) and suggests Erbb signaling is required to appropriately recruit perineurial processes to injury sites. Because Erbb signaling is required for many aspects of Schwann cell development (Taveggia et al., 2005; Garratt et al., 2000; Birchmeier, 2009; Riethmacher et al., 1997; 1Lyons et al., 2005), I wanted to verify that the 84-96 hpf treatment window inhibited Erbb signaling while producing minimal effects on Schwann cell development to that point. To this end, I treated *olig2:dsre*d larvae with either DMSO or AG1478 from 84-96

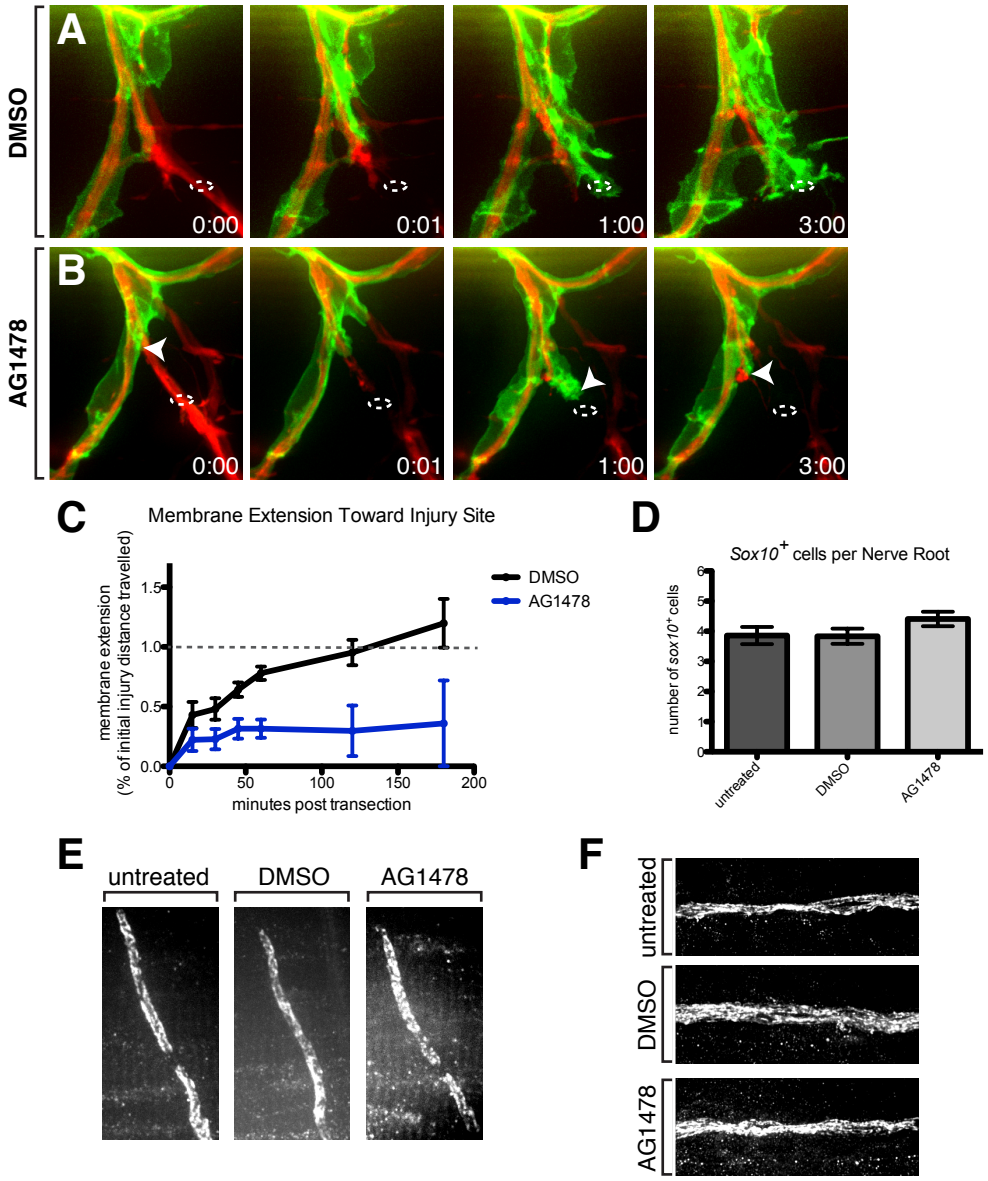

Figure 5-7: Recruitment of perineurial processes to transection sites is impaired in AG1478 treated larvae. All images are anterior to left and dorsal to top. (A-B) Frames taken from time-lapse movies of 4 dpf *nkx2.2a:gfp;olig2:dsred* larvae treated with DMSO or AG1478 beginning at 84 hpf. (A) Transection of an unensheathed axon tract induced extension of perineurial membrane to the injury site in a DMSO treated larva (n=5). (B) Perineurial membrane extension toward unensheathed axon injury is impaired in a larva teated with AG1478 (n=6). (C) Quantification of perineurial membrane extension in control and AG1478 treated larvae. (D) AG1478 treatment does not affect the number of sox10+ cells along motor roots at 96 hpf. (untreated, n=21 nerves in 6 fish; DMSO, n=24 nerves in 6 fish; AG1478, n=32 nerves in 7 fish) (E-F) MPB staining is present along the motor nerve (E) and PLLn (F) at 96 hpf in AG1478 treated larvae.

hpf, and immediately fixed and stained them with an antibody to sox10. I saw no significant difference in the number or location of *sox10*$^{+}$ cells along motor nerve roots in AG1478 treated larvae (Figure 5-7D). To assess any effect on Schwann cell differentiation, I stained control and AG1478 treated larvae with an antibody to MBP, a component of the myelin sheath. Schwann cells begin myelinating between 3 and 4 dpf, and expression of MBP at 96 hpf is reduced or absent when embryos are treated with AG1478 at earlier stages (Lyons et al., 2005). I observed that treatment from 84-96 hpf resulted in no visible reduction of MBP staining along the PLLn or motor nerves (Figure 5-7E,F). These data demonstrate that treatment with AG1478 from 84-96 hpf has minimal effects on Schwann cell development, but reduces the ability of perineurial glia to extend processes toward injury sites. This suggests that Schwann cells use signals produced downstream of Erbb activation to help recruit perineurial glia to sites of nerve damage. Interestingly, in both *erbb3* and AG1478 treated larvae, perineurial processes still exhibited an initial rapid attraction to the transection site during the first 15 mpt (Figure 5-6B,5-7B). This suggests that multiple signals act to attract perineurial glia to injury sites. The first signal acts immediately after the injury and is non-Schwann cell-derived, while the later signal is released by Schwann cells and acts over the course of several hours.

In Chapter 4 I reported that perineurial glia form an early tissue bridge between the proximal and distal nerve stumps after transection, and this bridge is essential for axon regrowth (Lewis and Kucenas, 2014). A recent study showed that axon regrowth was significantly impaired in *erbb3* mutants (Rosenberg et al., 2014), and I have seen this in my assay of motor nerve transection as well (Figure 5-8A,B). In light of these findings, I hypothesized that perineurial glia would be unable to bridge injury gaps in *erbb3* larvae. To

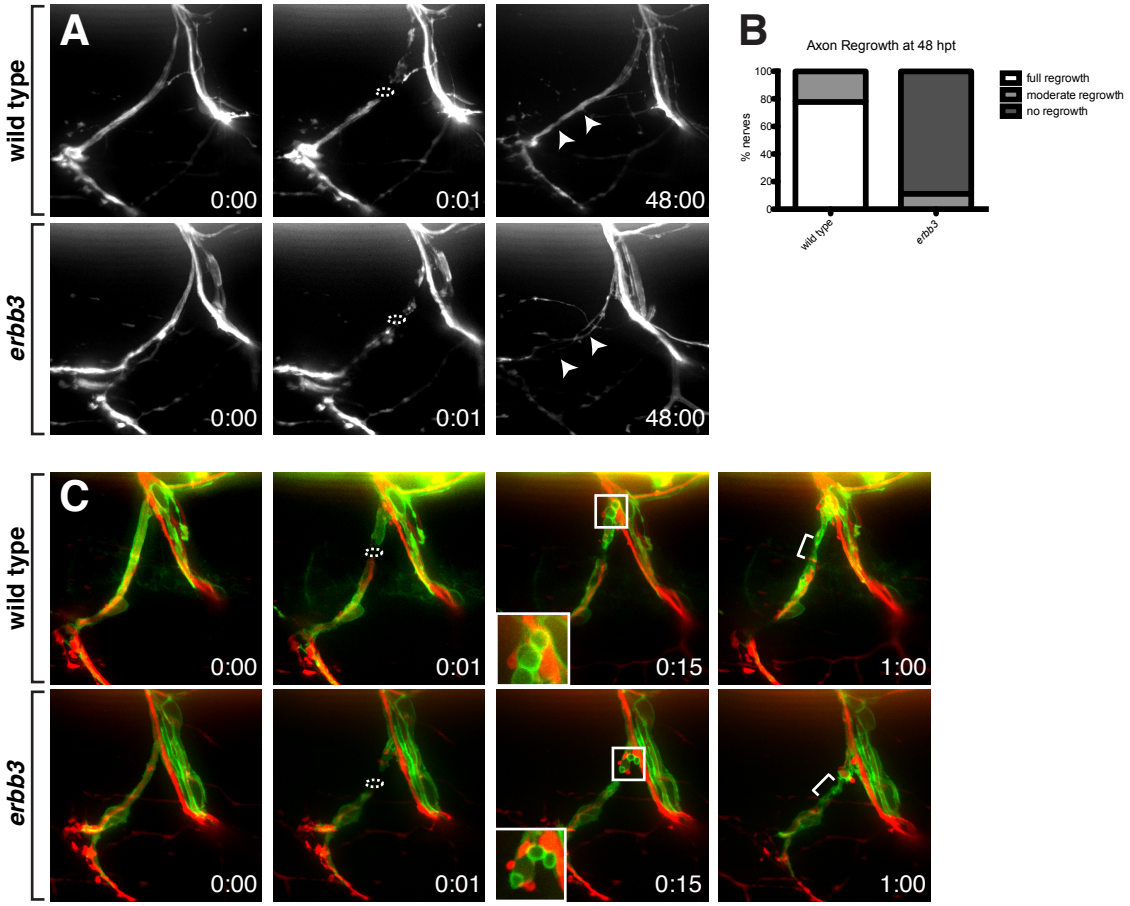

Figure 5-8: Perineurial glia form phagocytic vesicles and glial bridges in *erbb3* larvae. (A) Images are from *olig2:dsred* larvae and transections were performed at 6 dpf. Axons re-grew by 48 hpt in wild type, but not in *erbb3.* (B) Quantification of axon regrowth phenotypes in wild type (n=9) and *erbb3*(n-9) (C) Frames are taken from time-lapse movies of 6 dpf *nkx2.2a:gfp*;*olig2:dsred* larvae. Perineurial glia formed phagocytic vesicles and bridged the injury gaps of wild type and *erbb3* similarly. Dotted elipse denotes approximate ablated ROI.

test this, I transected the rostral motor nerve tract of 6 dpf *nkx2.2a:gfp;olig2:dsred* larvae as previously described (Chapter 3,4 and Lewis and Kucenas, 2013; 2014) and assessed the ability of perineurial glia to bridge the gap in both wild type and *erbb3*. In accordance with my previous findings, wild type perineurial glia responded to the transection by extending processes toward the injury site, forming phagocytic vesicles, and bridging the injury gap in 90% of cases (n=10). Surprisingly, the perineurial response in *erbb3* was similar, with perineurial glia forming phagocytic vesicles and bridging injury gaps in 75% of cases (n=4, not significantly different from wild type) (Figure 5-8C). This indicates that perineurial glia are able to overcome the loss of a Schwann cell-derived attractive cue when bridging injury gaps in *erbb3*. This is consistent with the idea that perineurial glia receive attractive cues from multiple cell types (both Schwann cell and not), and that some compensation or redundancy exists. Taken with the observation that axons do not regrow in *erbb3* mutants, this data also suggests that perineurial bridges are necessary but not sufficient to direct axon regrowth, and that both perineurial glia and Schwann cells are needed for regeneration to be successful.

Discussion

Mechanisms for communication between axons and glia are numerous and well established, while very little is known about how (or if) glial cells communicate with each other. Previous studies have suggested that Schwann cells and perineurial glia signal reciprocally during development, but precisely what aspects of perineurial development rely on signals from Schwann cells has not been clearly elucidated. Here, I demonstrate that Schwann cells are mostly dispensable for perineurial migration from the CNS, but are required to direct their

proper differentiation. My previous work has suggested that Schwann cells also communicate with perineurial glia after nerve injury, and here I present evidence that Schwann cells aid in the recruitment of perineurial processes to injury sites using signals downstream of Erbb receptor activation. Furthermore, my data suggest that the perineurial glia utilize multiple signals from multiple cell types during their injury response. These data highlight the importance of glial-glial signaling in both the development and regeneration of the PNS.

Schwann cells influence perineurial glial migration from the CNS

During PNS development, perineurial glia migrate out of the spinal cord through MEPs, crossing the boundary between the CNS and PNS. The subject of how this boundary is regulated is hotly debated and poorly understood. Here I show that perineurial glia migrate into the periphery in both *gpr126* and *erbb3* mutants, which lack myelin and Schwann cells respectively along motor nerves. I concluded from these data that differentiated Schwann cells were not required for perineurial glia to exit the spinal cord. However, my data does not rule out the possibility that ventrally streaming neural crest cells, many of which later differentiate into Schwann cells, play a role in perineurial migration. Interestingly, neural crest cells successfully stream to motor nerve roots in *cls* and *erbb3* mutants, but die before differentiating into Schwann cells (Kucenas et al., 2009b; unpublished data from Morris et al. in prep). Both of these mutants have at least some perineurial glia in the periphery by 4 dpf (Figure 5-1C and Lewis and Kucenas, 2014). In contrast, *mob;mos* mutants lack migratory neural crest entirely (Wang et al., 2011), and perineurial glia send processes into the periphery, but their cell bodies never exit the spinal cord (Kucenas et al., 2009b). These data are all consistent with the idea that neural crest plays a role in perineurial glial exit from the

spinal cord, but how could neural crest in the periphery affect the migration of perineurial glia that reside in the CNS? One possible explanation is that motor neurons serve as an intermediary. When neural crest cells reach motor axons, they may direct changes in the motor neurons that then indirectly affect perineurial migration. Nrg1-Erbb signaling between Schwann cells and axons is bidirectional and supports neuron survival (Bao et al., 2003), and it is likely that additional neural crest/Schwann cell to axon signaling mechanisms exist. Another explanation is that perineurial glial processes sense neural crest directly. Previous work showed that perineurial glia extend membrane processes into the periphery as early as 45 hpf, but recent unpublished work from our lab has suggested these processes may be out and sensing the peripheral environment much earlier (Zhu et al., in prep). It is important to note that there appeared to be fewer ensheathing perineurial glia in *cls* and *erbb3* mutants (Figure 5-4B), suggesting perineurial migration from the spinal cord was not entirely normal. This is also fitting with a role for neural crest in perineurial exiting, as neural crest reaches motor axons in these mutants but then migrates away. It is possible that more extended signals from neural crest and/or differentiating Schwann cells are required for perineurial glia to migrate from the CNS normally.

It is also possible that oligodendrocytes play a role perineurial migration in *erbb3* mutants. We observed OPCs exit the spinal cord and myelinate motor nerves in *erbb3*. These OPCs could substitute some signal to perineurial glia that is ordinarily derived from Schwann cells, or produce a different cue that is less attractive but sufficient to draw perineurial glia out. This seems less likely because perineurial glia do not exit in *mob;mos,* in which OPCs also myelinate, and they do exit in *cls*, where OPCs exit the spinal cord, but do not ensheath axons and die (Kucenas et al., 2009b).

A recent study demonstrated that a novel population of peripheral glial cells known as motor exit point (MEP) glia, which are functionally similar to Schwann cells, help maintain the boundary between CNS and PNS by inhibiting the ability of OPCs to migrate into the periphery in zebrafish (Smith et al., 2014). The presence of OPCs in the periphery in *cls* and *erbb3* suggests that MEP glia may be absent or disrupted, which could have some effect on perineurial glia. However, we believe this is unlikely as MEP glia are not observed along peripheral nerves until approximately 56 hpf (Smith et al., 2014), after most perineurial glia have exited (Kucenas et al., 2008). Future studies are needed to further investigate the role of MEP glia in PNS development in both wild type and mutant backgrounds.

The only mechanism currently known to mediate perineurial migration from the CNS is Notch signaling. A recent study from our lab showed that chemically or genetically disrupting Notch signaling within perineurial glia during a discrete temporal window completely prevented the ability of perineurial cell bodies to exit the spinal cord (Binari et al., 2013). The source of the Notch ligand was not identified, but was hypothesized to come from either axons or neural crest/Schwann cells. However, axons are not suspected to express Notch ligands during the window of perineurial exiting (Kim et al., 2008), which further strengthens my hypothesis of a role for neural crest. It is also possible, and indeed likely, that more than one mechanism mediates perineurial migration from the CNS, and future studies will be needed to elucidate these.

Effect of Schwann cells on perineurial glial differentiation

My data clearly show that perineurial glial differentiation is dependent on Schwann cells. In *gpr126* mutants where Schwann cells are present but do not myelinate, perineurial glia

invade the nerve and form minifaicicles. And in *erbb3* mutants, where Schwann cells are absent and the nerve is myelinated by oligodendrocytes instead, perineurial glia produce an excess amount of the tight junction-associated protein, ZO-1.

Perineurial minifascicles have been reported previously in several contexts, and these studies have concluded that their formation during development is the result of a loss of Desert Hedgehog (Dhh) signaling from Schwann cells. Schwann cells begin expressing Dhh at the Schwann cell precursor stage, and continue to express it throughout development (Bitgood and McMahon, 1995; Parmantier et al., 1999). The Dhh receptor Patched (Ptc) is expressed within the perineurium, and in *Dhh* mouse mutants, the perineurium forms minifascicles (Parmantier et al., 1999). Interestingly, Schwann cells do not express Dhh in *Gpr126* mutant mice, which also have perineurial minifascicles (Monk et al., 2011). This places Gpr126 upstream of Dhh expression, and suggests that a loss of Dhh-Ptc signaling between Schwann cells and perineurial glia leads to the formation of the minifascicles that I see in *gpr126* zebrafish. Schwann cells in *Dhh* mice do produce myelin, whereas Schwann cells in *Gpr126* mice and *gpr126* zebrafish do not. Dhh is not expressed in the Schwann cells of any of these mutants, and perineurial minifascicles form in all of them. This further suggests that minifascicles form in response to a loss of Dhh-Ptc signaling, and not a loss of myelin itself.

Perineurial minifascicles have also been reported to form during peripheral nerve regeneration in mice. This occurs within the distal stump as new axons begin to regrow and become re-myelinated. Fasciculation eventually returns to normal once regeneration is complete (Morris et al., 1972). This suggests that minifascicles may represent the perineurium's attempt to create a smaller and more tightly regulated or insulated

microenvironment in response to stress. This would also suggest that minifascicle formation isn't so much a defect as an attempt at compensation. Interestingly, minifascicle formation during regeneration is even more extensive in *Dhh* mice (Bajestan et al., 2006), further indicating that Dhh regulates perineurial fasciculation.

If Dhh derived from Schwann cells is responsible for keeping the perineurium at the outer edge of the fascicle, then why are minifascicles not present in *erbb3* mutants? This may be related to the presence of myelinating oligodendrocytes. Although oligodendrocytes are not thought to express Dhh during normal development, it is possible that they turn on expression when ensheathing axons in the periphery. Consistent with this, Dhh is not expressed in migratory neural crest, but is turned on in Schwann cell precursors only after they have associated with motor axons (Bitgood and McMahon, 1995; Parmantier et al., 1999). Additionally, Sox10, a transcription factor expressed in both Schwann cells and OPCs, has been reported to bind and activate Dhh expression in vitro (Küspert et al., 2012). This suggests OPCs have the appropriate transcriptional machinery to activate expression of Dhh, and this may be affected by environmental cues. The notion that OPCs may turn on expression of Dhh is intriguing because it is not known to what extent OPCs that myelinate peripheral axons retain their identity. These cells do express *plp1a*, a component of central myelin (Smith et al., 2014), but future experiments are needed to elucidate a full and more informative expression pattern.

I also observed morphological defects in the perineurium of *erbb3* mutant larvae at 6 dpf. Significantly fewer nerves were ensheathed by perineurium than in wild type, and some perineurial glia exhibited an aberrant "stuck" morphology. Intriguingly, ensheathment appeared normal by adulthood, but their appeared to be an increase in ZO-1 staining within

the perineurium. ZO-1 is an intercellular protein component of tight junctions, which form between adjacent perineurial cells and allow them to serve as a diffusion barrier (Akert et al., 1976; Bourne, 1968). Nothing is known about the regulation of ZO-1 expression in perineurial glia, but my data suggests it could be dependent on Schwann cells. One study found that TNFα was able to decrease ZO-1 expression and increase permeability of tight junctions through activation of NF-Kappa B in an *in vitro* model of intestinal epithelium (Ma et al., 2004). Both TNFα and NF-Kappa B have reported roles in peripheral nerve development and regeneration, and future studies may reveal if these have a role in regulating ZO-1 expression in perineurial glia. As with the formation of minifascicles, it is debatable whether and increase in tight junctions in the perineurium should be considered a defect. Over-producing tight junctions may serve to add protection to impaired nerves, and thus may actually be beneficial. Future studies are needed to investigate the functional significance of perineurial abnormalities in both *gpr126* and *erbb3* mutants.

Schwann cell-derived signals recruit perineurial processes to injury sites

Following a nerve transection, my data demonstrate that the recruitment of perineurial processes to injury sites along unensheathed axons is impaired in *erbb3* mutants, which lack Schwann cells, and when Erbb receptor activation is inhibited. This led me to draw two conclusions. First, Schwann cells aid in attracting perineurial processes to injury sites, and second, this requires signals produced or released downstream of Erbb activation. The first conclusion is consistent with my previously published data showing that recruitment of perineurial processes is impaired in *cls* mutants, which also lack Schwann cells (Chapter 4). The observation that *erbb3* mutants have myelinating oligodendrocytes along motor nerves,

and *cls* mutants do not, suggests that oligodendrocytes are not able to compensate for the lost Schwann cell-derived attractive cue.

The requirement of Erbb activation for recruitment is intriguing. In theory, Schwann cells could release cues to attract perineurial glia by either activating a signaling cascade that results in the release of a signal, or by passively dumping intracellular contents upon cellular damage. My results suggest the former is more likely. Erbb2/3 signaling is required throughout development (Birchmeier, 2009), but is turned down in adulthood (Atanasoski et al., 2006). An abundance of evidence has suggested that Erbb signaling is re-activated after nerve injury, but instead of promoting differentiation, it promotes demyelination and transdifferentiation (Carroll et al., 1997; Kwon et al., 1997; Tapinos et al., 2006). As described in Chapter 1, these differing effects of Erbb activation may be due to differences in the concentration and type of Nrg1 ligand available (Syed et al., 2010). My results are consistent with the idea that Schwann cells activate Erbb signaling after nerve injury, although this was not investigated directly. Future studies are needed to investigate Erbb signaling and the specific effects of AG1478 on Schwann cells and axon regrowth during regeneration. Importantly, pharmaceutical inhibition is not cell type specific, and I cannot rule out the possibility that AG1478 treatment affected perineurial glia directly, but I believe this is unlikely as Erbb expression has not been reported in the perineurium (Carroll et al., 1997). Future experiments should focus on identifying the Schwann cell-derived paracrine signal that acts to recruit perineurial glia, as this may have therapeutic value.

The role of non-Schwann cell-derived signals in the perineurial injury response

Although the recruitment of perineurial processes was ultimately impaired in *erbb3* and AG1478-treated larvae, I still observed some extension toward transection sites in the initial 15 mpt. This suggests that perineurial glia initially respond to injuries via a non-Schwann cell-derived cue. I hypothesize that this cue is derived from injured axons at the transection site. Because these transections performed along axons that were not ensheathed by perineurium, the cue is unlikely to be perineurial-derived. Macrophages do not generally arrive at injury sites until after 15 mpt, making them unlikely candidates as well. This early cue is likely something that diffuses very quickly, and ATP is one possibility. In the mammalian CNS, ATP released from injury sites can stimulate the recruitment of microglial processes within minutes (Davalos et al., 2005), and ATP has been shown to induce calcium influx in mammalian perineurial cells via P2X receptors (Shinohe and Saino, 2000). This could provide a mechanism for activating perineurial injury behavior, and future experiments may help elucidate this.

The observation that perineurial processes were less attracted to transections in *erbb3* but were still able to bridge injury gaps was unexpected. However, it is fitting with the idea that the perineurial response to injury is mediated by multiple cues derived from multiple cell types. The transections used for these experiments created injury gaps that were relatively small (< 7 μm), and it is possible that the initial non Schwann cell-derived attractive cue is sufficient to attract perineurial processes into injury gaps in these cases, but that bridging of larger injuries would be impaired. Alternatively, Schwann cells may aid in the recruitment of perineurial processes, but this contribution may be minimal and not enough to effect bridging. Perineurial processes extend into injury gaps from both the proximal and distal

stump, and once processes are within close proximity or touching, it is likely that perineurial-perineurial interactions act to sustain their adhesion and the formation of the bridge. This is supported by the fact that I do not see dissociation of bridges once they form (Lewis and Kucenas, 2014). Together my data support a hypothesis whereby perineurial glia respond to several signaling cues mediating different aspects of their injury behavior. Future identification of these signals may prove valuable in treating peripheral nerve injuries.

Collectively, my data shows that perineurial glia require Schwann cells for aspects of their development and injury response. I show that perineurial glia are able to exit the spinal cord in the absence of Schwann cells, but do so less frequently, and their differentiation is abnormal. I also demonstrate that Schwann cells aid in the recruitment of perineurial processes to injury sites, and this requires Erbb receptor activation. This work serves an important step towards better understanding the role of perineurial glia in PNS development and regeneration.

Chapter 6

Discussion and future directions

Summary

In this dissertation, I have presented the first ever characterization of perineurial glial behaviors after nerve injury in a live animal. To accomplish this, I first created a novel assay to study glial responses to nerve transection, which I described in Chapter 3. This assay used a MicroPoint laser to transect the motor nerve in live transgenic zebrafish, and time-lapse confocal imaging to visualize the response of surrounding cells. In Chapter 4, I used this assay to investigate the response of perineurial glia to nerve transection in detail. I found that perineurial glia responded rapidly to transections by extending highly motile membrane processes toward injury sites and phagocytizing debris. Perineurial glia and macrophages appeared to spatially coordinate debris clearance, with perineurial glia acting primarily along the proximal stump and macrophages acting at the injury site and along the distal stump. Perineurial processes later bridged the gap between proximal and distal stumps. These glial bridges formed before Schwann cells or axons traversed the gap, and in their absence axon regrowth was impaired. Additionally, I showed that perineurial glia were less attracted to injury sites in a mutant that lacked Schwann cells. These data demonstrate that perineurial glia are active and essential players in nerve regeneration, and that perineurial glia rely on signals from Schwann cells for their attraction to injury sites. In Chapter 5, I further demonstrated this requirement for Schwann cells by showing that the recruitment of perineurial processes to injury sites was decreased in another mutant lacking Schwann cells. Moreover, inhibiting Erbb signaling,

which is activated in Schwann cells after nerve injury, mimicked this effect. Taken together, these data show that Schwann cells communicate with perineurial glia after nerve injury using signals released downstream of Erbb activation, and this aids in the recruitment of perineurial processes to injury sites. Collectively, my data demonstrate that perineurial glia respond dynamically to nerve injury and are integral for nerve regeneration. This work highlights the need for greater consideration of perineurial glia in future studies.

Why is so little known about the perineurium during regeneration?

One of the primary impediments to the study of perineurial cells during regeneration has been the lack of available markers to specifically label these cells. This is exacerbated by the dramatic changes that happen within the nerve following injury, which have made it historically difficult to distinguish cells from one another using conventional methods such as EM. In normal uninjured nerves, cells are generally identified by EM based on ultrastructural properties such as the presence or absence of a basal lamina, cell shape, appearance of processes, density of nuclear staining, and location in the nerve. However, nerve-associated cells undergo dramatic morphological changes after an injury, and subsequently identifying cells based on criteria set forth in uninjured nerves can be misleading. In an elegant and seminal EM study of regenerating rat sciatic nerves by Morris et al., the authors admitted it was difficult to distinguish between Schwann cells, endoneurial fibroblasts, and perineurial cells after injury (Morris et al., 1972).

The idea that it is difficult to distinguish the origin and identity of cells after injury suggests that perineurial cells may have roles in regeneration that have previously

been attributed to other cell types. Indeed, my work supports this notion. Several previous studies in mammals have reported that the gap between proximal and distal stumps after transection is bridged by fibroblast-like cells that later adopt features of perineurial cells. Whether these bridge cells are derived from the existing perineurium or from mesenchymal fibroblasts has been debated, but my work showing perineurial glia bridge injury gaps in zebrafish is consistent with a perineurial origin. My work also demonstrates that perineurial glia phagocytize debris after injury, which has not specifically been described in perineurial cells previously. Vacuoles have been observed in the inner layers of the proximal stump perineurium and in the bridge cells descried above, but it was not clear by EM if these were indicative of phagocytosis (Morris et al., 1972; Scaravilli, 1984). Interestingly, abundant phagocytic activity has been described in fibroblast-like cells in the endoneurium after injury. There has been debate as to whether these are endoneurial fibroblasts or a type of resident macrophage, as the distinction between these cells is not clear (Richard et al., 2012). Our data suggest a third possibility, that these cells could be activated perineurial glia.

Yet another area in which perineurial glia have been markedly overlooked is in microarray and RNA-seq analysis of distal nerve preparations. Injury-induced changes in expression are generally attributed to Schwann cells because they are the most abundant cell type within the nerve. However, these preparations typically contain other cell types, such as perineurial glia, whose changes in expression may be misleadingly attributed to Schwann cells or otherwise overshadowed.

The discovery of specific markers for perineurial glia will surely lead to major advancements in our knowledge of these poorly studied cells and their role in

regeneration. Although motor nerve perineurial glia can be labeled with the *nkx2.2a:gfp* transgene in zebrafish, this marker is not specific, and very little is known about what other markers are expressed by these cells. Interestingly, the perineurium of zebrafish sensory nerves does not express *nkx2.2a*, and only a subset of cells in the mouse perineurium express Nkx2.2 (Clark et al., 2014). Future studies should focus on identifying better and more specific markers for perineurial glia, as well as determining the expression pattern of these cells. This could be accomplished by several methods. Mouse perineurium could be dissected from sciatic nerves and analyzed by microarray or RNA-seq. Dissection of the perineurium would not be possible in zebrafish, but *nkx2.2a*$^{+}$ cells could be individually isolated by laser capture microdissection and their expression analyzed. Groups of *nkx2.2a*$^{+}$ cells could also be isolated by fluorescence-activated cell sorting (FACS) from the body tissue of zebrafish (the heads and spinal cords would need to be removed because *nkx2.2a* is abundantly expressed in the CNS). These experiments would only analyze motor nerve perineurial glia, but markers may be identified by this analysis that could potentially be expressed in both motor and sensory perineurium.

How do perineurial glia affect Schwann cells and macrophages?

In Chapter 4 I demonstrated that in the absence of perineurial glia (and therefore perineurial bridges), axon regrowth was impaired. However, I did not address whether the response of Schwann cells was affected. My data showed that perineurial glia bridged injury gaps before Schwann cells, and previous studies have shown that Schwann cells were important for guiding axon sprouts across this bridge (McDonald et al., 2006). Loss of a perineurial bridge may impact the ability of Schwann cells to traverse the gap and

appropriately guide regrowing axons. In support of this, Parrinello et al. recently showed that cultured nerve fibroblasts derived from the perineurium could induce Schwann cells to sort into discrete bands via ephrin/Eph signaling *in vitro*, and disrupting Eph signaling *in vivo* impaired Schwann cell organization and axon regrowth. Another recent study demonstrated that axon regrowth failed or was misdirected in several zebrafish mutants that lack Schwann cells (Rosenberg et al., 2014). I showed this as well in *erbb3* mutants in Chapter 5. Interestingly, I observed that perineurial glia were able to bridge injury gaps in *erbb3* even in the absence of Schwann cells, suggesting that both perineurial glia and Schwann cells must be present together to achieve optimal axon regrowth. These studies are consistent with the idea that perineurial bridges serve as a scaffold for Schwann cell bridges, which then guide regenerating axons across the gap. Further investigation into how perineurial glia affect Schwann cells during regeneration may be an interesting future direction for this project.

Macrophages are also important for nerve regeneration, and my work did not address if the macrophage response was affected in the absence of perineurial glia. There is an abundance of evidence to support the idea that Schwann cells recruit macrophages to injured nerves (Toews et al., 1998; Tofaris et al., 2002; Napoli et al., 2012), but it is possible that perineurial glia play a role as well. In zebrafish *cls* mutants, which lack Schwann cells but still have some perineurial glia, macrophages are recruited to transected motor nerves in normal numbers (Rosenberg et al., 2012). Additional lines of evidence also suggest that perineurial glia and macrophages communicate or interact in some way. The perineurium is an important component of the BNB, which is broken

down after injury to facilitate the infiltration of macrophages, and in Chapter 4, I showed that perineurial glia and macrophages cleared debris in spatially distinct regions.

The response of Schwann cells and macrophages to the absence of perineurial glia could be tested using the paradigm of DAPT treatment set forth in Chapter 4 (also described in Chapter 2: Materials and Methods). Useful assessments would include analysis of Schwann cell bridging, macrophage recruitment and debris clearance. Defects in the response of either of these cells would suggest that perineurial glia signal to Schwann cells and/or macrophages after injury, placing them in a central position to control cellular responses during regeneration.

Signals that affect the perineurial response to injury

The molecular cues that govern perineurial injury behavior are not known, but my work suggests there are at least 3 separate signaling interactions. The first is an immediate paracrine attractive/activation cue. Within the first 15 mpt, perineurial glia always begin to extend membrane processes toward injury sites and form phagocytic vesicles. In Chapters 4 and 5 I showed that this happens even in mutants without Schwann cells and when Erbb signaling is inhibited. Perineurial glia do not respond to injuries to nearby muscle, suggesting this cue is nerve-derived. In Chapter 5 I proposed axon-derived ATP as a candidate for this signal, although this has not yet been investigated. The second signaling interaction is one between Schwann cells and perineurial glia, which acts to sustain the attraction of perineurial processes toward injury sites over longer periods of time. This is evidenced by the decreased recruitment of perineurial processes over the first several hours in mutants that lack Schwann cells. This signal may be produced

downstream of Erbb activation, as inhibiting Erbb mimicked the response seen in Schwann cell mutants. The third interaction mediates the formation of perineurial bridges. The existence of this signal is evidenced by the fact that perineurial glia can bridge injury gaps in the absence of Schwann cells, and that once bridges form, they do not disassociate. I hypothesize that bridging is mediated by perineurial-perineurial interactions, which act over a close range or upon contact to maintain the adhesion of membrane processes.

Future studies should focus on identifying the signals described above. One way to accomplish this could be through forward genetic screens or drug screens. A forward genetic screen could be used to identify mutations that affect perineurial attraction, phagocytic activity or bridging. This would be most useful in identifying genes that are involved in regeneration, but not development. If mutations resulted in significant developmental defects it would be difficult to assess their role in injury responses. Drug screening may be more useful in identifying signaling pathways that are also used in development. Zebrafish larvae can be easily treated with pharmaceutical libraries by adding drugs directly to the egg water. Identifying receptors or pathways in this manner could then be followed by more targeted genetic experiments. Discovering the molecular signals that drive perineurial responses is of particular importance because these may be useful in the development of injury therapies.

Implications for PNS injury therapies

Recovery from complete nerve transection, clinically termed neurotmesis, is generally poor and often leaves patients with little or no sensation and muscle control in the area

innervated by the nerve. This is particularly debilitating when the affected nerve serves a large area, such as the brachial plexus or sciatic nerve, which control large portions of the arm and leg respectively. Treatment generally requires surgical intervention, and the approach varies depending on the injury. The best results are usually achieved through direct nerve repair, where the ends are reapposed and sutured through the epineurium or perineurium. In cases where the nerve is more severely damaged, a nerve autograft may be required to connect the stumps. Autografting involves harvesting a portion of healthy nerve from one area of the body and using it to re-join the injured nerve. Grafts are usually harvested from non-essential sensory nerves, such as the sural nerve, which provides sensation to the lateral foot. However, autografts are most successful when the donor nerve has a similar size, shape, and number of fascicles as the injured nerve, and this often difficult to achieve. An additional concern with grafting is that patients will usually experience deficits in the donor nerve region. This can be avoided by using synthetic conduits to join the nerves. Historically, conduits have not performed as well as autografts, although recent work has shown promising results using bioabsorbable conduits to bridge small gaps (Deal et al., 2012). The success of regeneration through a graft or conduit decreases as the length of the inserted segment increases. Improving outcomes for patients with long segmental injuries will require an improvement of these traditional techniques (Wolford and Stevao, 2003).

An intriguing area of current research is in the use of autologous Schwann cells to improve the efficacy of grafts and conduits (Rodríguez et al., 2000). This involves isolating Schwann cells, culturing them, and reseeding them into grafts or conduits that are used in nerve repair. This technique improved the gap distance that could be repaired

in rats, and was recently tried in a human case of sciatic nerve transection with good results (Berrocal et al., 2013). My work suggests that in addition to Schwann cells, perineurial glia may be interesting to consider when designing new therapies. I observed that axon regrowth was reduced in the absence of perineurial bridges, and previous work has shown that Schwann cells and perineurial glia are intimately associated in the nerve bridge. Conduits or grafts seeded with both Schwann cells and perineurial glia may show improvement over grafts seeded with Schwann cells alone. Elucidating the molecular signals that drive perineurial injury behavior may prove useful as well. Conduits, grafts, and regions of direct nerve repair could be treated with factors that stimulate perineurial activation and bridging, which may improve overall regeneration.

Do perineurial glia undergo dedifferentiation/transdifferentiation after injury?

After a nerve injury, mature Schwann cells transdifferentiate into repair cells that are reminiscent of ISCs. As described in Chapter 1, this processes is marked by dramatic changes in expression and behavior, and is essential for the success of regeneration (Arthur-Farraj et al., 2012). Similarly, I observed that perineurial glia underwent rapid and dramatic changes in behavior in response to nerve transection, but my work did not elucidate if this represented a true dedifferentiation or transdifferentiation. As mentioned above, previous EM studies have shown that cells in the early nerve bridge resemble fibroblasts, but later adopt features of differentiated perineurial cells, such as a basal lamina and pinocytic vesicles. My work showed that perineurial glia form early bridges across injury gaps. Taken together, this suggests the fibroblast-like cells observed by EM may be a form of activated perineurial glia that have lost their differentiated features.

This could indicate a change in differentiation state. Future studies may elucidate this by determining if perineurial glia markedly change their expression pattern after injury. This would require that a baseline of perineurial expression be established first, as descried above. Analyzing changes in perineurial expression after injury may also help reveal some of the signaling mechanisms that drive their responses.

Does regeneration recapitulate development?

Whether regeneration recapitulates development is a topic of debate. However, in recent years, evidence has been mounting that in the PNS, these processes appear distinct. The expression profile of Schwann cells during repair is different than during development, and axons utilize guidance cues from Schwann cells during regeneration that are not present during initial pathfinding (Arthur-Farraj et al., 2012). Additionally, myelination by Schwann cells during development is strongly dependent on axon-derived Nrg1 (Taveggia et al., 2005), whereas recent evidence suggests Nrg1 may come from other sources during regeneration (Stassart et al., 2012; Fricker et al., 2013). My data is also consistent with the notion that regeneration is different from development. In a paper published by Binari et al. in 2013, we reported that Notch signaling was required for perineurial migration and differentiation during development. However, I did not observe activation of Notch signaling in perineurial glia during regeneration (Figure 6-1)(Binari et al., 2013). In Chapter 4, I observed that perineurial glia bridged injury gaps before Schwann cells or axons. This is in contrast to development, where axons pathfind and Schwann cells associate with axons before perineurial glia exit the spinal cord. Additionally, perineurial glia become phagocytic after injury, which is not a behavior that

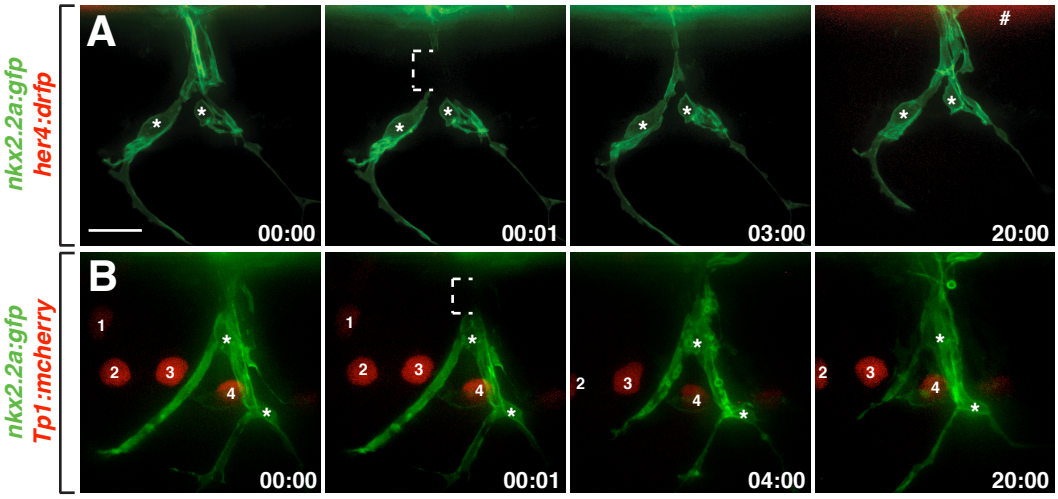

Figure 6-1: Notch activity is not detected in perineurial glia after injury. All images are lateral views with dorsal to top and anterior to left. (A,B) Images taken from *nkx2.2a:gfp;her4:drfp* (A) and *nkx2.2a:gfp;Tp1:mcherry* (B) larva after motor nerve root injury beginning at 6 dpf. *her4:drfp* and *Tp1:mcherry* are reporters of Notch activity. Motor nerve-associated perineurial glia never express RFP or mCherry after nerve injury in either line. Numbers in lower right denote time lapsed from first frame. Number sign denotes RFP expression in the spinal cord. 1-4 mark *mCherry*$^{+}$ cells in the periphery. Brackets show inury zones. Scale Bar: 10 µm.

has been observed during development. Taken together, my data strongly suggests that perineurial behavior differs between development and regeneration.

Implications for CNS regeneration

Unlike the PNS, the CNS is not able to regenerate after injury. This is due to differences in the intrinsic properties of CNS and PNS neurons (for review see Liu et al., 2011) and differences in the environment created by glial cells. PNS injury stimulates glia to become activated, clear debris, and aid in regrowth. In contrast, CNS injury results in reactive gliosis, substantial amounts of un-cleared debris and the formation of scars that block regrowth.

The axons of CNS neurons are wrapped and myelinated by oligodendrocytes. Unlike Schwann cells, oligodendrocytes do not transdifferentiate after injury and are not efficient at clearing myelin debris. This hinders regeneration, as several myelin components, such as Nogo, myelin associated glycoprotein (MAG), and oligodendrocyte myelin glycoprotein (OMgP), are inhibitory to axon regrowth. Debris clearance is further hindered by the inability of peripheral macrophages to access CNS tissue through the blood-brain-barrier (BBB), which does not break down like the BNB of the PNS. The CNS has its own class of resident immune cells, called microglia, which are capable of engulfing microorganisms and apoptotic cells. However, these cells clear myelin at an extremely slow rate (Vargas and Barres, 2007).

Astrocytes are another class of glia found in the CNS, which surround neurons and are essential for their trophic support, maintenance and function. After a CNS injury, astrocytes undergo a process termed “reactive gliosis”, which is characterized by cellular

hypertrophy, proliferation, and changes in gene expression. This includes the upregulation of chondroitin sulfate proteoglycans (CSPGs), which are ECM molecules that are highly inhibitory to axon growth. Reactive gliosis eventually leads to the formation of a glial scar, which both physically and molecularly obstructs axon regrowth through the injury site (Lutz and Barres, 2014).

The hostile glial environment in the CNS after injury creates a barrier to regeneration, while glial responses in the PNS create a growth permissive environment. This stark contrast in glial responses has led researchers to experiment with ways of using PNS cells to alter the CNS environment after injury. Several studies have reported that repair of spinal cord injury (SCI) is improved with the use of Schwann cell grafts. Combining Schwann cell transplantation with other therapeutic strategies, such as bioabsorbable conduits, glial scar inhibitors, and trophic factors, has shown particular promise (Tetzlaff et al., 2011; Kanno et al., 2014). My work suggests it may be useful to consider perineurial glia when designing SCI therapies as well. Perineurial glia could be transplanted into CNS injury sites or seeded into grafts with Schwann cells. Future studies elucidating the mechanisms of perineurial responses may also inform new strategies to treat SCI.

In the absence of Schwann cells in *erbb3* zebrafish mutants, OPCs exit the CNS and myelinate peripheral motor roots (Chapter 5; Morris et al., in prep; Smith et al., 2014). This presents a unique opportunity to study the response of oligodendrocytes to injury in the PNS, an environment that is usually permissive to regrowth. In Chapter 5 I reported that in *erbb3,* peripherally wrapping oligodendrocytes did not extend significant processes toward transections on neighboring axons during the imaging window of 3 hpt.

However, this was not investigated in detail and I did not image later time points. Additionally, this experiment investigated the response of cells to transections on adjacent axons and not the axons that they wrap directly. Future experiments using *erbb3* larvae to investigate the differences between oligodendrocyte responses in the CNS and PNS may reveal new information as to how oligodendrocyte behavior is (or is not) affected by the surrounding environment. This may ultimately inform the way we think of CNS regeneration and the ability of oligodendrocytes to help or hinder this process.

Glial subtypes and their potential role in regeneration

The PNS is classically thought of as being comprised of 5 distinct cell types: neurons, Schwann cells, endoneurial cells, perineurial cells, and epineurial cells. In recent years, evidence has been mounting that suggests there is a surprising amount of heterogeneity within each of these cell populations. The significance of this is still poorly understood, but may change the way we think about defining cell types and their respective roles in development and regeneration in the future.

In a recent groundbreaking study of the mouse CNS, Zeisel et al. utilized quantitative single-cell RNA-seq to reveal that each major class of CNS cell type had several molecularly distinct subclasses within it. Amongst glia, this included 2 subtypes of astrocytes and 6 subclasses of oligodendrocytes (Zeisel et al., 2015). There is evidence that this heterogeneity exists in PNS glia as well. It is known that Schwann cells can be either myelinating or non-myelinating, but there are likely additional subclasses within these groups. Schwann cells that myelinate strictly motor or sensory axons express different levels of growth factors after injury (Höke et al., 2006), as do Schwann cells that

myelinate more proximal or distal axon regions (Brushart et al., 2013). Smith et al. recently identified a new class of myelinating glia, termed motor exit point (MEP) glia, along the motor root in zebrafish. MEP glia appeared to be functionally similar to Schwann cells, but were derived from the CNS as opposed to neural crest (Smith et al., 2014). This finding was supported by previous studies in chick that showed myelinating glia were present along motor roots after neural crest ablation (Lunn et al., 1987). There are likely subclasses of perineurial cells as well. As stated above, perineurial cells along zebrafish sensory roots and the PLLn do not express *nkx2.2a* like motor nerve perineurial glia (Kucenas et al., 2008), and it is currently unclear if all perineurial cells share a CNS origin. The finding that only a subset of cells in the perineurium express Nkx2.2 in mice further suggesting a subclassification of perineurial cells (Clark et al., 2014). Future studies may be able to use quantitative single-cell RNA-seq on peripheral nerves, similar to the study of CNS by Zeisel et al., to more definitively define these PNS glial subclasses.

It is possible that different subclasses of glia may have different responses to injury or roles in regeneration. Indeed, motor axons preferentially regenerate through grafts derived from motor nerves, and likewise sensory axons prefer sensory grafts (Höke et al., 2006). This suggests there are distinct differences between these tracts. Along sensory dorsal root ganglion (DRG) neurons, regeneration of the peripheral branch is more successful than the central branch, which may be due to differences in both axon intrinsic factors and the glial environment (Chong et al., 1996). Another interesting notion is the idea that there may be metaplasia between subtypes during regeneration. Injury induces drastic changes in cellular expression and morphology, and to what extent

cells maintain their previous identity is not known. This would be an intriguing avenue of future study, and may impact the development of future nerve injury therapies. Grafts harvested from nerves with similar glial subtypes as the injured nerve may be more effective.

The assay I developed here may be a useful way to study differences in the injury-induced behavior of glial subtypes *in vivo* in the future. However, before these issues can be addressed, the complexity of glial subtypes must first be elucidated, and accurate markers developed as described above. This brings this issue to the forefront of importance in glial biology.

Appendix: Abbreviations

Abbreviations are listed in the order they appear. For abbreviations of transgenes and mutant lines see Tables 2-1 and 2-2 on page 27.

CNS	central nervous system
PNS	peripheral nervous system
BNB	blood-nerve-barrier
pMN	motor neuron progenitor domain
MEP	motor exit point
SCP	Schwann cell precursor
ISC	immature Schwann cell
Sox10	SRY (sex determining region Y)-box 10
Nrg1	Neuregulin 1
ERK	extracellular signal-regulated kinase
PLLn	posterior lateral line nerve
Gpr126	G protein-coupled receptor 126
ECM	extracellular matrix
GFP	green fluorescent protein
MO	morpholino oligonucleotide
Dhh	desert hedgehog
Ptc	patched
AAD	acute axonal degeneration

Wlds	Wallerian degeneration slow
LIF	leukemia inhibitory factor
MCP-1	monocyte chemoattractant protein-1
EM	electron microscopy
RFP	red fluorescent protein
ZO-1	zonal occludins-1
MBP	myelin basic protein
OPC	oligodendrocyte precursor cell
BBB	blood-brain-barrier
SCI	spinal cord injury
DRG	dorsal root ganglion

Reference for zebrafish ages and post-injury time-lapses:

hpf	hours post fertilization
dpf	days post fertilization
mpt	minutes post transection
hpt	hours post transection

References

Adalbert R, Gillingwater TH, Haley JE, Bridge K, Beirowski B, Berek L, Wagner D, Grumme D, Thomson D, Celik A, Addicks K, Ribchester RR, Coleman MP (2005) A rat model of slow Wallerian degeneration (WldS) with improved preservation of neuromuscular synapses. European Journal of Neuroscience 21:271–277.

Akert K, Sandri C, Weibel ER, Peper K, Moor H (1976) The fine structure of the perineural endothelium. Cell and Tissue Research 165:281–295.

Arduini BL, Bosse KM, Henion PD (2009) Genetic ablation of neural crest cell diversification. Development 136:1987–1994.

Arthur-Farraj PJ, Morwena Latouche, Daniel K Wilton, Quintes S, Chabrol E, Banerjee A, Woodhoo A, Jenkins B, Rahman M, Turmaine M, Wicher GK, Mitter R, Greensmith L, Behrens A, Raivich G, Mirsky R, Kristjan R Jessen (2012) c-Jun Reprograms Schwann Cells of Injured Nerves to Generate a Repair Cell Essential for Regeneration. Neuron 75:633–647.

Atanasoski S, Scherer SS, Sirkowski E, Leone D, Garratt AN, Birchmeier C, Suter U (2006) ErbB2 Signaling in Schwann Cells Is Mostly Dispensable for Maintenance of Myelinated Peripheral Nerves and Proliferation of Adult Schwann Cells after Injury. Journal of Neuroscience 26:2124–2131.

Avery MA, Rooney TM, Pandya JD, Wishart TM, Gillingwater TH, Geddes JW, Sullivan PG, Freeman MR (2012) WldS Prevents Axon Degeneration through Increased

Mitochondrial Flux and Enhanced Mitochondrial Ca2+ Buffering. Current Biology 22:596–600.

Bajestan SN, Umehara F, Shirahama Y, Itoh K, Sharghi-Namini S, Jessen KR, Mirsky R, Osame M (2006) Desert hedgehog-patched 2 expression in peripheral nerves during Wallerian degeneration and regeneration. J Neurobiol 66:243–255.

Banerjee S, Isaacman-Beck J, Schneider VA, Granato M (2013) A Novel Role for Lh3 Dependent ECM Modifications during Neural Crest Cell Migration in Zebrafish Mallo M, ed. PLoS ONE 8:e54609.

Bao J, Wolpowitz D, Role LW, Talmage DA (2003) Back signaling by the Nrg-1 intracellular domain. The Journal of Cell Biology 161:1133–1141.

Barrallo-Gimeno A, Holzschuh J, Driever W, Knapik EW (2004) Neural crest survival and differentiation in zebrafish depends on mont blanc/tfap2a gene function. Development 131:1463–1477.

Berrocal YA, Almeida VW, Levi AD (2013) Limitations of nerve repair of segmental defects using acellular conduits. Journal of Neurosurgery 119:733–738.

Binari LA, Lewis GM, Kucenas S (2013) Perineurial Glia Require Notch Signaling during Motor Nerve Development but Not Regeneration. Journal of Neuroscience 33:4241–4252.

Birchmeier C (2009) ErbB receptors and the development of the nervous system. Experimental Cell Research 315:611–618.

Birchmeier C, Nave K-A (2008) Neuregulin-1, a key axonal signal that drives Schwann cell growth and differentiation Jessen KR, Mirsky R, Salzer J, eds. Glia 56:1491–1497.

Bitgood MJ, McMahon AP (1995) Hedgehog and Bmp Genes Are Coexpressed at Many Diverse Sites of Cell–Cell Interaction in the Mouse Embryo. Developmental Biology 172:126–138.

Bourne GH (1968) The Structure and Function of Nervous Tissue. In. New York: Academic Press.

Britsch S, Derk E Goerich, Riethmacher D, Reto I Peirano, Moritz R, Nave K-A, Birchmeier C, Wegner M (2001) The transcription factor Sox10 is a key regulator of peripheral glial development. Genes and Development 15:66–78.

Brushart TM, Aspalter M, Griffin JW, Redett R, Hameed H, Zhou C, Wright M, Vyas A, Höke A (2013) Schwann cell phenotype is regulated by axon modality and central–peripheral location, and persists in vitro. Experimental Neurology:1–10.

Bukrinsky A, Griffin KJP, Zhao Y, Lin S, Banerjee U (2009) Essential role of spi-1-like (spi-1l) in zebrafish myeloid cell differentiation. Blood 113:2038–2046.

Bunge MB, Wood PM, Tynan LB, Bates ML, Sanes JR (1989) Perineurium originates from fibroblasts: demonstration in vitro with a retroviral marker. Science 243:229–231.

Burkel WE (1967) The Histological Fine Structure of Perineurium. Anatomical Record 158:177–190.

Busse D, Arteaga CL, Ramsey TT, Russell WE, Price JO, Flanagan WM, Shawver LK (2000) Reversible G_1 Arrest Induced by Inhibition of the Epidermal Growth Factor Receptor Tyrosine Kinase Requires Up-regulation of p27KIP1 Independent of MAPK Activity. Journal of Biological Chemistry 275:6987–6995.

Carroll SL, Miller ML, Frohnert PW, Kim SS, Corbett JA (1997) Expression of Neuregulins and their Putative Receptors, ErbB2 and ErbB3, Is Induced during Wallerian Degeneration. The Journal of Neuroscience 17:1642–1659.

Ceci ML, Mardones-Krsulovic C, Sanchez M, Valdivia LE, Allende ML (2014) Axon-Schwann cell interactions during peripheral nerve regeneration in zebrafish larvae. 9:1–21.

Chazotte B (2011) Labeling Lysosomes in Live Cells with LysoTracker. Cold Spring Harbor Protocols 2011; doi:10.1101/pdb.prot5571.

Chen Z-L, Yu W-M, Strickland S (2007) Peripheral Regeneration. Annu Rev Neurosci 30:209–233.

Chong MS, Woolf CJ, Turmaine M, Emson P, Anderson PN (1996) Intrinsic versus extrinsic factors in determining the regeneration of the central processes of rat dorsal root ganglion neurons: the influence of a peripheral nerve graft. J Comp Neurol 370:97–104.

Clark JK, O'keefe A, Mastracci TL, Sussel L, Matise MP, Kucenas S (2014) Mammalian Nkx2.2 +perineurial glia are essential for motor nerve development. Dev Dyn doi: 10.1002/dvdy.24158.

Davalos D, Grutzendler J, Yang G, Kim JV, Zuo Y, Jung S, Littman DR, Dustin ML, Gan W-B (2005) ATP mediates rapid microglial response to local brain injury in vivo. Nat Neurosci 8:752–758.

Deal ND, Griffin JW, Hogan MV (2012) Nerve Conduits for Nerve Repair or Reconstruction. Journal of the AAOS 20:63–68.

Du Plessis G, Mouton YM, Muller CJF, Geiger DH (1997) An ultrastructural study of the development of the chicken perineurial sheath. Journal of Anatomy 189:631–641.

Dutton KA, Pauliny A, Lopes SS, Elworthy S, Carney TJ, Rauch J, Geisler R, Haffter P, Kelsh RN (2001) Zebrafish colourless encodes sox10 and specifies non-ectomesenchymal neural crest fates. Development 128:4113–4125.

Eisen JS (1991) Developmental Neurobiology of the Zebrafish. The Journal of Neuroscience 11:311–317.

Ellett F, Pase L, Hayman JW, Andrianopoulos A, Lieschke GJ (2011) mpeg1 promoter transgenes direct macrophage-lineage expression in zebrafish. Blood 117:e49–e56.

Fleck D, van Bebber F, Colombo A, Galante C, Schwenk BM, Rabe L, Hampel H, Novak B, Kremmer E, Tahirovic S, Edbauer D, Lichtenthaler SF, Schmid B, Willem M, Haass C (2013) Dual Cleavage of Neuregulin 1 Type III by BACE1 and ADAM17

Liberates Its EGF-Like Domain and Allows Paracrine Signaling. Journal of Neuroscience 33:7856–7869.

Fricker FR, Antunes-Martins A, Galino J, Paramsothy R, La Russa F, Perkins J, Goldberg R, Brelstaff J, Zhu N, McMahon SB, Orengo C, Garratt AN, Birchmeier C, Bennett DLH (2013) Axonal neuregulin 1 is a rate limiting but not essential factor for nerve remyelination. Brain 136:2279–2297.

Garratt AN, Britsch S, Birchmeier C (2000a) Neuregulin, a factor with many functions in the life of a Schwann cell. BioEssays 22:987–996.

Garratt AN, Voiculescu O, Topilko P, Charnay P, Birchmeier C (2000b) A Dual Role of erbB2 in Myelination and in Expansion of the Schwann Cell Precursor Pool. The Journal of Cell Biology 148:1035–1046.

Gaudet AD, Popovich PG, Ramer MS (2011) 1742-2094-8-110. Journal of Neuroinflammation 8:110.

George EB, Glass JD, Griffin JW (1995) Axotomy-Induced Axonal Degeneration Is Mediated by Calcium Influx Through Ion-Specific Channels. Journal of Neuroscience 15:6445–6452.

Geuna S, Raimondo S, Ronchi G, Di Scipio F, Tos P, Czaja K, Fornaro M (2009) Chapter 3 - Histology of the Peripheral Nerve and Changes Occurring During Nerve Regeneration, 1st ed. Elsevier Inc.

Griffin JW, George R, Lobato C, Tyor WR, Yan LC, Glass JD (1992) Macrophage

responses and myelin clearance during Wallerian degeneration: relevance to immune-mediated demyelination. Journal of Neuroimmunology 40:156–166.

Guertin AD, Zhang DP, Mak KS, Alberta JA, Kim HA (2005) Microanatomy of Axon/Glial Signaling during Wallerian Degeneration. Journal of Neuroscience 25:3478–3487.

Hirata K, Kawabuchi M (2002) Myelin phagocytosis by macrophages and nonmacrophages during Wallerian degeneration. Microsc Res Tech 57:541–547.

Hirasawa Y, Saiki T, Nakao Y, Katsumi Y (1994) Regeneration of the perineurium after nerve injury and autografting. International Orthopaedics 18:229–235.

Höke A, Redett R, Hameed H, Jari R, Zhou C, Li ZB, Griffin JW, Brushart TM (2006) Schwann Cells Express Motor and Sensory Phenotypes That Regulate Axon Regeneration. Journal of Neuroscience 26:9646–9655.

Jessen KR, Mirsky R (2005) The origin and development of glial cells in peripheral nerves. Nat Rev Neurosci 6:671–682.

Jessen KR, Mirsky R (2008) Negative regulation of myelination: Relevance for development, injury, and demyelinating disease Jessen KR, Mirsky R, Salzer J, eds. Glia 56:1552–1565.

Joseph NM, Mukouyama Y-S, Mosher JT, Jaegle M, Crone SA, Dormand E-L, Lee K-F, Meijer D, Anderson DJ, Morrison SJ (2004) Neural crest stem cells undergo multilineage differentiation in developing peripheral nerves to generate endoneurial

fibroblasts in addition to Schwann cells. Development 131:5599–5612.

Kanno H, Pressman Y, Moody A, Berg R, Muir EM, Rogers JH, Ozawa H, Itoi E, Pearse DD, Bunge MB (2014) Combination of Engineered Schwann Cell Grafts to Secrete Neurotrophin and Chondroitinase Promotes Axonal Regeneration and Locomotion after Spinal Cord Injury. Journal of Neuroscience 34:1838–1855.

Kaplan S, Odaci E, Unal B, Sahin B, Fornaro M (2009) Chapter 2 - Development of the Peripheral Nerve, 1st ed. Elsevier Inc.

Kelsh RN, Brand M, Jiang Y-J, Heisenberg C-P, Lin S, Haffter P, Odenthal J, Mullins MC, van Eeden FJM, Furutani-Seiki M, Granato M, Hammerschmidt M, Kane DA, Warga RM, Beuchle D, Vogelsang L, Nusslein-Volhard C (1996) Zebrafish pigmentation mutations and the processes of neural crest development. Development 123:369–389.

Kerschensteiner M, Schwab ME, Lichtman JW, Misgeld T (2005) In vivo imaging of axonal degeneration and regeneration in the injured spinal cord. Nature Medicine 11:572–577.

Key A, Retzius G (1876) Studien in der Anatomie des Nervensystems und des Bindegewebes. Stockholm: Norstedt & Söner.

Kim H, Shin J, Kim S, Poling J, Park H-C, Appel B (2008) Notch-regulated oligodendrocyte specification from radial glia in the spinal cord of zebrafish embryos Satir P, Fallon JF, eds. Developmental Dynamics 237:2081–2089.

Kimmel CB, Ballard WW, Kimmel SR, Ullmann B, Schilling TF (1995) Stages of Embryonic Development of the Zebrafish. Developmental Dynamics 203:253–310.

Kirby BB, Takada N, Latimer AJ, Shin J, Carney TJ, Kelsh RN, Appel B (2006) In vivo time-lapse imaging shows dynamic oligodendrocyte progenitor behavior during zebrafish development. Nat Neurosci 9:1506–1511.

Klimaschewski L, Hausott B, Angelov DN (2013) The Pros and Cons of Growth Factors and Cytokines in Peripheral Axon Regeneration, 1st ed. Elsevier Inc.

Kristensson K, Olsson Y (1971) The perineurium as a diffusion barrier to protein tracers. Acta Neuropathologica 17:127–138.

Kucenas S, Snell H, Appel B (2009a) nkx2.2a promotes specification and differentiation of a myelinating subset of oligodendrocyte lineage cells in zebrafish. Neuron Glia Biol 4:71.

Kucenas S, Takada N, Park H-C, Woodruff E, Broadie K, Appel B (2008) CNS-derived glia ensheath peripheral nerves and mediate motor root development. Nat Neurosci 11:143–151.

Kucenas S, Wang WD, Knapik EW, Appel B (2009b) A Selective Glial Barrier at Motor Axon Exit Points Prevents Oligodendrocyte Migration from the Spinal Cord. Journal of Neuroscience 29:15187–15194.

Küspert M, Weider M, ller JM, Hermans-Borgmeyer I, Meijer D, Wegner M (2012) Desert Hedgehog Links Transcription Factor Sox10 to Perineurial Development. The

Journal of Neuroscience 32:5472–5480.

Kwon YK, Anita Bhattacharyya, Alberta JA, William V Giannobile, Cheon K, Stiles CD, Pomeroy SL (1997) Activation of ErbB2 during Wallerian Degeneration of Sciatic Nerve. Journal of Neuroscience 17:8293–8299.

Levitzki A, Gazit A (1995) Tyrosine Kinase Inhibition: An Approach to Drug Development. Science 267:1782-1788.

Leskovar A, MORIARTY LJ, Turek JJ, Schoenlein IA, Borgens RB (2000) The Macrophage in Acute Neuronal Injury: Changes in Cell Numbers over Time and Levels of Cytokine Production in Mammalian Central and Peripheral Nervous Syetems. The Journal of Experimenrtal Biology 203:1783–1795.

Lewis GM, Kucenas S (2013) Motor nerve transection and time-lapse imaging of glial cell behaviors in live zebrafish. Journal of Visualized Experiments 76:e50621, doi:10.3791/50621.

Lewis GM, Kucenas S (2014) Perineurial Glia Are Essential for Motor Axon Regrowth following Nerve Injury. Journal of Neuroscience 34:12762–12777.

Lin W, Burgess RW, Dominguez B, Pfaff SL, Lee JRSK-F (2001) Distinct roles of nerve and muscle in postsynaptic differentiation of the neuromuscular synapse. Nature 410:1057–1064.

Liu HM, Yang LH, Yang YJ (1995) Schwann Cell Properties: 3. C-Fos Expression, bFGF Production, Phagocytosis and Proliferation During Wallerian Degeneration.

Journal of Neuropathology and Experimental Neurology 54:487–496.

Liu K, Tedeschi A, Park KK, He Z (2011) Neuronal Intrinsic Mechanisms of Axon Regeneration. Annu Rev Neurosci 34:131–152.

Lunn ER, Perry VH, Brown MC, Rosen H, Gordon S (1989) Absence of Wallerian Degeneration does not Hinder Regeneration in Peripheral Nerve. European Journal of Neuroscience 1:27–33.

Lunn ER, Scourfield J, Keynes RJ, Stern CD (1987) The neural tube origin of ventral root sheath cells in the chick embryo. Development 101:247–254.

Lutz AB, Barres BA (2014) Contrasting the Glial Response to Axon Injury in the Central and Peripheral Nervous Systems. Developmental Cell 28:7–17.

Lyons DA, Pogoda H-M, Voas MG, Woods IG, Diamond B, Nix R, Arana N, Jacobs J, Talbot WS (2005) erbb3 and erbb2 Are Essential for Schwann Cell Migration and Myelination in Zebrafish. Current Biology 15:513–524.

Ma TY, Iwamoto GK, Hoa NT, Akotia V, Pedram A, Boivin MA, Said HM (2004) TNF-alpha-induced increase in intestinal epithelial tight junction permeability requires NF-Kappa B activation. AJP: Gastrointestinal and Liver Physiology 286:367G–376.

MacDonald JM, Beach MG, Porpiglia E, Sheehan AE, Watts RJ, Freeman MR (2006) The Drosophila Cell Corpse Engulfment Receptor Draper Mediates Glial Clearance of Severed Axons. Neuron 50:869–881.

Martin SM, O'Brien GS, Portera-Cailliau C, Sagasti A (2010) Wallerian degeneration of

zebrafish trigeminal axons in the skin is required for regeneration and developmental pruning. Development 137:3985–3994.

McDonald D, Cheng C, Chen Y, Zochodne D (2006) Early events of peripheral nerve regeneration. Neuron Glia Biol 2:139.

McDonald DS, Zochodne DW (2003) An injectable nerve regeneration chamber for studies of unstable soluble growth factors. Journal of Neuroscience Methods 122:171–178.

Meier C, Parmantier E, Brennan A, Mirsky R, Jessen KR (1999) Developing Schwann Cells Acquire the Ability to Survive without Axons by Establishing an Autocrine Circuit Involving Insulin-Like Growth Factor, Neurotrophin-3, and Platelet-DerivedGrowth Factor-BB. Journal of Neuroscience 19:3847–3859.

Moldovan M, Alvarez S, Krarup C (2008) Motor axon excitability during Wallerian degeneration. Brain 132:511–523.

Monk KR, Naylor SG, Glenn TD, Mercurio S, Perlin JR, Dominguez C, Moens CB, Talbot WS (2009) A G Protein-Coupled Receptor Is Essential for Schwann Cells to Initiate Myelination. Science 325:1402–1405.

Monk KR, Oshima K, Jors S, Heller S, Talbot WS (2011) Gpr126 is essential for peripheral nerve development and myelination in mammals. Development 138:2673–2680.

Montero-Balaguer M, Lang MR, Sachdev SW, Knappmeyer C, Stewart RA, La Guardia

De A, Hatzopoulos AK, Knapik EW (2006) The mother superiormutation ablates foxd3activity in neural crest progenitor cells and depletes neural crest derivatives in zebrafish. Developmental Dynamics 235:3199–3212.

Morris AD, Lewis GM, Kucenas S (in prep) Peripheral glial interactions are essential during motor nerve development.

Morris JH, Hudson AR, Wenddell G (1972) A Study of Degeneration and Regeneration in the Divided Rat Sciatic Nerve Based on Electron Microscopy. Zeitschrift Fur Zellforschung Und Mikroskopische Anatomie 124:165–203.

Morris JK, Lin W, Hauser C, Marchuk Y, Getman D, Lee K-F (1999) Rescue of the Cardiac Defect in ErbB2 Mutant Mice Reveals Essential Roles of ErbB2 in Peripheral Nervous System Development. Neuron 23:273–283.

Myers PZ, Eisen JS, Westerfield M (1986) Development and Axonal Outgrowth of Identified Motoneurons in the Zebrafish. The Journal of Neuroscience 6:2278–2289.

Napoli I, Noon LA, Ribeiro S, Kerai AP, Parrinello S, Rosenberg LH, Collins MJ, Harrisingh MC, White IJ, Woodhoo A, Lloyd AC (2012) A Central Role for the ERK-Signaling Pathway in Controlling Schwann Cell Plasticity and Peripheral Nerve Regeneration In Vivo. Neuron 73:729–742.

Nguyen QT, Sanes JR, Lichtman JW (2002) Pre-existing pathways promote precise projection patterns. Nat Neurosci 5:861–867.

O'Brien GS, Martin SM, SOllner C, Wright GJ, Becker CG, Portera-Cailliau C, Sagasti A

(2009) Developmentally Regulated Impediments to Skin Reinnervation by Injured Peripheral Sensory Axon Terminals. Current Biology 19:2086–2090.

O'Donnell KC, Vargas ME, Sagasti A (2013) WldS and PGC-1 Regulate Mitochondrial Transport and Oxidation State after Axonal Injury. Journal of Neuroscience 33:14778–14790.

Parkinson DB, Bhaskaran A, Arthur-Farraj P, Noon LA, Woodhoo A, Lloyd AC, Feltri ML, Wrabetz L, Behrens A, Mirsky R, Jessen KR (2008) c-Jun is a negative regulator of myelination. The Journal of Cell Biology 181:625–637.

Parmantier E, Lynn B, Lawson D, Turmaine M, Namini SS, Chakrabarti L, McMahon AP, Jessen KR, Mirsky R (1999) Schwann Cell–Derived Desert Hedgehog Controls the Development of Peripheral Nerve Sheaths. Neuron 23:713–724.

Parrinello S, Napoli I, Ribeiro S, Digby PW, Fedorova M, Parkinson DB, Doddrell RDS, Nakayama M, Adams RH, Lloyd AC (2010) EphB Signaling Directs Peripheral Nerve Regeneration through Sox2-Dependent Schwann Cell Sorting. Cell 143:145–155.

Peri F, Nüsslein-Volhard C (2008) Live Imaging of Neuronal Degradation by Microglia Reveals a Role for v0-ATPase a1 in Phagosomal Fusion In Vivo. Cell 133:916–927.

Perry VH, Brown MC (1992) Role of Macrophages in Peripheral Nerve Degeneration and Repair. BioEssays 14:401–406.

Perry VH, Brown MC, Gordon S (1987) The macrophage response to central and

peripheral nerve injury. Journal of Experimental Medicine 165:1218–1223.

Perry VH, Tsao JW, Fearn S, Brown MC (1995) Radiation-induced reductions in macrophage recruitment have only slight effects on myelin degeneration in sectioned peripheral nerves of mice. European Journal of Neuroscience 7:271–280.

Petersen SC, Luo R, Liebscher I, Giera S, Jeong S-J, Mogha A, Ghidinelli M, Feltri ML, Schöneberg T, Piao X, Monk KR (2015) The Adhesion GPCR GPR126 Has Distinct, Domain-Dependent Functions in Schwann Cell Development Mediated by Interaction with Laminin-211. Neuron 85:755–769.

Prasad MK, Reed X, Gorkin DU, Cronin JC, McAdow AR, Chain K, Hodonsky CJ, Jones EA, Svaren J, Antonellis A, Johnson SL, Loftus SK, Pavan WJ, McCallion AS (2011) SOX10 directly modulates ERBB3 transcription via an intronic neural crest enhancer. BMC Dev Biol 11:40.

Prendergast A, Linbo TH, Swarts T, Ungos JM, McGraw HF, Krispin S, Weinstein BM, Raible DW (2012) The metalloproteinase inhibitor Reck is essential for zebrafish DRG development. Development 139:1141–1152.

Quarles RH, Macklin WB, Morell P (2006) Myelin Formation, Structure and Biochemistry. In: Basic Neurochemistry: Molecular, Cellular and Medical Aspects, pp 51–71. Elsevier, Inc.

Rhodes J, Hagen A, Hsu K, Deng M, Liu TX, Look AT, Kanki JP (2005) Interplay of Pu.1 and Gata1 Determines Myelo-Erythroid Progenitor Cell Fate in Zebrafish. Developmental Cell 8:97–108.

Richard L, Topilko P, Magy L, Decouvelaere A-VR, Charnay P, Funalot B, Vallat J-M (2012) Endoneurial Fibroblast-Like Cells. J Neuropathol Exp Neurol 71:938–947.

Riethmacher D, Sonnenberg-Riethmacher E, Brinkmann V, Yamaai T, Birchmeier GRLC (1997) Severe neuropathies in mice with targeted mutations in the ErbB3 receptor. Nature 389:725–730.

Rodríguez FJ, Verdú E, Ceballos D, Navarro X (2000) Nerve Guides Seeded with Autologous Schwann Cells Improve Nerve Regeneration. Experimental Neurology 161:571–584.

Rosenberg AF, Isaacman-Beck J, Franzini-Armstrong C, Granato M (2014) Schwann Cells and Deleted in Colorectal Carcinoma Direct Regenerating Motor Axons Towards Their Original Path. Journal of Neuroscience 34:14668–14681.

Rosenberg AF, Wolman MA, Franzini-Armstrong C, Granato M (2012) In Vivo Nerve-Macrophage Interactions Following Peripheral Nerve Injury. Journal of Neuroscience 32:3898–3909.

Roytta M, Salonen V, Peltonen J (1987) Reversible endoneurial changes after nerve injury. Acta Neuropathologica 73:323–329.

Scaravilli F (1984) Regeneration of the perineurum across a surgically induced gap in a nerve encased in a plastic tube. Journal of Anatomy 139:441–424.

Schmidt H, Rickert C, Bossing T, Vef O, Urban J, Technau GM (1997) The Embryonic Central Nervous System Lineages of *Drosophila melanogaster*. Developmental

Biology 189:186–204.

Schroder J, May R, Weis J (1993) Perineurial cells are the first to traverse gaps of peripheral nerves in silicone tubes. Clinical Neurology and Neurosurgery:S78–S83.

Shinohe Y, Saino T (2000) Effects of ATP on intracellular calcium dynamics of the perineurium of peripheral nerve bundles. Histochem Cell Biol 114:497–504.

Smith CJ, Morris AD, Welsh TG, Kucenas S (2014) Contact-Mediated Inhibition Between Oligodendrocyte Progenitor Cells and Motor Exit Point Glia Establishes the Spinal Cord Transition Zone Barres BA, ed. PLoS Biol 12:e1001961.

Stassart RM, Fledrich R, Velanac V, Brinkmann BG, Schwab MH, Meijer D, Sereda MW, Nave K-A (2012) A role for Schwann cell–derived neuregulin-1 in remyelination. Nat Neurosci 16:48–54.

Stoll G, Griffin JW, Li CY, Trapp BD (1989) Wallerian degeneration in the peripheral nervous system: participation of both Schwann cells and macrophages in myelin degradation. Journal of Neurocytology 5:671–683.

Stoll G, Muller HW (1999) Nerve injury, axonal degeneration and neural regeneration: basic insights. Brain Pathol 9:313–325.

Sullivan WE, Mortensen OA (1934) Visualization of the Movement of a Brominized Oil Along Peripheral Nerves. The Anatomical Record 59:493–501.

Syed N, Reddy K, Yang DP, Taveggia C, Salzer JL, Maurel P, Kim HA (2010) Soluble Neuregulin-1 Has Bifunctional, Concentration-Dependent Effects on Schwann Cell

Myelination. Journal of Neuroscience 30:6122–6131.

Tapinos N, Ohnishi M, Rambukkana A (2006) ErbB2 receptor tyrosine kinase signaling mediates early demyelination induced by leprosy bacilli. Nature Medicine 12:961–966.

Tetzlaff W, Okon EB, Karimi-Abdolrezaee S, Hill CE, Sparling JS, Plemel JR, Plunet WT, Tsai EC, Baptiste D, Smithson LJ, Kawaja MD, Fehlings MG, Brian K Kwon (2011) A Systematic Review of Cellular Transplantation Therapies for Spinal Cord Injury. Journal of Neurotrauma 28:1611–1682.

Taveggia C, Zanazzi G, Petrylak A, Yano H, Rosenbluth J, Einheber S, Xu X, Esper RM, Loeb JA, Shrager P, Chao MV, Falls DL, Role L, Salzer JL (2005) Neuregulin-1 Type III Determines the Ensheathment Fate of Axons. Neuron 47:681–694.

Thomas PK (1963) The connective tissue of peripheral nerve: an electron microscope study. Journal of Anatomy 97:35–44.

Thomas PK, Jones DG (1967) The cellular response to nerve injury. 2. Regeneration of the perineurium after nerve section. Journal of Anatomy 101:45–55.

Thomas PK, Jones DG (1967) The cellular response to nerve injury. Journal of Anatomy 101:45–55.

Thomas PK, Olsson Y (1984) Microscopic anatomy and function of the connective tissue components of peripheral nerve (Dyck J, Thomas PK, eds). Philidelphia, Pa: Saunders.

Toews AD, Barrett C, Morell P (1998) Monocyte Chemoattractant Protein 1 Is Responsible for Macrophage Recruitment Following Injury to Sciatic Nerve. Journal of Neuroscience Research 53:260–267.

Tofaris GK, Patterson PH, Jessen KR, Mirsky R (2002) Denervated Schwann Cells Attract Macrophages by Secretion of Leukemia Inhibitory Factor (LIF) and Monocyte Chemoattractant Protein-1 in a Process Regulated by Interleukin-6 and LIF. The Journal of Neuroscience 22:6696–6703.

Vargas ME, Barres BA (2007) Why Is Wallerian Degeneration in the CNS So Slow? Annu Rev Neurosci 30:153–179.

Villegas R, Martin SM, Donnell KCO, Carrillo SA, Sagasti A, Allende ML (2012) Dynamics of degeneration and regeneration in developing zebrafish peripheral axons reveals a requirement for extrinsic cell types. Neural Development 7:1–1.

Waller A (1850) Experiments on the Section of the Glossopharyngeal and Hypoglossal Nerves of the Frog, and Observations of the Alterations Produced Thereby in the Structure of Their Primitive Fibres. Philosophical Transactions of the Royal Society of London 140:423–429.

Wang JT, Medress ZA, Barres BA (2012) Axon degeneration: Molecular mechanisms of a self-destruction pathway. The Journal of Cell Biology 196:7–18.

Wang W-D, Melville DB, Montero-Balaguer M, Hatzopoulos AK, Knapik EW (2011) Developmental Biology. Developmental Biology 360:173–185.

Webber C, Zochodne D (2010) The nerve regenerative microenvironment: Early behavior and partnership of axons and Schwann cells. Experimental Neurology 223:51–59.

Westerfield M, McMurray JV, Eisen JS (1986) Identified Motoneurons and Their Innervation of Axial Muscles in the Zebrafish. The Journal of Neuroscience 6:2267–2277.

Witzel C, Rohde C, Brushart TM (2005) Pathway sampling by regenerating peripheral axons. J Comp Neurol 485:183–190.

Wolford LM, Stevao EL (2003) Considerations in nerve repair. BUMC Proceedings 16:152–156.

Xiao Y, Faucherre A, Pola-Morell L, Heddleston JM, Liu TL, Chew TL, Sato F, Sehara-Fujisawa A, Kawakami K, Lopez-Schier H (2015) High-resolution live imaging reveals axon-glia interactions during peripheral nerve injury and repair in zebrafish. Disease Models & Mechanisms 8:553–564.

Yamamoto M, Okui N, Tatebe M, Shinohara T, Hirata H (2011) Regeneration of the perineurium after microsurgical resection examined with immunolabeling for tenascin-C and alpha smooth muscle actin. Journal of Anatomy 218:413–425.

Zeisel A, Munoz-Manchado AB, Codeluppi S, Lonnerberg P, La Manno G, Jureus A, Marques S, Munguba H, He L, Christer Betsholtz, Rolny C, Castelo-Branco G, Hjerling-Leffler J, Linnarsson S (2015) Cell types in the mouse cortex and hippocampus revealed by single-cell RNA-seq. Science 347:1138–1142.

Ziegenfuss JS, Doherty J, Freeman MR (2012) Distinct molecular pathways mediate glial activation and engulfment of axonal debris after axotomy. Nat Neurosci 15:979–987.

Zochodne DW (2012) The challenges and beauty of peripheral nerve regrowth. Journal of the Peripheral Nervous System 17:1–18.